UNIVERSITAT DE BARCELONA

Genetic disruption of transfer RNA modifications in human cancer

Laia Coll San Martin

UNIVERSITAT DE BARCELONA

Genetic disruption of transfer RNA modifications in human cancer

LAIA COLL SAN MARTÍN

BARCELONA, 2021

UNIVERSITAT DE BARCELONA

FACULTAT DE MEDICINA

PROGRAMA EN BIOMEDICINA

Instituto de Investigación
CONTRA LA LEUCEMIA
Josep Carreras

IDIBELL
Institut d'Investigació
Biomèdica de Bellvitge

UNIVERSITAT DE
BARCELONA

UNIVERSITAT DE BARCELONA - FACULTAT DE MEDICINA

PROGRAMA DE DOCTORAT EN BIOMEDICINA 2021

Genetic disruption of transfer RNA modifications in human cancer

Memòria presentada per Laia Coll San Martín per optar al grau de Doctora per la Universitat de Barcelona

Dr. Manel Esteller Badosa

Director i tutor

Dra. María Verónica Davalos Vega

Co-directora

Laia Coll San Martín

Autora

ACKNOWLEDGEMENTS

ACKNOWLEDGEMENTS

En primer lloc voldria agrair al Dr. Manel Esteller Badosa per haver-me donat l'oportunitat de poder créixer com a científica en un grup tant punter, a més de ser un exemple de dedicació a la ciència.

No menys importat ha estat la guia de la Dra. Verónica Dávalos, sempre empàtica i disposada a ser l'estrella polar que no deixa que em perdi al llarg d'aquesta dura travessia.

Moltes persones han format part d'aquest viatge que va començar amb les pràctiques de grau durant l'estiu del 2014, i de cadascuna d'elles m'enduc records i ensenyaments.

A la Vanessa i l'Alberto que no només són grans científics a dia d'avui, sinó que tinc la sort de poder dir-los amics i encara que els nostres camins es puguin allunyar, espero que es segueixin creuant al llarg de la vida. Perquè els seus consells i suport han estat claus per poder arribar fins aquí.

Al Fer que és la definició de bondat i amor a la ciència. Per tot el que m'has ensenyat durant els viatges en cotxe.

A les mames gatunes Laura i Lorea perquè amb la seva temprança i frenesí, respectivament, balancejaven el despatx.

A la Lida i el Pere que m'han ensenyat a relativitzar els petits drames del dia a dia.

A la Laia i l'Edi perquè sempre que posaven un peu al despatx aquest s'omplia de la seva energia.

A la Sugey per ser sempre tant dolça i amable.

Al Maxime i al Gerardo per ser exemples de perseverança i resiliència, i sempre estar disposats a baixar a dinar d'hora.

A l'Oriol per ser sempre amable i pacient amb els xerrameques del despatx.

Als eterns Marta i Miguel, i la més recent Laila per la seva temprança i paciència.

A l'Eva, la Rosaura, l'Olga, el David, el Manu, l'Helena, l'Espe, i el Martí per cada paraula amable i estar sempre disposats a donar-me un cop de mà.

A les persones de la plataforma de citogenètica per la seva amabilitat i predisposició a ensenyar-me a interpretar el mar de llums de les FISH.

Al Can Ruti PhD Committee, esperava cada reunió i activitat amb delit (sobretot per estar al dia de les tafaneries dels diferents centres). Per que, tot i que l'organització del PhD Day va ser una bogeria, em va permetre aprendre a molts nivells.

A la Rosa Hernández i la Laura Pintado, dos estrelles fugaces que van deixar una estela molt brillant de filosofies de vida, alegria i energia.

A la Paola, per ser la meva primera mentora científica en el laboratori i em va fer enganxar a la investigació.

Res d'això hagués estat possible sense el suport dels meus pares. Per haver-me ensenyat la importància de l'esforç i sempre haver recolzat les meves decisions. Per estar sempre en els moments durs i els d'alegria, i haver-se alegrat per cada pas que anava traçant.

A la Berta, la meva germana, per ella que representa el futur de la ciència, perquè tot i veure tot el que implica la investigació, segueix entestada en submergir-s'hi. Perquè és un exemple d'esforç, i admiro la persona en la que s'està convertint.

Pel amics del Prat, perquè escolten les nostres peripècies científiques, i ens fan tocar de peus a terra. Al Pau per tots i cadascun dels moments de gim i nyam, per compartir amb mi l'afició pastissera. I a la Sara i al Carles perquè cadascun dels dos a la seva manera han estat exemples de lluita per al que un desitja.

A la lliga, perquè amb vosaltres no només vivim aventures d'aquest món. Perquè el que més recordo de la carrera són els bons moments compartits i perquè, tot i només veure'ns de tant en tant, sembla que no hagi passat el temps.

Al Marc, per que ets el millor company de viatge que podria haver tingut la sort de trobar. Per estar allà i recolzar-me en tots moments, per entendre'm millor que ningú i empènyer a ser la millor versió de mi.

TABLE OF CONTENT

INDEX

LIST OF FIGURES

LIST OF TABLES

TABLE OF ABBREVIATURES

Ψ	Pseudouridine
AaRS	Aminoacyl-tRNA synthetase
ADC	Adenocarcinoma
ALKBH8	AlkB Homolog 8, TRNA Methyltransferase
ANGPTL4	Angiopoietin Like 4
APL	Acute promyelocytic leukaemia
As_2O_3	Arsenic trioxide
ASCL1	Achaete-scute homolog 1
bHLH	Basic helix-loop-helix
CDK5RAP1	Cdk5 regulatory subunit associated protein 1
CDKAL1	CDK5 regulatory subunit associated protein 1-like 1
CN	Copy number
CNS	Central nervous system
COL3A1	Collagen Type III Alpha 1 Chain
CTL	Cytotoxic T lymphocyte
CTLA-4	Cytotoxic T-lymphocyte-associated protein 4
DMAPP	Dimethylallyl pyrophosphate
DMOG	Dimethyloxalylglycine
DNA	Deoxyribonucleic acid
eEF	Eukaryotic translation elongation factor
eEFSec	Eukaryotic selenocysteine-specific elongation factor
eIF	Eukaryotic translation initiation factor
eRF1	Eukaryotic release factor 1
FC	Fold change
FDA	US Food and Drug Administration
FISH	Fluorescence *in situ* hybridisation

FTSJ1	FtsJ RNA methyltransferase 1
GPX	Glutathione peroxidase
GPX4	Glutathione Peroxidase 4
GSEA	Gene set enrichment analysis
HIFs	Hypoxia-inducible factors
HIF1α	Hypoxia-induced factor 1α
hm^{5}C	5-hydroxymethylcytidine
I	Inosine
i^{6}A	N^6-isopentenyladenosine
IC50	Half-maximal inhibitory concentration
iCLIP	Individual-nucleotide resolution Cross-Linking and Immunoprecipitation
ICI	Immune checkpoint inhibitors
ID1	Inhibitor of DNA Binding 1, HLH Protein
ID3	Inhibitor of DNA Binding 3, HLH Protein
io^{6}A	N^6-(cis-hydroxyisopentenyl) adenosine
itRNA	Initiation tRNA
LAMA4	Laminin Subunit Alpha 4
LCC	Large cell carcinoma
LC-MS	Liquid chromatography-coupled mass spectrometry
lncRNA	Long non-coding RNA
LOF	Loss-of-function
m^{1}A	1-methyladenosine
m^{5}C	5-methylcytidine
m^{6}A	N^6-methyladenosine
m^{6}Am	N^6-2′-O-dimethyladenosine
mcm^{5}U	5-methoxycarbonylmethyl-uridine
mcm^{5}Um	5-methoxycarbonylmethyl-2′-O-methyluridine
MELAS	Mitochondrial encephalomyopathy, lactic acidosis and stroke-like episodes

MERRF	Myoclonus epilepsy with ragged-red fibres
miRNA	MicroRNA
MLPA	Multiplex ligation-dependent probe amplification
mRNA	Messenger RNA
ms^2i^6A	2-methylthio-N^6-isopentenyladenosine
ms^2io^6A	2-methylthio-N^6-(cis-hydroxyisopentenyl) adenosine
ms^2t^6A	2-methylthio-N^6-threonylcarbamoyladenosine
$msms^2i^6A$	2-methylthiomethylenethio-N^6-isopentenyl-adenosine
MT1X	Metallothionein 1X
MTT	3-(4,5-dimethylthiazol-2-yl)-2,5-diphenyltetrazolium bromide
NE	Neuroendocrine
NEUROD1	Neurogenic differentiation factor 1
NSCLC	Non-small cell lung cancer
ORF	Open reading frame
OS	Overall survival
OXPHOS	Oxidative Phosphorylation System
PCI	Prophylactic cranial irradiation
PD-1	Programmed cell death
PD-L1	Programmed death-ligand protein 1
PFS	Progression-free survival
PI	Propidium iodide
POU2F3	POU domain class 2 homeobox
PSTK	O-phosphoserine by Phosphoseryl-tRNA Kinase
RIP-Seq	RNA immunoprecipitation sequencing
RPL30	Ribosomal protein L30
RNA	Ribonucleic acid
ROS	Reactive oxygen species
rRNA	Ribosomal RNAs
RR	Response rate

RT-qPCR	Real-time quantitative PCR
SA-β-gal	Senescence-associated β-galactosidase
SARS1	Seryl-tRNA Synthetase 1
SCC	Squamous cell carcinoma
SCLC	Small cell lung cancer
SCLY	Selenocysteine lyase
SCR	Scramble
Sec	Selenocysteine
SECIS	Selenocysteine insertion sequence
SECISBP2	Selenocysteine insertion sequence-binding protein 2
SELENOP	Selenoprotein P
SeMet	Selenomethionine
SEPHS2	Selenophosphate 2 synthetase
SEPSECS	Sep (O-Phosphoserine) tRNA:Sec (Selenocysteine) tRNA Synthase
shRNAs	Short hairpin RNAs
SMRT	Single-molecule real-time sequencing
SNP	Single nucleotide polymorphisms
snRNA	Small nuclear RNAs
tgm	tRNA-gene mediated
TNM	Tumour-node-metastasis
TRIT1	tRNA Isopentenyltransferase 1
tRNA	Transfer RNA
TXNRD	Thioredoxin reductases
UPR	Unfolded protein response
WES	Whole exome sequencing
WHO	World Health Organisation
YAP1	Yes-associated protein 1

I. INTRODUCTION

I. INTRODUCTION

1. Cancer.

1.1. Definition.

Cancer was reported as the second leading cause of death in 2018 by the World Health Organisation (WHO). Nowadays, cancer is responsible for more than 9.96 million deaths worldwide every year, affecting the health and economy of people and communities [1]. As a result of the improvements in treatment and detection and the decrease in smoking, the cancer death rate has fallen for a total decline of 31% since the end of the last century [2]. According to the National Cancer Institute, more than 100 types of cancer exist. The most frequent causes of cancer death are lung, colorectal, liver, stomach, and breast cancers.

Cancer is defined as the set of diseases that proceeds in multiple phases generating a transformation lead by an accumulation of genetic (mutations, copy number), epigenetic (CpG methylation, histone modifications), and epitranscriptomic alterations [3,4]. Hanahan and Weinberg listed all these alterations that confer the neoplastic characteristics in 2000 and extended them in 2011 [5,6]. They are known as the hallmarks of cancer (**Figure 1**).

- Resisting cell death: Apoptosis and other cell death forms serve as a natural barrier to cancer development. They are triggered in response to various physiologic stresses that cancer cells experience as DNA damage. Tumour cells use various strategies to evade cell death as the loss of proapoptotic tumour suppressor genes and elevated levels of antiapoptotic oncogenes.

- Deregulating cellular energetics: The constant cancer cell proliferation may require some glucose metabolism adjustments to produce enough energy. This is achieved through the aerobic glycolysis state that can be accentuated under hypoxic conditions and increases glycolytic intermediates' availability required for proliferation.

- Sustaining proliferative signalling: Cancer cell deregulate the cell division and growth signals. Homeostasis is altered by changes in stimulation, activation and receptors levels, ligands and downstream molecules. Chronic alteration affects the tissue architecture and other cell-biological properties.

- Evading growth suppressors: Several tumour suppressor genes participate in programs that negatively regulate cell growth and proliferation. Cancer cells are characterised by shutting down these constriction mechanisms, although a high functional redundancy level reinforces them.

- Avoiding immune destruction: Immune system is able to detect many initiating tumours and eradicates them. However, weakly immunogenic cancers escape this control and generate solid tumours.

- Activating invasion and metastasis: Cancer cells harbour alterations in cell-cell/matrix attachment proteins that allow them to spread from their original sites. Metastasis is a sequential process that starts with the local invasion, follows with cancer cells circulating through the lymphatic and haematogenous systems and end with those cells colonising a distant tissue.

- Tumour-promoting inflammation: Tumours have an associated inflammatory response that enhances tumorigenesis and progression by supplying bioactive molecules to the tumour microenvironment.

- Enabling replicative immortality: Normal cell lineages have barriers that limit proliferation thanks to the protection of chromosome ends by telomeres. Once telomeres are short enough after several cell growth-and-division cycles, cells enter senescence and crisis/apoptosis. Nevertheless, cancer cells can avoid telomeres' erosion, mainly increasing telomerase levels and becoming immortal.

- Inducing angiogenesis: Tumours generate new vasculature through activation of angiogenesis. Tumour expansion requires a high amount of nutrients and oxygen and needs to evacuate metabolic wastes and carbon dioxide. Changes in the expression of angiogenesis regulators allow maintaining this process chronically.

- Genome instability and mutation: Mutations naturally occur during DNA replication, but they are almost always correctly repaired. However, systems that detect DNA damage, repair mutations, and protect DNA may be lost during tumour progression. Mutation accumulation generates subclones of cells with genomic instability and a neoplastic selective advantage.

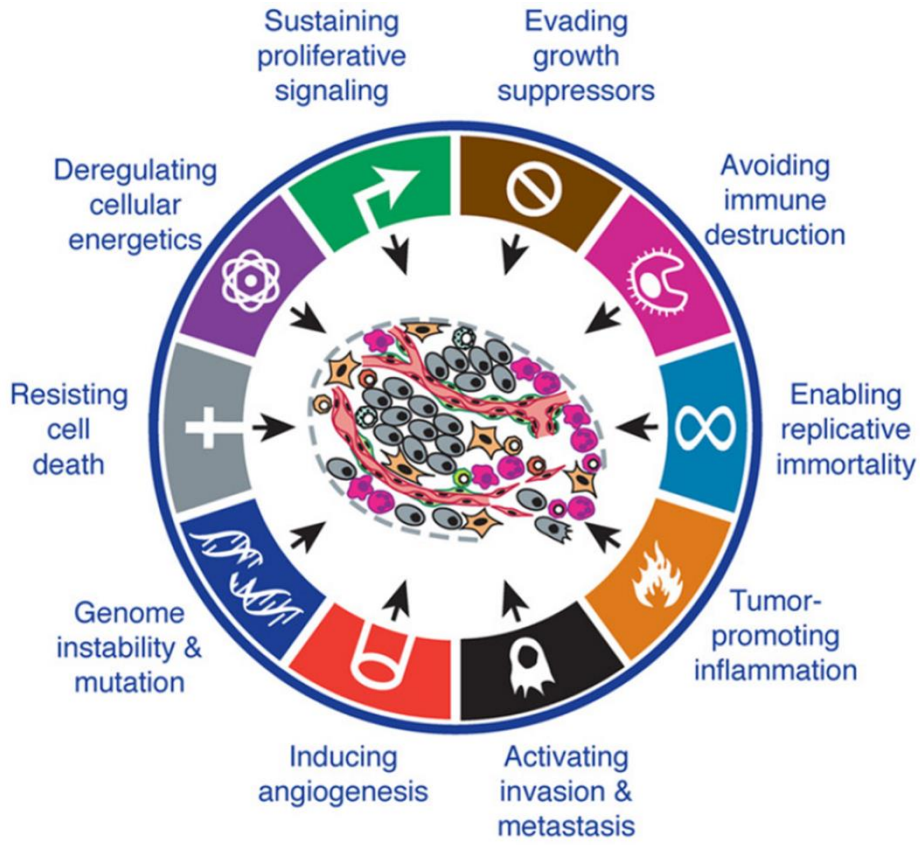

Figure 1. Hallmarks of cancer. Adapted from Hanahan and Weinberg, 2011 [6].

1.2. Lung cancer.

Lung cancer is the primary cause of cancer-related deaths and the second in incidence (**Figure 2A**) [1]. 82% of cancer deaths are associated to tobacco smoking, although other air carcinogens also increase the risk [2,7]. The over 60 chemical carcinogens in tobacco contribute to lung carcinogenesis, activating an inflammatory response, forming DNA adducts that will trigger mutations in critical genes, and altering the metabolic processes activating carcinogenic pathways [8].

Lung cancer is mainly diagnosed among people aged 65–74, being 71 years the median age of diagnosis (**Figure 2B**). It is commonly diagnosed at advanced stages, leading to a 5-year survival of about 21% (**Figure 2C**), one of the lowest survival rates after pancreas (10%), liver (20%) and oesophagus (20%) cancers [9,10]. Nevertheless, mortality for lung cancer has declined in recent years due to improvements in treatment and the reduction of cigarette consumption at the population level [2,7].

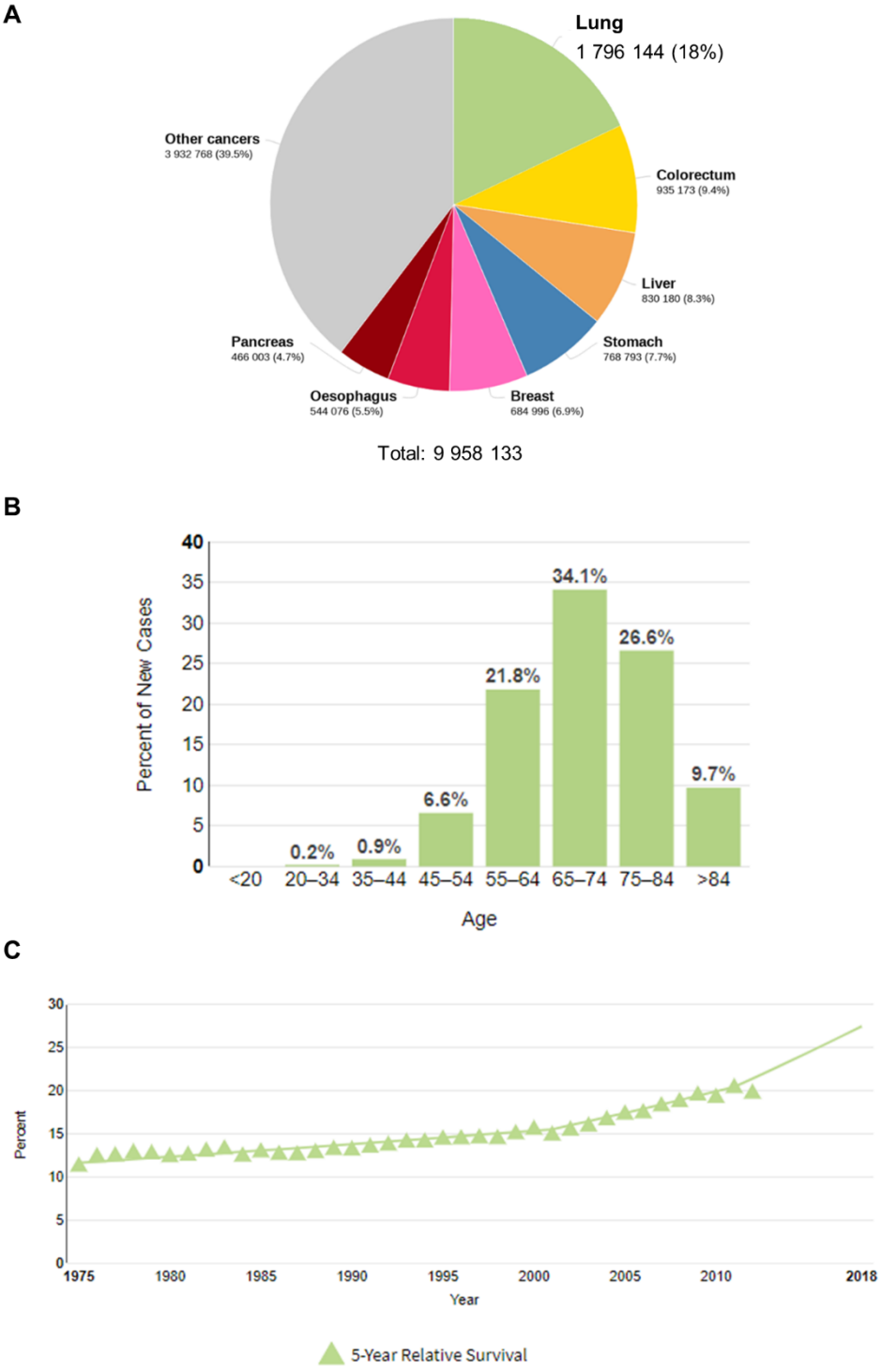

Figure 2. Statistical analysis of cancer incidence in worldwide population. **(A)** Estimated number of cancer deaths in 2020 (GLOBOCAN 2020) [1]. **(B)** Percent of new cases by age group of lung and bronchus cancer between 2013 and 2017 (SEER) [9]. **(C)** 5-Year relative survival percent from 1975-2012 of lung and bronchus cancer (SEER) [9].

The clinical manifestations may include a new cough, recurrent pneumonia in the exact anatomic location, shortness of breath (dyspnea), developing pulmonary embolus, pneumothoraces, pleural effusions, or pericardial effusions [11].

Lung cancer is historically subdivided according to resection specimens in small cell lung cancer (SCLC) and non-small cell lung cancer (NSCLC) [7,12]. NSCLC accounts for about 85% of lung cancers. The most common NSCLC pathologic subtypes are adenocarcinoma (ADC), squamous cell carcinoma (SCC), and large cell carcinoma (LCC). Patients with NSCLC have a better survival rate than those with SCLC with a 2-year survival of about 42% [2,13].

In 2015, the World Health Organization actualised the classification according to morphology based on immunochemistry and the tumour genetic profile. This new classification includes five main groups: Epithelial tumours, mesenchymal tumours, lymphohistiocytic tumours, tumours of ectopic origin and metastatic tumours. The new classification aims to improve the assignment of a personalised medicine according to the assigned tumour type [14].

1.2.1. Small cell lung cancer (SCLC).

SCLC is the most lethal and aggressive subtype of lung cancer, responsible of 200,000 deaths globally each year. As classified for the World Health Organization, small cell lung cancer is an epithelial tumour with neuroendocrine features representing 10-15% of all lung tumours. According to Siegel et al. 2021, 2-year relative survival for small cell lung cancer remains about 14% [2]. In 95% of the cases, SCLC is strongly associated with tobacco smoke habit [15].

Histopathologically, SCLC consists of small round to fusiform cells with scant cytoplasm, poorly defined cell borders, finely dispersed granular nuclear chromatin, and nuclear moulding with absent or inconspicuous nucleoli. Necrosis is usually extensive, and the mitotic rate is high, with about 60 mitoses per 2 mm^2. Genetically, SCLC is one of the most mutated cancers being the mutation rate highly associated with smoking and presenting a characteristic tobacco carcinogen-associated molecular signature. Early *TP53* (80–90%) and *RB1* (60–90%) inactivating mutations are molecular hallmarks of SCLC [14-17]. In brief, p53 protein—known as the guardian of the genome—induces cell cycle arrest, apoptosis, senescence, DNA repair, or changes in metabolism; and RB protein negatively regulates the cell cycle [18-20].

SCLC is a highly aggressive and fast-growing malignancy with a remarkable poor prognosis. It easily spreads through lymph nodes to the body, and over 60% of SCLC patients present metastasis when cancer is diagnosed. This tumour type frequently metastasises to the brain, liver, adrenal glands, and bone [21].

Symptoms of SCLC, as symptoms in all lung tumours, include coughing (sometimes coughing up blood), dyspnoea, wheezing or post-obstructive pneumonia. Also, if the tumour has extended, patients can present vocal hoarseness, chest or throat pain, or dysphagia. Paraneoplastic syndromes are more frequently documented in SCLC than in other histological types of lung cancer. The tumour at presentation tends to be large, often lobulated, and show an advanced stage because of the rapid growth compared with NSCLC tumours. The tumour mass is usually located in the perihilar region as the central part of the major airways is the most exposed to tobacco smoke and its genotoxic effects, and it is usually detected in chest imaging.

Although the first-line therapy is very effective in almost all cases, the tumour will broadly recur within 1 or 2 years. Relapsed patients can be divided into having chemotherapy-sensitive or chemotherapy-refractory diseases. The sensitive cases response to first-line chemotherapy is maintained for at least 2 to 3 months after completion of therapy, and are more prone to respond to second-line chemotherapy. The refractory relapse is extremely chemoresistant (response rates under 10% with single-agent chemotherapy) what causes disease progression during initial therapy or within 3 months after its completion. Therefore, refractory cases have shorter median survival than sensitive relapse [22,23]. However, this scenario is improving with the emergence of the immunotherapy.

Historically, SCLC is divided into two stages, limited (LD-SCLC) or extensive (ED-SCLC), in order to assign the treatment. Limited disease patients have the tumour mass confined to one hemithorax and associated regional lymph nodes. Meanwhile, extensive disease patients present the tumour mass outside the previous limits and include patients with malignant pericardial and pleural effusion. Nowadays, tumour-node-metastasis (TNM) classification is preferred because it distinguishes between different prognostic groups, previowsly grouped as limited disease. The TNM gives information about the primary tumour (T), the nearest lymph nodes (N), and metastasis (M) [11,22,24]. T is subdivided into four groups (1, 2, 3 and 4) depending on the tumour size, the lung invasion and the presence of atelectasis or obstructive pneumonitis. N is subdivided into four groups, N0 means no regional lymph node metastasis, and N1, 2 and 3 indicate an increasing

spreading of pulmonary lymph node metastasis. Finally, M indicates the absence (M0) or the presence (M1) of distant metastasis (**Table 1**). The TNM classification is grouped in the following TNM staging system that serves as a guide for the treatment election:

- TNM stage I: Few patients are detected at this stage; for that reason, clinical trials cannot be conclusive with the best treatment strategy. The application of surgery and fractioned radiotherapy administration is controversial. There are favourable data for stereotactic ablative radiotherapy. Cisplatin-etoposide chemotherapy is used as an adjuvant.

- TNM stage I-III: Cancer has spread through the lungs and regional lymph nodes, but dissemination to distant organs is not detected. The treatment depends on the size of the primary tumour and the status of the patient. Chemotherapy and radiotherapy are the usual treatment choice.

- TNM stage IV: Patients with metastatic disease are treated with chemotherapy and more recently, with immune checkpoint inhibitors (ICI). Prophylactic cranial irradiation (PCI) is recommended in patients without central nervous system (CNS) metastasis [25].
- Recurrent disease: Great majority of patients relapse within six months after concluding the initial treatment [26,27]. The response rate (RR) of oral topotecan is 6–17% [28]. Regular monitoring is crucial in order to detect recurrence as soon as possible. Unfortunately, the response to second-line chemotherapy is poor.

Despite this action plan, SCLC treatment was maintained invariably until the last years. First-line chemotherapy has been based on the combination of etoposide with a platinum-based agent (cisplatin or carboplatin) and second-line chemotherapy using the topoisomerase I inhibitor topotecan [24]. Nowadays, increasing clinical trials are trying to establish new therapies and combinations to increase overall survival (OS) substantially. Research is focus on the identification of molecular biomarkers and ICIs. On the one hand, lots of studies tried to develop new therapeutic options based on targeting the vascular system, transcription and epigenetic factors, errant signal cascades, specific surface markers, and anti-apoptotic markers. Although, some of them increased the progression-free survival (PFS), but there were no benefits in OS or shown increased toxicity [29,30]. On the other hand, the use of ICIs therapies based on anti-PD-L1 (programmed death-ligand 1), anti-PD-1 (programmed cell death protein 1) and anti-CTLA-4 (cytotoxic T-lymphocyte-associated protein 4) monoclonal antibodies has been

a revolution in the treatment of aggressive tumour types including melanoma and lung cancer, particularly NSCLC [10]. Blocking of immune checkpoint molecules can stimulate the reactivation of cytotoxic T cell immunity. In SCLC, the US Food and Drug Administration (FDA) approved in 2020 the use of the atezolizumab (anti-PD-L1) in combination with chemotherapy to treat extensive-stage disease [31]. Additionally, durvalumab (anti-PD-L1) plus platinum-etoposide has improved OS in patients with extensive-stage SCLC [26,32]. However, these novel treatments have slightly improved progression-free survival and overall survival in SCLC [31-33].

Table 1. TNM staging system. The TNM system and its associated median survival considering optimal chemoradiation or chemotherapy [15].

Stage	Tumour	Node	Metastasis	Median survival
Ia	T1a	N0	M0	60 months
	T1b	N0	M0	
Ib	T2a	N0	M0	43 months
IIa	T1a	N1	M0	34 months
	T1b	N1	M0	
	T2a	N1	M0	
	T2b	N0	M0	
IIb	T2b	N1	M0	18 months
	T3	N0	M0	
IIIa	T1	N2	M0	14 months
	T2	N2	M0	
	T3	N1	M0	
	T3	N2	M0	
	T4	N0	M0	
	T4	N1	M0	
IIIb	T4	N2	M0	10 months
	T1	N3	M0	
	T2	N3	M0	
	T3	N3	M0	
	T4	N3	M0	
IV	T Any	N Any	M1	6 months

Nowadays, expectations are focus on a novel molecular classification of SCLC as it would provide new targetable biomarkers to treat patients, but a better understanding of their biology is still needed to successfully translate the molecular findings in benefit of patients [34-36]. The molecular classification proposed by Rudin et al. 2020 is mainly based on the expression pattern of the four genes: achaete-scute homolog 1 (*ASCL1*), neurogenic differentiation factor 1 (*NEUROD1*), POU domain class 2 homeobox 3 (*POU2F3*) and yes-associated protein 1 (*YAP1*) [34]. The four subtypes have been called SCLC-A, SCLC-N, SCLC-P and SCLC-Y, respectively. SCLC-A and SCLC-N are considered neuroendocrine (NE) subtypes as ASCL1 and NEUROD1 are neuronal transcription factors, even though SCLC-A express more NE makers than SCLC-N [34,37]. Meanwhile, SCLC-P and SCLC-Y have a non-neuroendocrine profile, showing a low dependence on ASCL1 and NEUROD1. However, SCLC-Y is the less characterised, and it is not clear if YAP1 drives the phenotype. Thus, Gay et al. 2021 have proposed a SCLC-I subtype characterised by low expression of ASCL1, NEUROD1 and POU2F3, and an inflamed gene signature [38].

2. Epitranscriptomics.

Although RNA modifications were detected for the first time in 1951, it was not until 2012 that the term epitranscriptomics was coined to describe this field of study [39,40]. RNA modifications are inserted in transcripts derived from both coding (messenger RNAs, mRNAs) and non-coding (transfer RNAs, tRNAs; ribosomal RNAs, rRNAs; small nuclear RNAs, snRNAs; microRNAs, miRNAs) and long non-coding RNAs (lncRNAs)) genes [3]. The development of new sequencing methods and highly sensitive mass spectrometry technologies for gaining insight in detection, mapping and quantification of these modifications has boosted the epitranscriptome information in the last years.

RNA modification knowledge is expanding in parallel with detection techniques development. The most abundant modifications are 5-methylcytidine (m^5C), N^6-methyladenosine (m^6A), N^6-2′-O-dimethyladenosine (m^6Am), pseudouridine (Ψ), 1-methyladenosine (m^1A), 5-hydroxymethylcytidine (hm^5C) and inosine (I), which are the best characterised and the ones that have the more advanced detection techniques. At the beginning, approaches only identified modified ribonucleosides based on their physicochemical properties. These techniques include two-dimensional thin-layer chromatography and capillary electrophoresis. They are laborious and time-consuming, use radioactive labelling, and are semiquantitative [41-43]. After, liquid chromatography-coupled mass spectrometry (LC-MS) allowed identification and quantification of multiple

modified ribonucleosides in less time than previous techniques [44-46]. Unfortunately, LC-MS does not provide information about the location of the modification in the transcript and the transcript itself. Transfer RNAs have been the best-characterised mainly due to their abundance and short sequence [47]. Next generation sequencing technologies provide the tools to accurately map some modified nucleosides [40,48,49]. These techniques include RNA immunoprecipitation sequencing (RIP-Seq), RNA chemical treatment before sequencing (CHEM-seq), RNA mismatch signatures produced during the conversion of RNA to cDNA by reverse transcriptase, methylated RNA immunoprecipitation sequencing (MeRIP-Seq), and individual-nucleotide resolution Cross-Linking and ImmunoPrecipitation (iCLIP) [50,51]. Inconveniently, some of them are not suitable for transcriptome-wide sequencing of the modifications as they are lost in the RNA to cDNA conversion for sequencing [52]. Third Revolution in Sequencing technology eliminates all these flaws, mapping the (epi)transcriptome of full-length reads [53-56]. Single-molecule real-time sequencing (SMRT) was the first of these technologies, although labour-intensive and expensive [40]. Oxford Nanopore Technologies emerges as a promising technology as it enables direct native RNA sequencing. Nevertheless, there is still a long way to go to facilitate the analysis of the complex raw data generated with these technologies.

Until now, more than 160 modifications have been identified through the three domains of life (Archaea, Bacteria, and Eukarya) (**Figure 3**) [57,58]. These modifications are added to ribonucleotide residues on the purine/pyrimidine ring or ribose, and a significant number of enzymes regulates their dynamic. The identification of these enzymes in charge of inserting (writers), detecting (readers) and removing (erasers) all these modifications is nowadays a field of extensive research. The role of these modifications ranges from provide stability, to be involved in export, maturation, splicing, folding and function of the RNA; however, there are still many gaps to fill.

Transfer RNAs show the highest density of modifications, with an average of 76 nucleotides and 13 modifications per molecule [59,60]; although, mitochondrial tRNAs are generally modified to a lesser extent, containing an average of 5 modifications per molecule [61]. During different maturation steps, modifications are anchored to tRNAs, allowing the correct folding of their secondary and tertiary structures through correct base-pairing, codon recognition and binding. These ensure translation fidelity, structural stability, and integrity, allowing the global protein synthesis rate control [59,62].

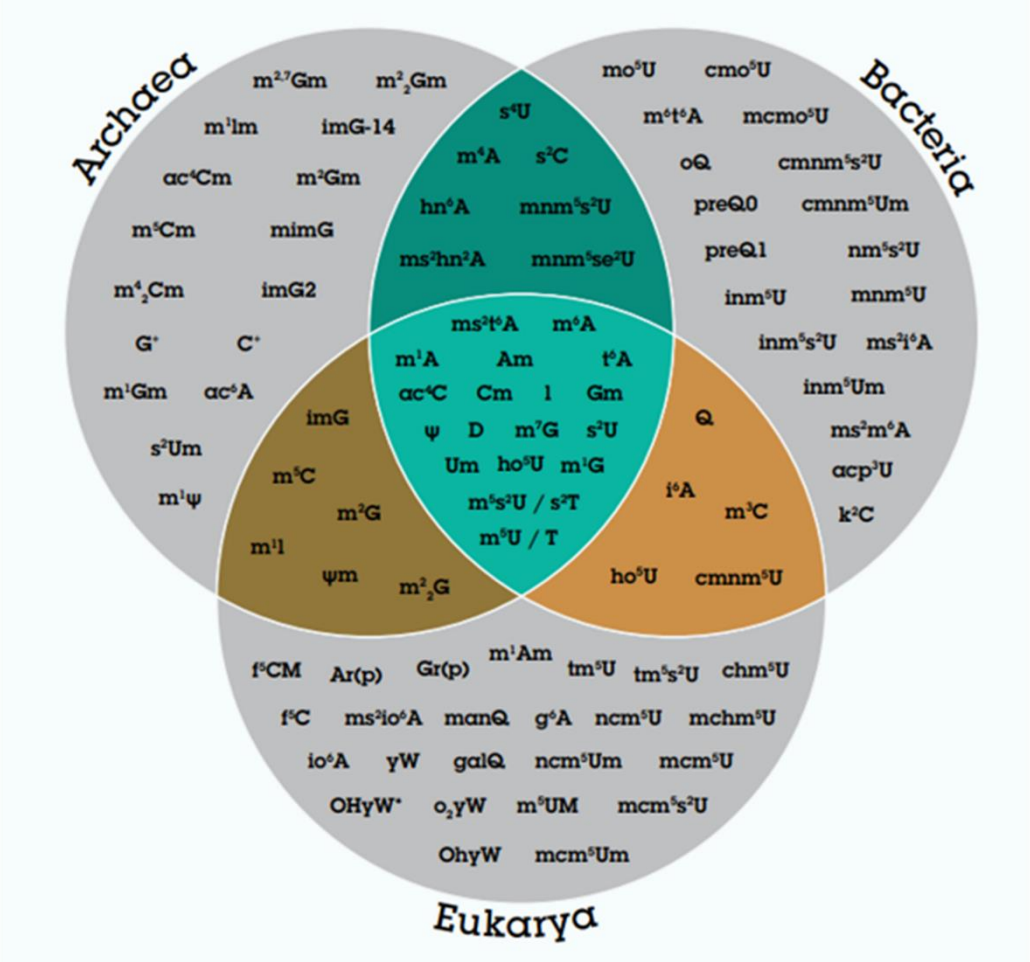

Figure 3. RNA modifications identified in the three domains of life. Some modifications are present in more than one domain. Adapted from Lorenz 2017 [63].

2.1. Transfer RNAs.

tRNA plays a fundamental role in protein biosynthesis as an adaptor molecule acting as a biological link between mRNA and protein sequences on the ribosome during the translation process [59,64]. Apart from this role, tRNA fragments regulate protein synthesis during stress situations, gene silencing and signalling [65]. For the decoding of the 21 amino acids, the human genome harbours about 429 high confidence cytoplasmic tRNA encoding genes, and 22 mitochondrial tRNA species, which are often tissue-specifically expressed [66,67].

2.1.1. tRNA transcription and processing.

Genes that codify tRNAs show an extreme evolutionary conservation as their sequence reflects the secondary structure of the gene product [59]. In eukaryotes, RNA polymerase III transcribes several small non-coding genes as tRNAs in the nucleus [68], and mitochondrial tRNAs are transcribed by the complex composed of TFB2M, TFAM and POLRMT [69].

Three deeply interrelated and coordinated processes are responsible to generate mature tRNAs in eukaryotes. On the one hand, the tRNA sequence folds in the cloverleaf secondary structure that is further folded to the three-dimension L-shape structure (**Figure 4**). L-shape is needed for the tRNA to fit onto the ribosome. tRNA architecture is organised in five functional arms or loops stabilised by Watson-Crick base pairing. The anticodon arm contains the three nucleosides that pair with the mRNA codon in the ribosome, whereas the acceptor stem is where the aminoacyl synthase charges the corresponding amino acid. The T-loop contains a conserved TψC sequence and serves in the ribosome:tRNA interaction, the D-loop charges dihydrouridines, and the variable arm length differs in each tRNA [63,70]. However, there are some mitochondrial RNAs structures that differ from the canonical one [71-73]. In these mt-tRNAs, structure stability seems to lay into RNA modifications [74,75]. Concomitantly, chemical modifications are incorporated into the structure and lead to folding and stabilisation [76].

Once correctly folded, the pre-tRNAs undergo 5′ and 3′ end processing by RNase P (mt-RNase P in mitochondria) complex and ELAC2, respectively, and TRNT1 polymerises CCA to the processed 3′ end. If needed, the TSEN complex splits the intron part, and the tRNA-splicing ligase complex joins the ends (**Figure 5**) [70,77]. Then mature nuclear-synthesised tRNA is bond to RAN:GTP, and the complex interacts with the nuclear export receptor XPOT that translocate the tRNA to the cytosol through the nuclear pore [70]. Once on cytoplasm, more epitranscriptomic modifications are attached to the tRNA conferring the need characteristics to accomplish their function.

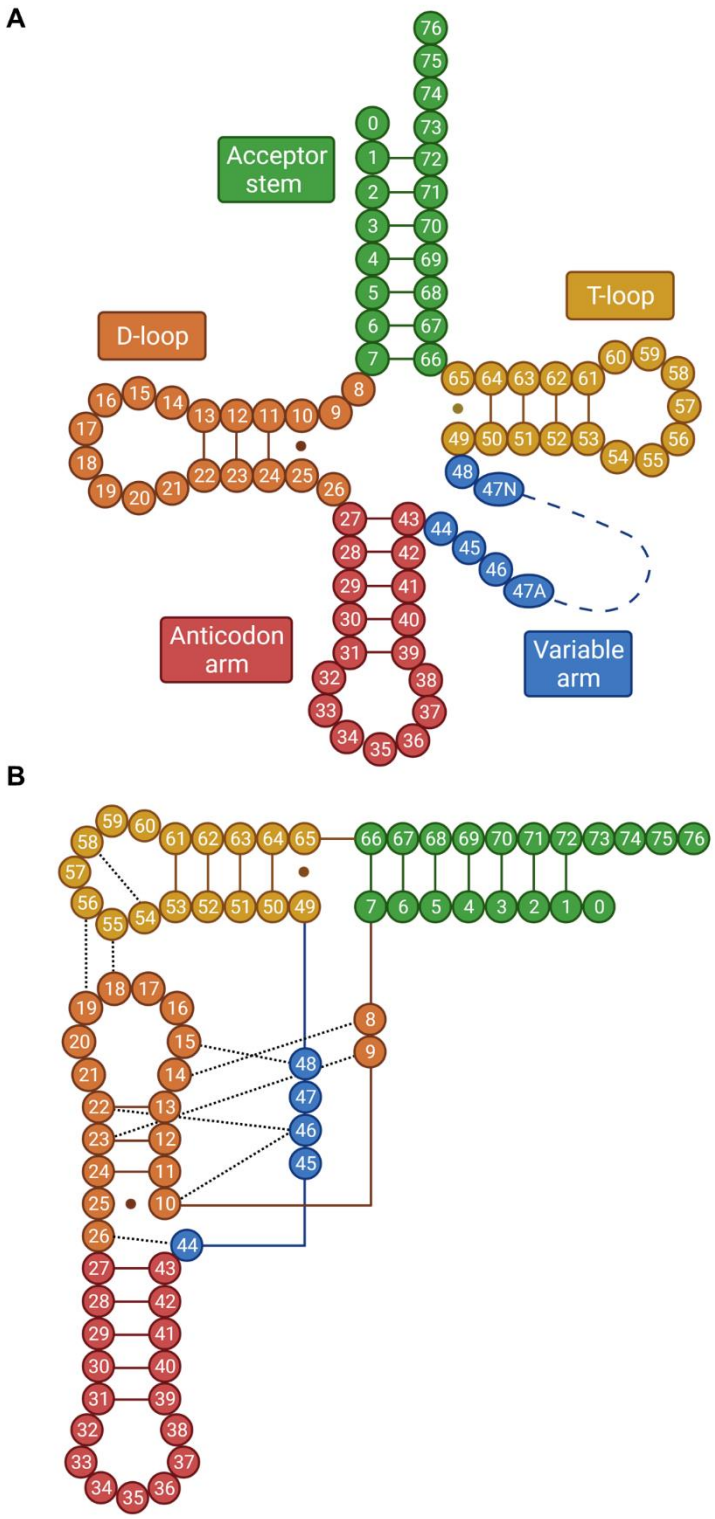

Figure 4. Transfer RNA structure. (**A**) Cloverleaf secondary structure of tRNA. (**B**) Three-dimension L-shape structure of tRNA with the interactions between the arms represented with a black dashed line. The acceptor stem is represented in green, the T-loop is yellow, the D-loop is orange, the variable arm is blue, and the anticodon arm is red.

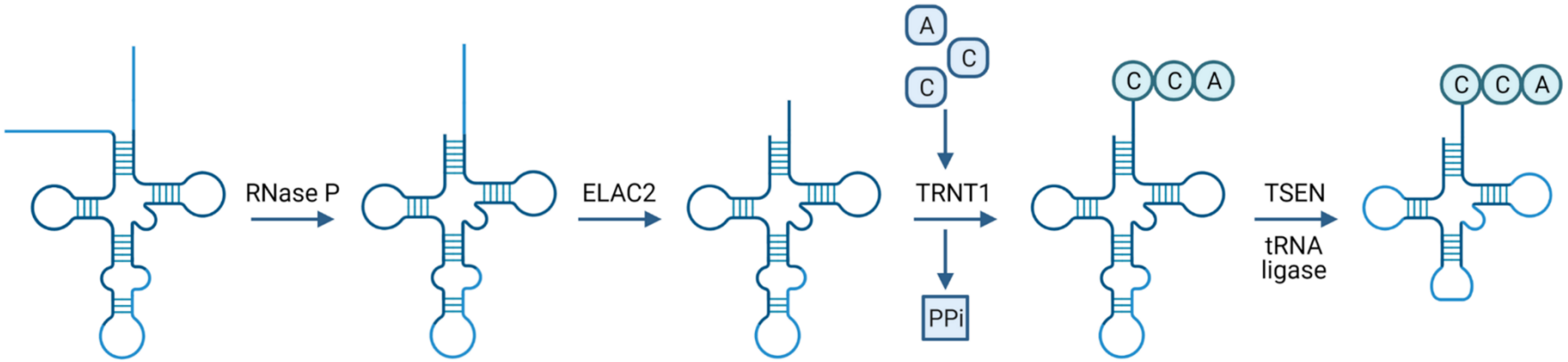

Figure 5. Transfer RNA processing in the nucleus. Cleavage of the 5' and 3' ends by the RNAase P complex and ELAC2, respectively. Next, incorporation of the CCA nucleotide sequence, and finally cleavage of the intron (TSEN, tRNA ligase).

2.1.2. tRNA aminoacylation.

In the cytoplasm or mitochondria, mature tRNAs are attached to the appropriate amino acid through an aminoacylation reaction. Aminoacyl-tRNA synthetases (aaRSs) catalyse the covalent pairing. In eukaryote, there are one aaRS for each amino acid (except selenocysteine that follows an indirect aminoacylation pathway), and they can act in the cytoplasm, the mitochondria, or in both locations. Firstly, the aaRS incorporates its corresponding amino acid and an ATP molecule and forms a complex releasing pyrophosphate in a process named amino acid activation. Next, the specific tRNA binds to the complex and forms a covalent bond with the amino acid releasing AMP, and the amino acid is covalently incorporated into the ribose of the terminal adenosine of the CCA sequence at the 3' end. Finally, the charged tRNA detaches from the aaRS (**Figure 6**) [78-80].

As previously described, there are more tRNA genes than codons, meaning that various tRNAs exist for the same anticodon, and they are named "isodecoders" [59]. AaRs has a high specificity for their substrates, and tRNAs isodecoders have recognition sequences called identity elements. The main identity element is the anticodon, but other specific nucleotides provide structural characteristics for aaRS recognition [80-82].

2.1.3. Translation.

Once the tRNA is aminoacylated, it can perform its role in translation. The translation process of decoding the mRNA sequence in the ribosome into protein is divided in initiation, elongation, and termination [81,83].

Firstly, the initiation process is led by eukaryotic translation initiation factors (eIFs) that incorporates the initiation tRNA that carries a methionine ($itRNA^{Met}$) at the AUG codon.

The elongation process is carried out by the eukaryotic translation elongation factors (eEFs). The ribosome, eEFs and tRNA have various mechanisms to maximise the decoding accuracy, ensuring the correct codon-anticodon pairing.

A stop codon (UAA, UAG, or UGA in universal code) marks the end of the polypeptide chain's elongation. In mammals only the tRNA selenocysteine complements the UGA codon in certain circumstances, but all three codons are considered termination signals in the universal code. When one of these codons is present, the polypeptide chain release factor 1 (eRF1) is incorporated in the ribosome, liberates the polypeptide chain into the cytoplasm, and then, the mRNA-tRNA-ribosomal complex is dissociated.

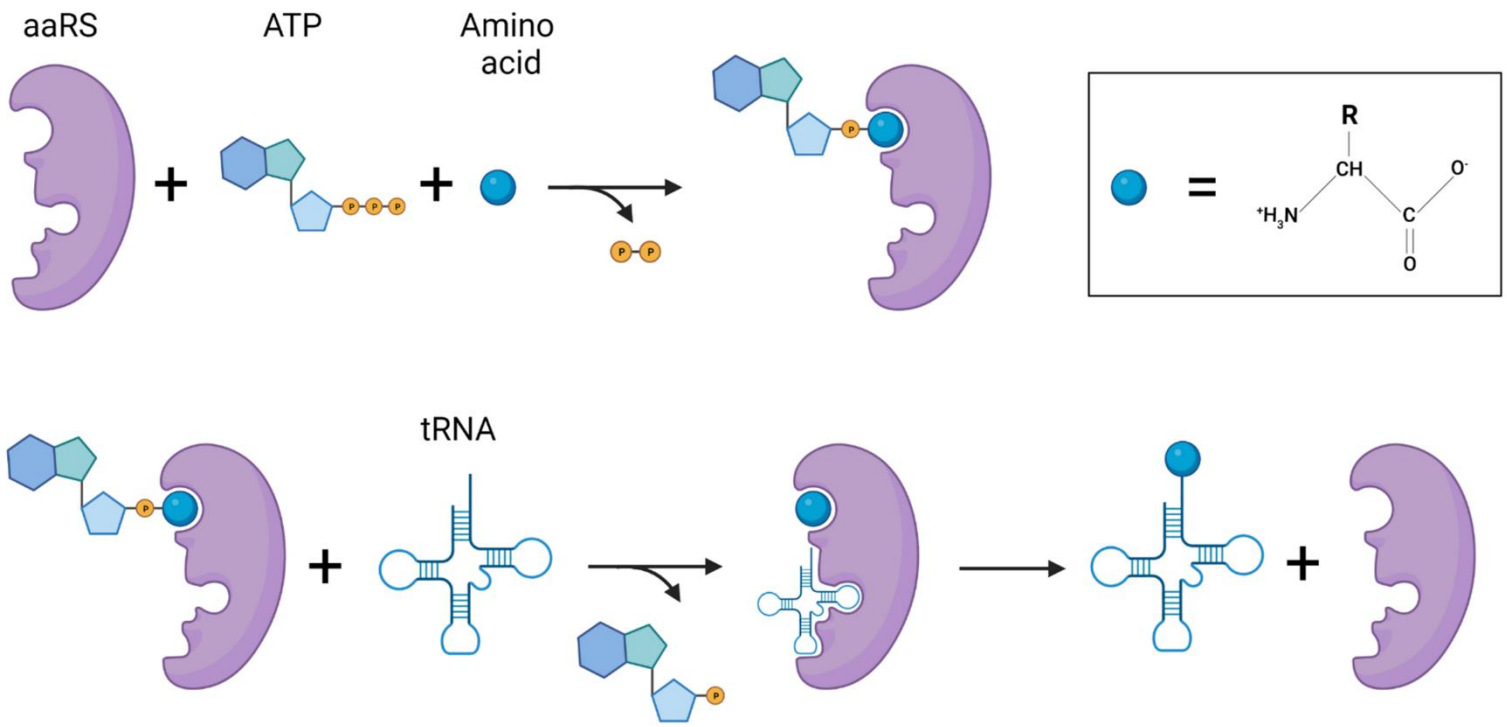

Figure 6. Transfer RNA aminoacylation. The charging of the amino acid onto the corresponding aminoacyl-tRNA synthetase (aaRS) releases a pyrophosphate from an ATP molecule. Then, the tRNA molecule is attached to the charged amino acid releasing an AMP molecule. Finally, the charged tRNA is released. The amino acid is represented as a blue sphere.

2.1.4. tRNA modifications.

Although a significant amount of tRNA modifications were discovered many years ago, the enzymatic machinery behind is still being identified [60,84]. These are modifications present in almost all tRNAs and others tRNA-specific [85]. Cytoplasmic and mitochondrial tRNAs can also show different modification patterns; for example, mammalian mt-tRNA$^{Ser(GCU)}$ lacks the complete D-arm and, hence lacks the characteristic dihydrouridine [86,87]. Moreover, environmental factors regulate the presence of some modifications that allow the cellular readjustment to a stress situation and promote the translation of specific transcripts [88-90].

tRNA modification location in the structure, stage of anchorage and chemical group properties will determine their function [91]. Modifications can be divided into two groups depending on its position through the L-shape structure, modifications in the tRNA body and modifications found in the anticodon-loop region. Modifications in the body usually play a structural and stabiliser role, helping to form the correct base-pairings and bending until the final shape [85,92]. On the other hand, the anticodon-loop region is a hotspot of highly diverse modifications. They can also be involved in tRNA structure; but they have particular relevance in translation, including accurate mRNA decoding, codon-anticodon pairing, reading frame maintenance, affinity for the ribosome and translation efficiency [93-95].

The great majority of modifications are found at positions 34 and 37 in the anticodon stem-loop. Francis Crick's Wobble hypothesis states that some tRNA can interact in a noncanonical base-pairing manner at position 34 with the third codon base [96]. Wobble position expands the initially proposed anticodon:codon pairing of the Universal Genetic Code [97]. A significant proportion of the cytosolic tRNAs have the position 34 modified, and some of them are conserved throughout all kingdoms of life [62,97]. Modifications at wobble position enhance, expand or contract the number of codons that anticodons recognise [98]. In eukaryotes, U in the wobble position of the mRNA can be decoded by A, G or I at position 34, and G34 or I34 can decode C in the mRNA. Meanwhile, A and G are only decoded by U and C, respectively [81,99,100]. It has been reported that the modification state at this position is sensitive to stress, operating as a detector of changes in the environment that stimulate the translation of particular codons present in mRNA transcripts of stress-response proteins [101].

Base 37 is also called the extended anticodon as it acts as a support for the anticodon presentation [102,103]. There have been proposed several roles for modifications in this position. Chemically, it has been described how tRNA anticodon structure is modulated by avoiding illicit intermolecular base-pairing and providing energetic stability and accuracy to the chemical bond between codon and anticodon [82,104]. This translates into a more stable interaction with the mRNA, increased efficiency in translation, prevention of frameshifting, and better tRNA recycling [97].

The so-called “circuits” refers to the dependence of some modifications on the previous presence of other ones establishing an order of introduction. This phenomenon has been well described in the anticodon-loop region. It has been hypothesised that those primary modifications can act as a recognition target or induce the folding in a recognisable structure for the subsequent modification enzyme or can avoid illicit base pairings maintaining the canonical anticodon-loop folding [105].

2.1.4.1. tRNA modification enzymes.

The tRNA modification enzymes can form macromolecular complexes to perform their function or act as a single protein (**Table 2**) [95]. They chemically alter the nucleotides through reactions of isomerization (pseudouridine formation), group addition (methyl-, formyl-, acetyl-, or more prominent groups such as isopentenyl- or threonyl carbamoyl groups) and group exchange (adenosine deamination into inosine) [43,89].

Transfer RNA modifiers require a specific tRNA architecture and sequence to incorporate the modification at the appropriate tRNA maturation stage. For instance, some enzymes require the presence, and others the removal, of the intron. The enzymes can base their specificity on the chemical nature of the target nucleoside, the location of the correct nucleoside, or the tRNA identity [89].

Table 2. Transfer RNA modifications. Functions of the modification and location where it is introduced are also described.

Modification*	Enzyme	Role	Localization	Ref.
G0	THG1L	$tRNA^{His}$ maturation. Translation fidelity.	Cytoplasm, mitochondria	[106-108]
m^{5}G0	BCDIN3D	$tRNA^{His}$ stability.	Cytoplasm	[109]
m^{1}G9	TRMT10A		Nucleus (nucleolus)	[110,111]
m^{1}A9	TRMT10B		Nucleus	[111]

m^{1}A/G9	TRMT10C, HSD17B10	tRNA structure.	Mitochondria	[74,112,113]
Ψ13	PUS7			[114]
acp^{3}U20**,** **acp**^{3}D20a	DTWD1, DTWD2			[115]
D20/a	DUS2		Nucleus, cytoplasm	[116-118]
m$^{2}{}_{2}$G26	TRMT1, TRMT1L	tRNA structure.	Nucleus	[119-121]
Ψ28	PUS1		Cytoplasm, mitochondria	[122]
m^{3}C32	METTL2A, METTL2B, DALRD3			[123,124]
m^{3}C32	METTL6		Cytoplasm, mitochondria	[123,125]
Y**m**32	FTSJ1, WDR6			[126,127]
m^{5}C34	NSUN2	tRNA stability.	Nucleus	[128-131]
m^{5}C34	NSUN3	Codon recognition and translation.	Mitochondria	[132-135]
hm^{5}C34	TET2		Nucleus	[136]
hm^{5}C34 **f**^{5}C34	ALKBH1	Expand codon recognition.	Nucleus, mitochondria	[131,133,134,137]
hm^{5}C**m**34 f^{5}C**m**34	FTSJ1		Cytoplasm	[126,131]
cm^{5}U34	ELP1-6	Translation efficacy.		[138-141]
mcm^{5}U34 (S)-mc**h**m^{5}U34	ALKBH8, TRMT112 TRMT9B, TRMT112	Efficiency of UGA decoding.	Cytoplasm	[140,142-150]
mcm^{5}**s**^{2}U34	CTU1, CTU2, URM1, MOCS3, ATPBD3, NFS1	Translation efficacy.	Nucleolar, cytoplasmic, mitochondria	[140,151-154]
τm^{5}U34	MTO1, GTPBP3	Ribosome progression.	Mitochondria	[155-157]
τm^{5}**s**^{2}U34	TRMU		Mitochondria	[156,158,159]
N**m**34	FTSJ1, WDR6			[126,127]
C**m**34	SNORD97, SNORD133	Prevent angiogenin-mediated cleavage.		[160]
I34	ADAT2, ADAT3	Modulate the pairing capacity of A34 containing codons.	Nucleus	[161,162]

Q34	QRTR1, QRTR2	Decoding. Circuit (m^5C38). Prevent angiogenin-mediated cleavage and frameshifting. Efficient translation.	Cytoplasm, mitochondria	[163-167]
i^6A37	TRIT1	Codon-anticodon interaction. Circuit (m3C32).	Cytoplasm, mitochondria	[104,168-170]
ms^2i^6A37	CDK5RAP1	Decoding fidelity.	Mitochondria	[171-173]
t^6A37	YRDC, KEOPS complex (GON7, LAGE3, OSGEP, TP53RK, TPRKB)	Translation regulation. Circuit (m^3C32).	Mitochondria	[174-177]
m^6t^6A37	TRMO			[178]
ms^2t^6A37	CDKAL1	Decoding AAG and AAA codons. Codon-anticodon interaction.	Cytoplasm	[179-182]
m^1G37	TRMT5	Diminished paucity at G37.	Mitochondria	[183-187]
imG-14 37	TYW1			[184]
yW-86 37	TRMT12	Ribosome frameshift.	Cytoplasm	[184,187]
yW-72 37	TYW3			[184]
OHyW*37	TYW5			[184,187]
OHyW37	TYW4			[184]
I37	ADAT1		Nuclear	[188]
m^5C38	TRDMT1		Cytoplasm	[189]
Ψ39	PUS3	Frameshift efficiency.		[190-192]
m^7G46	METTL1, WDR4	Ribosome progression.	Nuclear	[193-195]
m^5C48, **m^5**C49, **m^5**C50	NSUN2	Preventing angiogenin-mediated cleavage.	Cytoplasm, mitochondria	[129,130,135,196]
m^5U54	TRMT2A, TRMT2B		Nucleus, mitochondria	[197,198]
Ψ55	TRUB1		Nucleus	[199,200]
Ψ55	TRUB2		Mitochondria	[61,200,201]
Ψ54, **Ψ**55	PUS10		Cytoplasm	[200,202,203]

m^{1}A58	TRMT6, TRMT61A		Nucleus	[204]
m^{1}A58	TRMT61B	Circuit (enhances TRUB2).	Mitochondria	[200,205]
m^{5}C72	NSUN6		Cytoplasm	[206]

*****The modification added by the enzymes is highlighted in bold.

2.1.4.2. TRIT1.

TRIT1 gene encodes the enzyme tRNA-isopentenyltransferase-1 that transfers an isopentenyl group from a dimethylallyl pyrophosphate (DMAPP) to form the N^6-isopentenyladenosine (i^6A) at position 37 of some cytoplasmic and mitochondrial tRNAs in humans [93,168]. DMAPP that donate the isopentenyl chain is an intermediate of the mevalonate pathway [207].

Transfer RNA isopentenyltransferases are conserved through evolution; they are present in Bacteria and Eukarya [208]. Homologous tRNA isopentenyl transferase enzymes have been identified in bacteria (MiaA), yeast (Mod5 in *Saccharomyces cerevisiae*, *tit1* in *Schizosaccharomyces pombe*), plants (IPT2 in *Arabidopsis thaliana*), roundworm (GRO-1), and mammals (TRIT1) [209]. The first to be identified was Mod5 in $tRNA^{Ser}$ from *S. cerevisiae* in 1966 [210].

Human *TRIT1* gene was cloned in 2000. Golovko A et al. inferred the *TRIT1* sequence considering the conserved regions in known tRNA isopentenyl transferases such as Mod5 of *S. cerevisiae* (53% of protein homology) and MiaA of *E. coli* (47% of protein homology) [168]. They expressed the putative cDNA on a *S. cerevisiae* deficient in Mod5, and the modification was restored into the tRNAs [168]. Multiple alternative splicing isoforms of TRIT1 are expressed, but only the full-length mRNA isoform is biochemically active [211].

Transfer RNAs modified by TRIT1 in humans are cytoplasmic (cy) $tRNA^{[Ser]Sec}$ and $tRNA^{Ser(HGA)}$, and mitochondrial (mt) $tRNA^{Cys(GCA)}$, $tRNA^{Tyr(GUA)}$, $tRNA^{Trp}$, $tRNA^{Ser(UGA)}$, and $tRNA^{Phe(GAA)}$ (**Figure 7**) [61,104,170,212,213]. The determinants that predispose for TRIT1 modification in these tRNAs remain to be elucidated. Although, the relevance of the A36-A37-A38 recognition sequence has been described, not all tRNAs with this sequence are modified; therefore, other anticodon stem-loop determinants should be critical for the addition of the isopentenyl group by TRIT1 [170].

N^6-isopentenyladenosine modification can be further modified in 2-methylthio-N^6-isopentenyladenosine (ms^2i^6A) in four mitochondrial tRNAs (mt-$tRNA^{Tyr(GUA)}$, mt-$tRNA^{Trp}$,

mt-tRNA$^{Ser(UGA)}$, and mt-tRNA$^{Phe(GAA)}$) in mammalian cells (**Figure 7**) [104]. This conversion is carried out by the methylthiotransferase Cdk5 regulatory subunit associated protein 1 (CDK5RAP1) [171]. Ms^{2}i^{6}A modification is highly correlated with mitochondrial activity in mammals, particularly in tissues with a high-energetic demand [173,214]. I^{6}A and ms^{2}i^{6}A modifications, as also described for other modifications at position 37 of tRNAs, have a role in stabilising the AU codon-anticodon base pairs interaction and increasing the tRNA affinity for the ribosome, resulting in an enhancement of the reading frame maintenance during translation [215-217]. I^{6}A37 is a prerequisite for m^{3}C32 incorporation by AlkB Homolog 8, TRNA Methyltransferase (ALKBH8) on tRNA^{Ser} [103]. In bacteria, I^{6}A and ms^{2}i^{6}A are also modified into other ribonucleosides such as N^6-(cis-hydroxyisopentenyl) adenosine (io^{6}A), 2-methylthio-N^6-(cis-hydroxyisopentenyl) adenosine (ms^{2}io^{6}A), and 2-methylthiomethylenethio-N^6-isopentenyl-adenosine (msms^{2}i^{6}A) (**Figure 8**) [104,218,219].

In addition, other roles of TRIT1 have been demonstrated in *S. cerevisiae*. The TRIT1 homologue Mod5 is required for silencing near tRNA genes, in a tRNA-gene mediated (tgm) silencing mechanism [220]. Also, it has been shown that a cytotoxic T lymphocyte (CTL)–defined antigen that is derived from an open reading frame (ORF) sequence on the 3′-UTR of *TRIT1* gene sensitised melanoma cells to lysis [221].

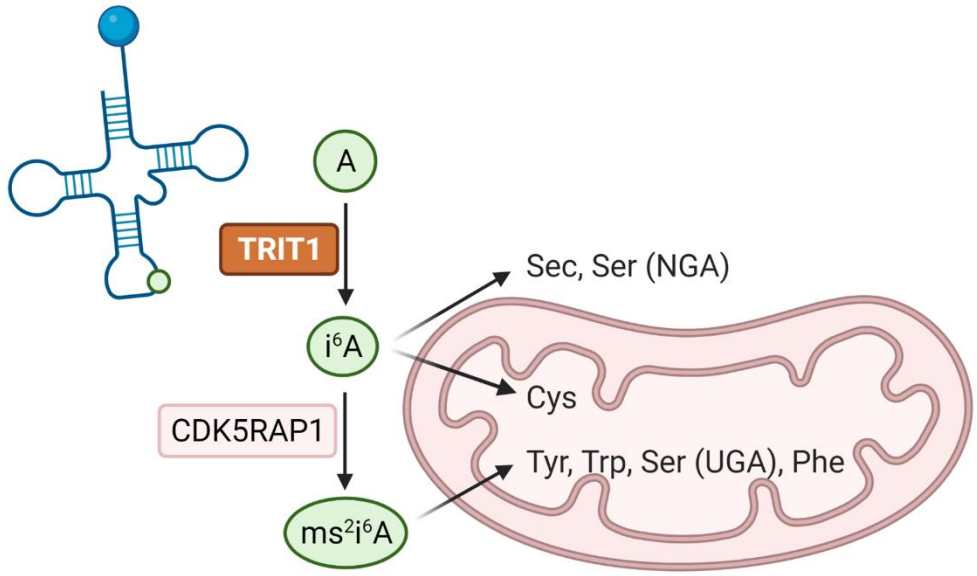

Figure 7. Transfer RNAs modified by tRNA-isopentenyltransferase-1 (TRIT1) in humans. A37 of cytoplasmic tRNA$^{[Ser]Sec}$ and tRNA$^{Ser(HGA);}$ and mitochondrial tRNA$^{Cys(GCA)}$, tRNA$^{Tyr(GUA)}$, tRNA^{Trp}, tRNA$^{Ser(UGA)}$ and tRNA$^{Phe(GAA)}$ is modified into i^{6}A37 by TRIT1. Additionally, mitochondrial tRNA$^{Tyr(GUA)}$, tRNA^{Trp}, tRNA$^{Ser(UGA)}$, and tRNA$^{Phe(GAA)}$ are further modified to ms^{2}i^{6}A by Cdk5 regulatory subunit associated protein 1 (CDK5RAP1). The green dot at the tRNA represents the adenosine 37.

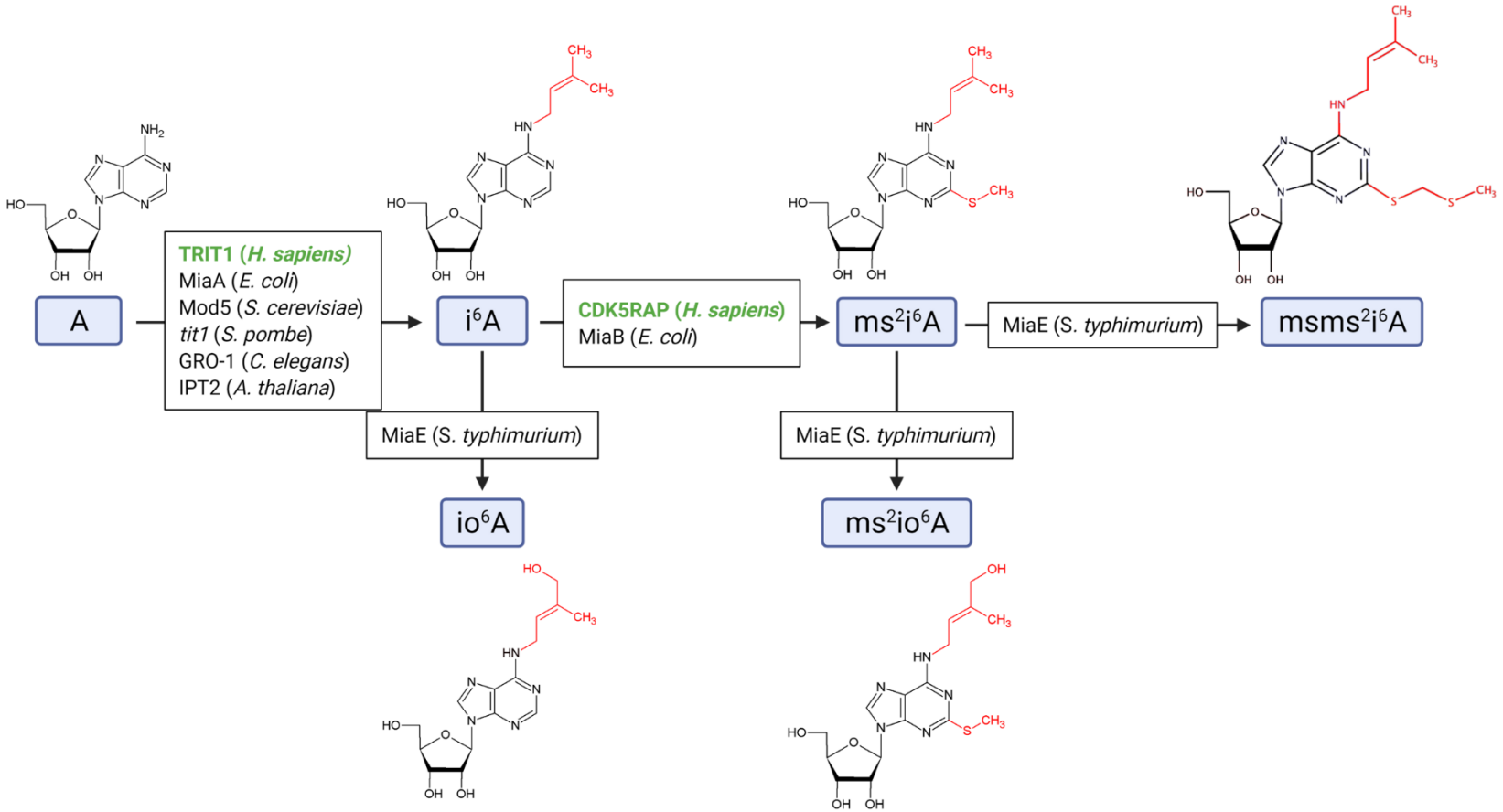

Figure 8. Transfer RNA isopentenyl transferase enzymes pathway. Representation of the hypermodifications that can suffer adenosine 37 starting witht isopentenylation. Enzymes involved in the different steps in various species are listed. Enzymes present in humans are highlighted in green.

2.1.4.2.1. Selenocysteine.

$tRNA^{[Ser]Sec}$ was the first tRNA described to contain i^6A37 in mammals [169,222]. $tRNA^{[Ser]Sec}$ carries the selenocysteine (Sec) amino acid that is incorporated in 25 proteins in humans called selenoproteins. Selenoprotein expression is reduced by TRIT1 knockdown as $tRNA^{[Ser]Sec}$ harbour the i^6A37 modification [169,222]. Selenocysteine contains a selenium atom in place of the sulphur atom of cysteine, and it is also called the 21st amino acid, which is considered a noncanonical amino acid as is decoded by the UGA stop codon. $tRNA^{[Ser]Sec}$ is encoded by the *TRU-TCA1-1* human gene on chromosome 19 and is 96 nucleosides long as its variable arm consists of 16 nucleosides (**Figure 9**) [223]. Despite being the largest tRNA in eukaryotes, it is only post-transcriptional modified in four bases. In the nucleus, m^1A at position 58 and ψ at position 55 are introduced. Studies in *Xenopus laevis* oocytes suggest that modification m^1A58 is required for Ψ55 formation, and Ψ55 influences the tertiary structure of $tRNA^{[Ser]Sec}$ [224]. Meanwhile, i^6A37 and 5-methoxycarbonylmethyl-uridine (mcm^5U) at position 34 are introduced by ALKBH8 in the cytoplasm. Mcm^5U34 base can be further methylated into 5-methoxycarbonylmethyl-2′-O-methyluridine (mcm^5Um34) by ALKBH8, and it requires the presence of i^6A37 modification. However, both $tRNA^{[Ser]Sec}$ isoforms coexist in the cell as this methylation reaction is not complete [224,225].

In contrast to canonical tRNAs, $tRNA^{[Ser]Sec}$ is not aminoacylated by an aaRS enzyme; instead, selenocysteine is synthesised in the tRNA following a process that involves several enzymes. First, the tRNA is conjugated with serine by the Seryl-tRNA Synthetase 1 (SARS1) enzyme. Then, it is phosphorylated to O-phosphoserine by Phosphoseryl-tRNA Kinase (PSTK). Finally, Sep (O-Phosphoserine) tRNA:Sec (Selenocysteine) tRNA Synthase (SEPSECS) converts the O-phosphoserine to selenocysteine incorporating a hydrogen selenide (HSe^-) (**Figure 10**) [223,226]. All selenoproteins contain a single Sec residue except from Selenoprotein P (SELENOP) that contains ten residues. SELENOP is secreted to plasma and distributes selenium from the liver, where it is mainly synthesised, to other tissues [223,227,228].

The HSe^- comes from a selenophosphate ($H_2SePO_3^{3-}$) generated from selenide by Selenophosphate 2 synthetase (SEPHS2), which is itself a selenoprotein [223]. Selenium is mainly incorporated in the body through plant diet in the form of selenomethionine (SeMet). The SeMet is absorbed over the intestinal transport channels and is stored in the methionine pool. SeMet can be incorporated into proteins in the position of methionine or be transsulfurated into Sec, predominantly in the liver. Sec is then

degraded by selenocysteine lyase (SCLY), producing selenide and alanine [227-229]. The selenocysteine residues from proteolytic degradation of selenoproteins are recycled by SCLY [230]. SCLY is especially important under selenium-deficient conditions for maintaining selenoprotein synthesis, and a selenoprotein hierarchy is created synthesising according to the cellular needs.

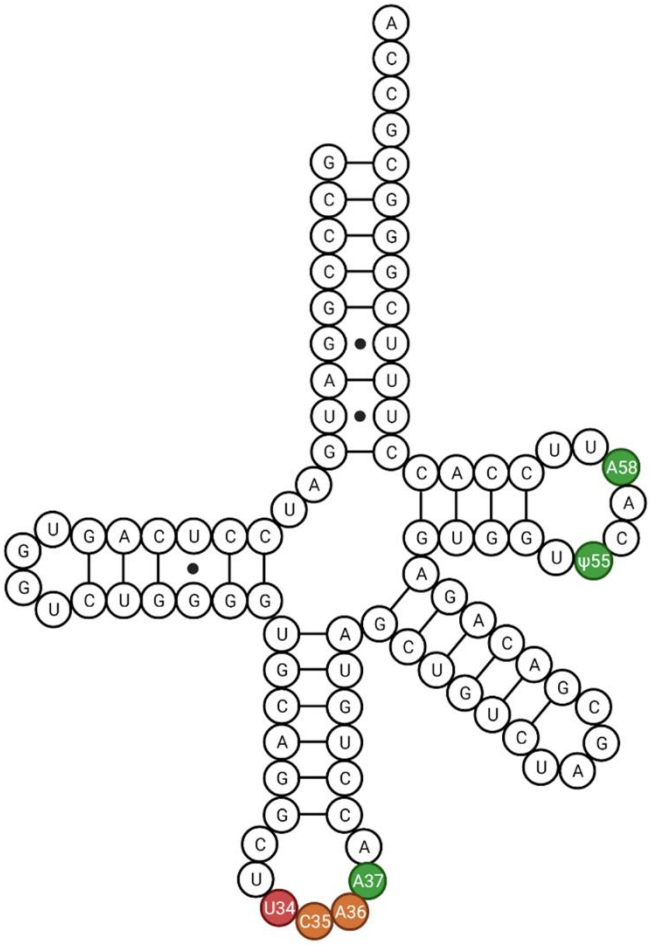

Figure 9. Selenocysteine tRNA. Modified nucleosides are coloured in green. The wobble base is coloured in red, and the remaining bases of the anticodon are coloured in orange.

Translation of the UGA codon as selenocysteine instead of functioning as a stop depends on selenocysteine insertion sequence (SECIS), an RNA secondary stem-loop structure in the 3′ UTR of the tRNA [231]. The mechanism is based on the binding of SECIS to Selenocysteine insertion sequence-binding protein 2 (SECISBP2), which recognises the T-loop and the variable arm, and the Selenocysteine-specific elongation

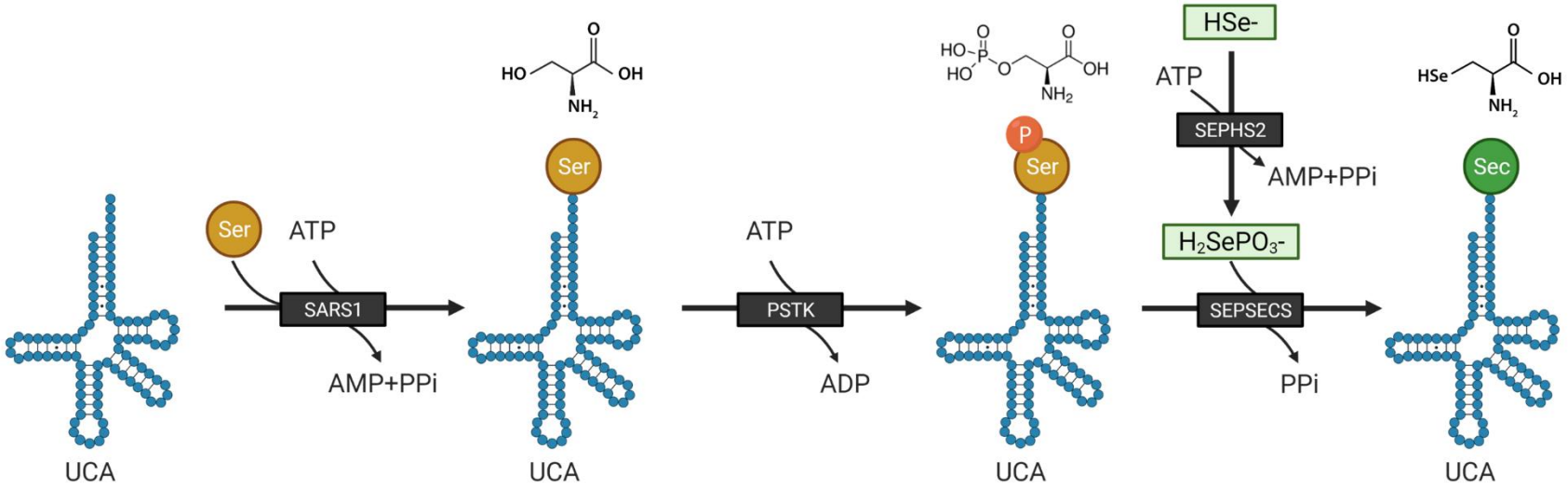

Figure 10. Selenocysteine tRNA aminoacylation. This process involves the sequential role of 3 enzymes: Seryl-tRNA Synthetase 1 (SARS1), Phosphoseryl-tRNA Kinase (PSTK) and Sep (O-Phosphoserine) tRNA:Sec (Selenocysteine) tRNA Synthase (SEPSECS) that charge and process an amino acid serine into a selenocysteine. Adapted from Vindry et al. 2018 [223].

factor (eEFSec), an analogue of the eIF component eEF1A, that specifically recruits the $tRNA^{[Ser]Sec}$ to the ribosome when UGA codon is present (**Figure 11**) [226]. The complete mechanism remains to be entirely well described, but other proteins involved include the translation initiation factor 4A3 (eIF4A3), nucleolin and ribosomal protein L30 (RPL30) [232]. Each selenoprotein has only one SECIS element in their mRNA, except SELENOP that has two to be able to translate the ten UGA codons that contain. Each SECIS sequence is distinct from the others and the characteristics of each SECIS element determines the decoding efficiency of each selenoprotein. Interestingly, all selenoproteins use UAA or UAG stop codons probably to avoid the wrong introduction of selenocysteine [223].

Selenoprotein translation can be modulated according to the cellular context. $tRNA^{[Ser]Sec}$ U34 modifications mcm^5U and mcm^5Um promote the translation of two different groups of selenoproteins. Mcm^5U34 allows the expression of housekeeping selenoproteins necessary for cell survival, and its expression is promoted in selenium-deficient conditions. Whereas mcm^5Um34 is responsive to the translation of stress-related selenoproteins, increases in oxidative stress and is stimulated by selenium supplementation [149,224,227,233]. These differences in translation seem to be related to the change in tertiary structure induced by the methyl group introduced by the ALKBH8 and TRMT12 enzymes [233,234]. Methylated isoform depends on i^6A modification as lack of i^6A modification causes effects similar to selenium deficiency and difficult the binding of the $tRNA^{[Ser]Sec}$ to the UGA codon because of inhibition of the maturation process [222,225,235].

ALKBH8 expression and, therefore, mcm^5Um modification is increased in response to ROS stress and is required to express stress-related selenoproteins as GPX1, GPX3, GPX6, MSRB1, SELENOT, SELENOW and SELENOP [149,223,227,228,235]. Meanwhile, TXNRD3 is a housekeeping protein, and GPX4 and TXNRD1 have been assigned to groups depending on the study [149,227,228,235,236]. Glutathione peroxidase (GPX) enzymes catalyse the reduction of oxidative stress in the organism, and the thioredoxin reductases (TXNRD) regulate thiol redox status by reducing thioredoxin [237-239].

Deficiencies in $tRNA^{[Ser]Sec}$ expression have been linked to reduced levels of selenoproteins, seizures and a variety of other symptoms in mouse models (being even lethal) and human patients [104,236]. Mutations in protein genes implied in the

selenocysteine pathway such as ALKBH8 and SEPSECS cause intellectual disability, cerebellocerebral atrophy and seizures, and selenoprotein synthesis reduction [223,240].

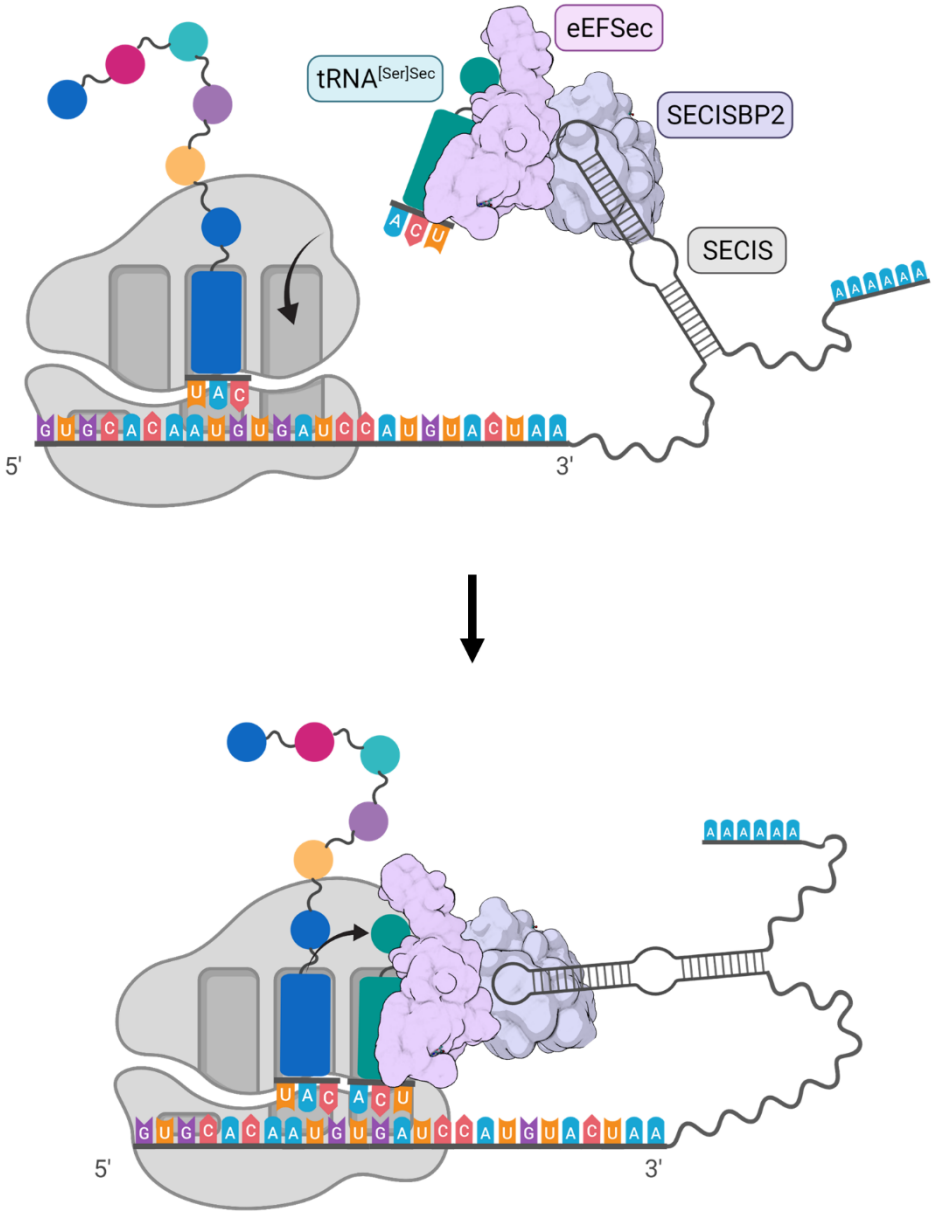

Figure 11. UGA codon translation into selenocysteine in eukaryotes. A complex formed by the tRNA[Ser]Sec, eEFSec and SECISBP2 binds to the SECIS sequence of the selenoprotein mRNA. Once the UGA codon should be translated, the tRNA[Ser]Sec is inserted at the corresponding pocket of the ribosome. Adapted from Vindry et al. 2018 [223].

2.2. Epitranscriptomic diseases.

RNA modifications can be introduced co-transcriptionally in the nucleus or post-transcriptionally in the nucleus, the cytoplasm and the mitochondria. Each modification is specifically inserted on a determined localisation and order, as sometimes sequential circuits of modifications are required. This process is rigorously regulated, and alterations in homeostasis have been associated to disease. It has been demonstrated that single nucleotide polymorphisms (SNPs) and alterations in epitranscriptomic genes are associated with development, immune, neurologic, mitochondrial and metabolic diseases, as well as cancer [50,62,85,241-243].

Disruption of the RNA modification and processing has been proved to affect the development and, specifically, neuronal development [244]. For example, FtsJ RNA methyltransferase 1 (FTSJ1) is highly expressed in the brain during foetal development [245], and both loss-of-function mutations and duplication of the gene cause mild dysmorphic features [126,246].

Mitochondrial RNA modification defects can generate a slippery-slope effect starting from a deficiency in protein synthesis and ending in diminished ATP production and increased superoxide levels [247]. Several mutations in RNA modifiers can cause mitochondrial encephalomyopathy, lactic acidosis and stroke-like episodes (MELAS) and myoclonus epilepsy with ragged-red fibres (MERRF), diseases with a neuronal-mitochondrial profile. Homozygous pathogenic mutations in *TRIT1* have been reported in eight patients from six unrelated families [216,248-250]. The consequent i^6A37 hypomodification of cytoplasmic and mitochondrial tRNAs has been associated with neuronal disorders. Patients show microcephaly, neurodevelopmental delay, myoclonic epilepsy, and oxidative phosphorylation deficiencies [250]. Lack of i^6A modification will also avert the presence of ms^2i^6A on mitochondrial tRNAs affecting the translation of mitochondrial respiratory chain subunits (complex I, III and IV), jeopardising the correct respiratory complex assembly decreasing oxidative phosphorylation [104]. Moreover, mutations on TRIT1-target tRNAs also can impair isopentenyl incorporation, causing the described disorders [104,216].

Regarding metabolic diseases, the link between CDK5 regulatory subunit associated protein 1-like 1 (CDKAL1) and type 2 diabetes has been well described [182,251]. Reduced CDKAL1 expression, results in reduced levels of 2-methylthio-N^6-threonylcarbamoyladenosine (ms^2t^6A) at position 37 of $tRNA^{Lys3}$ that stack to the wobble

codon AAG. The correct decoding of this codon is essential for the proinsulin processing, thus, reduced levels of CDKAL1 cause a decrease in insulin secretion in β-cells that lead to the development of diabetes [182].

Furthermore, several RNA modifiers have been related to different types of cancer. Some act as tumour suppressor genes and others as oncogenes, even they can work one way or another depending on the tumour type. An antiangiogenic and proapoptotic effect of the TRIT1 product i^6A has been described in various tumours. In *in vitro* studies in glioma, CDK5RAP1 abrogated the antitumour effect of i^6A by converting i^6A to ms^2i^6A [207,214]. Also, CDK5RAP1 deficiency inhibits tumour growth in human breast and melanoma cell lines acting over cell cycle arrest and apoptosis via the reactive oxygen species (ROS) pathway [252,253]. Additionally, Spinola et al. detected the downregulation of TRIT1 expression in lung adenocarcinoma patients [211]. Nevertheless, it could not be proved to have an *in vivo* antitumoural activity in nude mice [254].

II. OBJECTIVES

II. OBJECTIVES

The main objective of this thesis was to identify a cancer-specific genetic or epigenetic alteration occurring in a gene encoding an epitranscriptomic enzyme, and how this alteration could promote tumorigenesis, as well as to assess its potential as putative druggable target for cancer treatment. For this aim, the following specific objectives are proposed:

1. Identify genes encoding tRNA modifying enzymes disrupted by copy number alterations or promoter-associated CpG aberrant methylation in cancer through the comprehensive study of a panel of molecularly well-characterised cancer cell lines.
2. Evaluate the impact of the identified genetic or epigenetic alteration in gene expression in cancer cell lines and validate the findings in cancer patients.
3. Investigate the biological function of the candidate gene in the context of cancer through *in vitro* functional assays in cancer cell lines and *in vivo* experiments in murine models.
4. Elucidate associations between the alteration status of the candidate gene and the response to a defined set of drugs in a panel of cancer cell lines, and validate the findings in murine models.

III. MATERIALS AND METHODS

III. MATERIALS AND METHODS

1. Cell lines.

For this study, NCI-H82 (American Type Culture Collection, ATCC), DMS273 (Sigma-Aldrich, St. Louis, MO, USA), HCC-33 (Leibniz Institute DSMZ (Jena, Germany)-German Collection of Microorganisms and Cell Cultures) and NCI-H1694 (ATCC) human small-cell lung cancer (SCLC) cell lines; HEK273 (ATCC) human embryonic kidney cell line; and HCT-116 (ATCC) human colon cancer cell line were used. NCI-H82, HCC-33 cell lines were cultured with Roswell Park Memorial Institute (RPMI1640, Gibco) medium; DMS273 cell lines was cultured with Waymouth (Gibco) media; NCI-H1696 was cultured with HITES (Gibco) medium; and HEK293 and HCT-116 was cultured with Dulbecco's Modified Eagle's Medium (DMEM). Culture medium were completed with 10% of Foetal Bovine Serum (FBS, Gibco, Waltham, MA, USA) and 1% of penicillin/streptomycin (Invitrogen, Carlsbad, CA, USA). Cell were cultured at 37ºC with 5% (v/v) of CO_2. All cell tested negative for mycoplasma.

2. Human samples.

DNAs isolated from tumour samples of 39 SCLC patients obtained between 1975 and 2010 at the National Cancer Center Hospital/National Cancer Center Biobank (Tokyo, Japan), Saitama Medical University (Saitama, Japan), and the University of Tsukuba (Ibaraki, Japan) were used in this study. The study was approved by the corresponding Institutional Review Boards [255].

3. Fluorescence *in Situ* Hybridization (FISH).

The UCSC genome browser was used to select the 1p34.2 region probe RP11-613D14 for TRIT1 detection. Bacterial artificial chromosome (BAC) clones were obtained from the BACPAC Resources Center at the Children's Hospital Oakland Research Institute (Oakland, CA, USA). Probe was labelled with Spectrum Red dUTP (Abbott, Chicago, IL, USA) and CGH Nick Translation Kit with control DNA (MPE 600, Abbott, Chicago, IL, USA). FISH was performed on cells fixed in Carnoy's solution. The sample and probe were codenatured by heating slides on a hotplate at 75 °C for 2 min. After that, they were hybridized with 5 µL of handmade probe mixture (BAC RP11-613D14, 1p34.2/TRIT1) or control (D-5099-100-OG, MetaSystems, 1p32.3) and incubated in a humidified chamber at 37°C overnight. Post-hybridization washes of hybridized slides were performed first

with 0.4X SSC (pH 7.0) at 72 °C for 2 min followed by a wash in 2X SSC, 0.05% Tween-20 (pH 7.0) at room temperature for 30 seg. Finally, slides were counterstained with ',6-diamidino-2-fenilindol (DAPI, D8417, Sigma Aldrich) and analysed under a fluorescent microscope (NIKON, Eclipse E400).

4. Cell lines DNA extraction.

DNA was extracted from cell pellets by incubating them with lysis buffer (10mM Tris-HCl, pH=7.4; 10mM EDTA; 200mM NaCl; 1% SDS, 0.4 mg/ml proteinase K (EO0492, Thermo Scientific)) overnight at 37ºC and inactivating the proteinase K for 15 min at 75ºC. Lysate was treated with 0.03mg/ml RNase, washed with 1.5M NaCl and centrifuged 5 min at 13000 rpm. Supernatant was collected and DNA was precipitated with isopropanol. DNA was centrifuged 15 min at 4ºC at maximum speed and washed with 70% ethanol. The dried pellet was resuspended in water.

5. Multiplex Ligation-Dependent Probe Amplification (MLPA).

MLPA assay in DNA samples from SCLC patients and cell lines were performed by qGenomics (Spain) using two probes for exons 4 and 9 of the TRIT1 gene. RAC1 (exon 6), TBCK (exon 15), TRPM7 (exons 17 and 18), and TRIP12 (exons 3 and 11) probes were used as references. MLPA ratios were calculated according Coffa J and van der Berg J, 2011 [256].

6. RNA extraction.

Total RNA was purified using Maxwell RSC simplyRNA Tissue kit (AS1340, Promega, Madison, WI, USA) with the Maxwell RSC display (Promega, Madison, WI, USA) according to the manufacturer guidelines.

7. Real-time quantitative PCR (RT-qPCR).

RNA concentrations were measured with a Nanodrop (Thermo Scientific, Waltham, MA, USA). About 1.5 µg of RNA were reversed transcribed into cDNA using the RevertAid First Strand cDNA Synthesis Kit (K1622, Thermo Scientific).

Real-time PCR reactions were performed using SYBR green PCR Master Mix (Thermo Scientific), specific primers for the region of interest (**Table 3**) and corresponding cDNAs. *HPRT1* expression was used as endogenous control. Reaction was run in the QuantStudio 5 Real-Time PCR System (Thermo Scientific). Three biological replicates were assessed for each experiment.

Fold change (FC) between samples was determined through the algorithm $2^{-\Delta\Delta Ct}$. ΔCt was calculated normalizing with the endogenous control. Then, ΔΔCt was determined relativizing against the control. Relative expression was calculated as the square of –ΔΔCt.

ΔCt= $\bar{x}$ sample Ct - $\bar{x}$ endogenous Ct

ΔΔCt= sample problem ΔCt - $\bar{x}$ reference sample ΔCt

$FC=2^{-\Delta\Delta Ct}$

FC were statistically compared using a two-tailed unpaired t-test and plotted in Graphpad Prism 5 (Version 5 for Windows, GraphPad Software, La Jolla, CA, USA).

Table 3. List of RT-qPCR primers used in the study. TRIT1 primers 1 were used for the analysis of cells cultured *in vitro* and primers 2 were used for the analysis of DMS-273-derived tumours in order to avoid the amplification of TRIT1 transcripts from mice.

Primer IDs	Sequence (5'-3')
TRIT1 F1	CTCCATGCAGGTCTATGAAG
TRIT1 R1	ATCTTCAATCAGAGCAGTTGC
TRIT1 F2	AATGGGCAGCGCACA
TRIT1 R2	CCTTCTCTTTAGGTTCTTTGTTATG
ID1 F	ACGTGCTGCTCTACGACAT
ID1 R	TCCGAGTTCAGCTCCAACTGA
ID3 F	TGACACCTCCAGAACGCA
ID3 R	CAGGTTTAGTCTCCAGGAAG
COL3A1 F	GTGCTAAGGGTGAAGTTGGA
COL3A1 R	CCAGGACTACCATTAATCCCA
MT1X F	GCTTCTCCTTGCCTCG
MT1X R	CTGACGTCCCTTTGCAG
LAMA4 F	GCCAAGAACTGTGCAGTGTG
LAMA4 R	AGCTTATGGTTGGGCAGTCC
ANGPTL4 F	CAGCCTGCAGACACAAC
ANGPTL4 R	CTGGCTTTGCAGATGC
GPX4 F	CCAGTGAGGCAAGACCG
GPX4 R	CGGCGAACTCTTTGATCT
HPRT1 F	TGACACTGGCAAAACAATGCA
HPRT1 R	GGTCCTTTTCACCAGCAAGCT

Abbreviations: F, Forward; R, Reverse

8. Western blot.

Cell pellets were resuspended in RIPA buffer (0.1% SDS, 50 mM Tris-HCl [pH 7.4], 150 mM NaCl, 1 mM EDTA, 1% NP-40, 12.23 mM deoxycholic acid) containing protease and the cOmplete™ (Roche, Basel, Switzerland) phosphatase inhibitor cocktail, then

incubated for 20 min on ice. The tubes were centrifuged for 5 min at 13,000 rpm, and the supernatant was collected. RIPA extracts were quantified using the Pierce™ BCA Protein Assay Kit (Thermo Scientific). Each sample was diluted 1:6 in water and 10 µL of each sample were loaded in triplicate into a 96-well plate. A standard curve of albumin was performed to determine protein concentration. Kit reagents were prepared and loaded according to the manufacturer's instructions. After 30 min, the 96-well plate was read at 562 nm.

Protein expression was analysed by Western blot. SDS-PAGE was performed on acrylamide gels with a variable acrylamide percentage in a range of 8-15% depending on the molecular weight of the protein. Membranes were blocked with 5% skimmed milk (232100, BD Difco) in 0.1% Tween-20 in PBS (PBS-Tween) during 1 h with shaking. Next, membranes were incubated overnight at 4 °C with the primary antibody (**Table 4**). Afterwards, membranes were washed three times with PBS-Tween and incubated with the secondary antibody for 1 h with shaking. Membranes were washed three times with PBS-Tween and developed using Luminata HRP-substrates (Millipore, Burlington, MA, USA). As a loading control, membranes were incubated with β-actin (Actin) HRP-conjugated antibody.

Table 4. List of antibodies used in this study.

Antibody	Dilution	Brand	Reference
Actin–HRP	1:5000	Sigma Aldrich	A3854
CDN1A	1:1000	Cell Signaling Technology (CST)	#2947
EIF2AK3	1:1000	CST	D11A8
ERO1A	1:1000	CST	#3264
GAPDH	1:1000	Trevigen	2275-PC-100
GPX4	1:1000	Abcam	ab125066
HSPA5	1:1000	CST	#3177
Lamin B	1:5000	Abcam	ab16048
OXPHOS cocktail	1:1000	Thermo Scientific	45-8199
TRIT1	1:1000	Novus Biologicals	NBP2-20727
Anti-rabbit HRP	1.10000	Sigma Aldrich	A0545
Anti-mouse HRP	1:5000	GE Healthcare	NA9310

9. Immunocytochemistry.

Cells were seeded on Shi-fix coverslips (SB-Shifix50, Shikar Biotech) in a 12 wells-plate. After 30 min in culture to allow cell attachment, unbound cells were washed with PBS.

Next, cells were fixed with 4% paraformaldehyde (15710-S, Electron Microscopy Sciences, Hatfield, PA, USA) for 15 min, washed with PBS and permeabilizated with 0.5% Triton X-100 (Sigma Aldrich) for 10 min. After blocking with 5% BSA (A7906, Sigma Aldrich) diluted in PBS for 2 h, cells were incubated overnight at 4 ºC with TRIT1 antibody (NBP2-20727, Novus Biologicals, 1:200 dilution in 5% BSA in PBS). Afterwards, coverslips were washed three times with PBS and incubated with Alexa Fluor 488 Donkey anti-Rabbit (A21206, Thermo Scientific, 1:5000 in 5% BSA in PBS). Finally, cells were washed, counterstained with DAPI (D8417, Sigma Aldrich) and analyzed under a confocal microscope (Leica TCS SPE).

10. TRIT1 overexpression.

The isoform 1 of TRIT1 gene (NM_017646.6) was cloned into the lentiviral expression vector pLVX-IRES-tdTomato (631238, Takara) through EcoRI and NotI restriction endonuclease sites (**Table 5**). PCR products were purified using Nucleospin columns (740609.250, Macherey-Nagel) after agarose gel electrophoresis. PCR products and vector backbones were enzymatically digested, purified and mixed using the following criteria: 1 µl T4 DNA ligase, 1 µl T4 buffer 1X, 50 ng of vector backbone and ng of insert according to the following formula:

ng of insert= [(3 x bp of insert) x 50ng of vector] / bp of vector

Competent bacteria *E. coli* DH5α (Thermo Scientific) were transformed with pLVX-IRES-tdTomato plasmids through thermal shock (42ºC 1 min followed by 2 min on ice). Bacteria were grown during 1h at 37ºC in agitation with 1ml of ampicillin-free LB media. Then, bacteria were seeded in ampicillin + LB Petri dishes. Bacteria colonies were analysed by PCR to confirm the plasmid incorporation. At least 6 clones were purified by miniprep and sequenced to select the plasmid containing the correct sequence.

To obtain the lentiviral particles, 10 µg of plasmid were mixed with 7.5 µg of ps-PAX2 and 2.5 µg of PMD2.G plasmid (Addgene, Watertown, MA, USA), using jetPRIME® Transfection Reagent (Polyplus Transfection, New York, NY, USA). The transfection mix was added to HEK293 cells grown at 80% confluence. After 72 h, medium with high-titer lentiviral particles was 0.45 µm-filtered and cells were cultured in virus-containing medium for 24 h. After five passages, red-fluorescent cells were sorted by fluorescence-activated single cell sorting (FACS).

Table 5. Primers used for TRIT1 cloning.

Primers IDs	Sequence (5'-3')
TRIT1 EcoRI F	aaaaaaaaGAATTCGCCGCCACCATGGCGTCCGTGGCGGCTGCACG
TRIT1 NotI R	aaaaaaaaGCGGCCGCTTAAACGCTGCATTTCAGCTCTTGATCATTCTGCCCTGG

Abbreviations: F, Forward; R, Reverse

11. Short-hairpin RNAs.

Lentiviral plasmids for TRIT1 human shRNA (TL300819, Origene, Rockville, MD, USA) and scrambled shRNA (TR30021, Origene, Rockville, MD, USA), both cloned in pGFP-C-shLenti vector, were used. To obtain the lentiviral particles, 10 µg of plasmid were mixed with 7.5 µg of ps-PAX2 and 2.5 µg of PMD2.G plasmid (Addgene, Watertown, MA, USA), using jetPRIME® Transfection Reagent (Polyplus Transfection, New York, NY, USA). The transfection mix was added to HEK293 cells grown at 80% confluence. After 72 h, medium with high-titer lentiviral particles was 0.45 µm-filtered and DMS-273 cells were cultured in virus containing medium for 24 h. After five passages, green-fluorescent cells were sorted by fluorescence-activated single cell sorting (FACS).

A shRNA designed against the Tomato fluorescent protein (shT1, CGCTGATCTACAAGGTGAA) and cloned into the pLVXshRNA2 vector was also used.

12. Minipreps and maxipreps.

Minipreps were performed in 96-well plates using the NucleoSpin® Plasmid kit (22740625.24, Cultek), and maxipreps using Plasmid DNA Maxiprep Kit (K2100-17, Thermo Scientific), both following manufacturer's instructions. In brief, transformed bacteria were grown at 37ºC overnight. Then, bacteria were pelleted by centrifugation, resuspended, lysed and neutralized. After that, the eluted product was purified using columns to retain the plasmid. Then, plasmids were washed, precipitated and resuspended in water. In case of 96-plated miniprep products, they were further purified before sequencing.

13. N^6-Isopentenyladenosine (i^6A) quantification.

Cells were lysed using TRI Reagent (T9424, Sigma Aldrich) and phase separation was performed with 1-bromo-3-chloropropane. The mixture was centrifuged in order to obtain the aqueous phase and the RNA was precipitated with 2-isopropanol. RNA pellets were washed with 70% ethanol, dried, and resuspended in water. RNA concentration was

measured with a Nanodrop (Thermo Scientific) spectrophotometer. Modification status of A37 was finally determined by liquid chromatography–mass spectrometry (LC/MS).

14. Measurement of ms^2i^6A modification in mitochondrial tRNAs by RT-q PCR.

This analysis was performed according to Wei and Tomizawa (2016) (**Figure 12**) [257]. First, two independent mixtures of 25 ng of RNA with the R1 or R2 reverse primer (10 µM) (**Table 6**) were denatured at 65 °C for 10 min and put on ice. Then 5X buffer, RNase inhibitor, dNTP Mix and enzyme from the RevertAid First Strand cDNA Synthesis Kit (K1622, Thermo Scientific) were added to each mixture, and the reverse transcription reaction was performed at 55 °C for 30 min followed by inactivation at 85°C for 5 min.

For the quantitative PCR, 2 µL of the obtained cDNA were mixed with the forward F1 and the reverse R1 primers (10 µM) (**Table 6**) and the SYBR Green PCR Master Mix (Thermo Scientific). Reactions were run in the QuantStudio 5 Real-Time PCR System (Thermo Scientific).

Ct values from samples (R1) and (R2) were obtained and represented the total tRNA level and ms^2i^6A modification level in individual tRNA, respectively (**Figure 12**). The normalized modification level in any RNA sample was calculated as ΔCt = Ct (R2) - Ct (R1) because the ΔCt value reflects the modification level [180].

Table 6. List of primers for ms^2i^6A quantification used in this study.

Primer IDs	Sequence (5'-3')
$tRNA^{Phe}$ F1	CTCCTCAAAGCAATACACTG
$tRNA^{Phe}$ R1	AGCCCGTCTAAACATTTTCA
$tRNA^{Phe}$ R2	GGGTGATGTGAGCCCGTCTA
$tRNA^{SerUCN}$ F1	GAGGCCATGGGGTTGG
$tRNA^{SerUCN}$ R1	CCCAAAGCTGGTTTCAAGC
$tRNA^{SerUCN}$ R2	AATCGAACCCCCCAAAGC
$tRNA^{Trp}$ F1	GGTTAAATACAGACCAAGAGC
$tRNA^{Trp}$ R1	CAACTTACTGAGGGCTTTGAA
$tRNA^{Trp}$ R2	TTAAGTATTGCAACTTACTGAGG
$tRNA^{Tyr}$ F1	GCTGAGTGAAGCATTGGACT
$tRNA^{Tyr}$ R1	AACCCCTGTCTTTAGATTTACA
$tRNA^{Tyr}$ R2	AGAGGCCTAACCCCTGTCTT

Abbreviations: F, Forward; R, Reverse

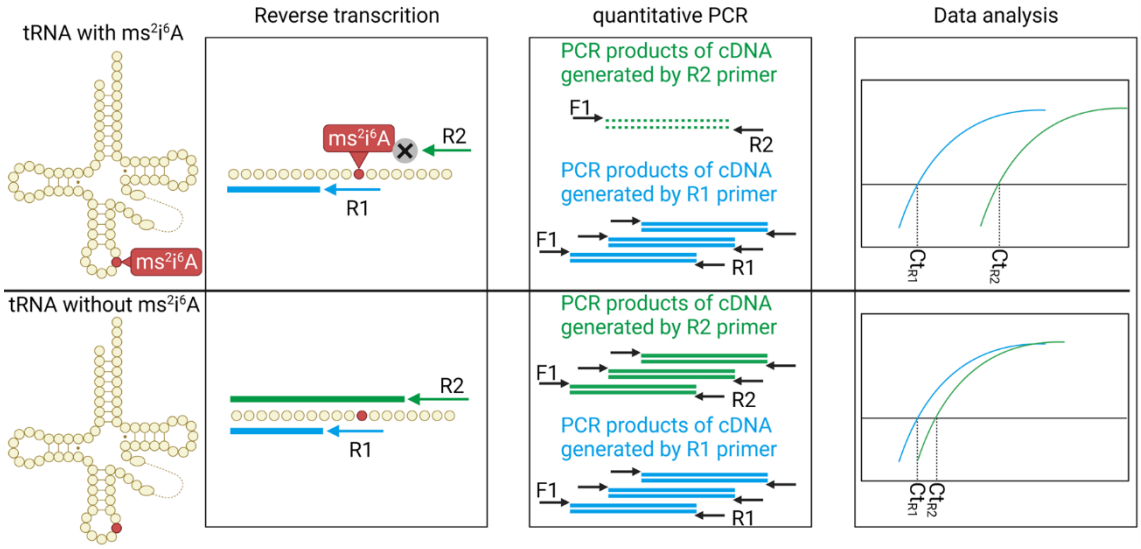

Figure 12. Workflow of the approach to detect ms^{2}i^{6}A modification. The mitochondrial tRNA is reversely transcribed by R1 primer and R2 primer, respectively. Because of the inhibitory effect of ms^{2}i^{6}A-modification to the reverse transcription, the amount of cDNA generated by R2 primer (Green lines) highly depends on the ms^{2}i^{6}A levels in each RNA sample. On the other hand, the cDNA generated by R1 primer (Blue lines) is independent of ms^{2}i^{6}A level, and is used as an internal control. The amount of each cDNA is quantified by a subsequent quantitative PCR (qPCR) using F1 and R1 primers. Adapted from Wei and Tomizawa 2016 [257].

15. Cell proliferation assay.

Cell proliferation was assessed by the MTT (3-(4,5-dimethyl-2-thiazolyl)-2,5-diphenyl-2H-tetrazolium bromide, M2128-10G, Sigma-Aldrich) assay. 3000 cells per well were seeded in 96-well plates. On 4 consecutive days, cells were treated with 10 µl of 5mg/ml MTT reagent. After 3 h of incubation at 37°C, cells were lysed for about 20 h with MTT lysis buffer (50% N,N dimethylformamide (161785.1612, PanReac AppliChem, Barcelona, Spain), 20% sodium dodecyl sulphate (A2572,1000, PanReac AppliChem), 2.5% glacial acetic acid (1.00063.2500, Merck, NJ, USA), 2.1% 1N HCl, at pH 4.7). Viable cells with active metabolism convert MTT into formazan leading to a colorimetric change from yellow to purple. Thus, the measured absorbance with an optical spectrometer at 560 nm is proportional to the number of viable cells. The mean absorbance of day 1 was taken as a reference and the following days were relativized according to it.

16. Colony assay.

Two hundred DMS-273 cells were seeded in 6-well plates in triplicate. Cells were cultured at standard conditions (37°C, 5% (v/v) CO_2) for 2 weeks. Then, culture media was removed, and cells were fixed with cold 100% methanol (200-659-6, Alcoholes Gual). After 10 minutes at room temperature, the methanol was aspirated, and 0.5% crystal violet (C3886-25G, Sigma Aldrich) diluted in methanol was added. Cell were incubated for 1 h at room temperature to allow staining of the colonies. After 3 washes with 1X PBS, the colonies were dried at room temperature. Finally, digital images were taken using the Hp Scanjet 4890 scanner, and colonies were counted using the ImageJ program (U. S. National Institutes of Health, Bethesda, Maryland, USA).

17. DNA content measurement for cell cycle analysis.

$1x10^7$ cells were collected and individualized in PBS, and fixed with 70% cold ethanol for at least 2 hours at -20ºC. Ethanol was decanted after centrifugation, and cells were washed with PBS. Then, cells were stained with 1 ml Propidium iodide (PI)/Triton X-100 staining solution containing 0.1mg PI (Sigma Aldrich), 0.1% (v/v) Triton X-100 (Sigma Aldrich), and 0.2 mg of DNase-free RNase A (10109169001, Sigma Aldrich)) for 15 min at 37°C. Cell fluorescence was measured with a flow cytometer set up for excitation with blue light (488-nm argon ion laser line) and detection of PI emission at red wavelengths (>600 nm filter). Data was analysed using the DNA content frequency histogram deconvolution in the FlowJo software v10.5.3 (BD Corporation, NJ, USA) and GraphPad Prism (Version 5 for Windows, GraphPad Software).

18. Apoptosis assay with Annexin V.

Cell viability was analysed using APC Annexin V Apoptosis Detection Kit (640930, Biolegend, San Diego, CA, USA), and DAPI (D8417, Sigma Aldrich) was used for the quantification of early and late apoptotic cells. DMS-273 cells were treated with 1uM of staurosporine (S4400, Sigma Aldrich) for 24h as positive control. DMS-273 cells without any treatment were used as negative control.

$5x10^5$ cells were collected and washed with Cell Staining Buffer and resuspended in Annexin V Binding Buffer. Cells were stained with 2.5 µl of APC Annexin V and 5 µl of PI for 15 min at room temperature in the dark, and 400 µl of Annexin V Binding Buffer were added. Cells were analysed by flow cytometry (FACS Canto, BD Biosciences). APC was analysed with an excitation wavelength of 633 nm and the FL6 detector (660/20 nm) was used for the emission wavelength. Meanwhile, DAPI was analysed with an excitation

wavelength of 405 nm and the FL9 detector (450/40 nm) was used for the emission wavelength. 10,000 cells were analysed for each sample. Data was analysed using the FlowJo software v10.5.3 (BD Corporation) and GraphPad Prism (Version 5 for Windows, GraphPad Software).

19. Senescence-associated β-galactosidase assay.

5×10^4 cells were seed in a 6-well plate and culture for at least 2 days. Then, cells were washed with PBS and fixed with 4% formaldehyde (28908, Thermo Scientific) for 3 min at room temperature. Cells were washed and stained with 2 ml of the SA-βgal staining solution (1 mg/mL 5-bromo-4-chloro-3-indolyl-beta-d-galactopyranoside (X-gal, BIMB1001-5G, Apollo Scientific Limited), 1X citric acid/sodium phosphate buffer (pH 6.0), 5 mM potassium ferricyanide, 5 mM potassium ferrocyanide, 150 mM NaCl, 2 mM $MgCl_2$) for 15 hours at 37ºC. Cells were washed with PBS and the blue SA-βgal-positive cells were counted under a microscope.

20. *XBP1* splice assay.

The XBP1 sequence from the cDNA of DMS-273 SCR and DMS-273 shTRIT1 cell lines were PCR-amplified using the primers XBP1 F (GCCAAGGGGAATGAAGTGAG) and XBP1 R (TGGGGAAGGGCATTTGAAGA).

The PCR conditions were one cycle of denaturation (95°C for 5 minutes), 30 cycles of amplification (95°C for 1 min, 62 °C for 30 sec, and 72°C for 30 sec) and a final cycle of extension (72°C for 10 min). The PCR products were run in 7% acrylamide at 90 V for 80 min. Gels were stained with a solution of TAE 1X 250 ml and 12 µl Sybr Safe (1691992, Invitrogen) during 15 min in an orbital shaker.

21. Murine models.

In order to assess tumour growth, DMS-273 SCR or shTRIT1 cells were subcutaneously injected into the flanks of five-week-old athymic nu/nu mice (Envigo Laboratories). $3x10^6$ cells in 50% Matrigel (354234, BD Biosciences) for each condition were injected into nine mice per group. Tumour development was monitored every 4-6 days, and tumour width (W) and length (L) were measured with a calliper to calculate the tumour volume ($V = \pi/6 \times L \times W^2$). Animals were sacrificed 20 days after injection.

For the arsenic trioxide treatment, DMS-273 SCR or shTRIT1 cells were subcutaneously injected in the mouse flanks as described above. Ten days after injection, the animals were randomized in two groups and treated with vehicle (0.015 N NaOH in saline) or

Arsenic Trioxide (A1010, Sigma-Aldrich) diluted in 0.015 N NaOH. Drug was administered by intraperitoneal injection at 5 mg/kg dosage following a schedule of 5 days ON 2 days/OFF for three consecutive weeks. Tumour growth was monitored and measured as described above and animals were sacrificed 28 days after cell injection. All mouse experiments were approved by the Institutional Animal Care Committee of Bellvitge Biomedical Research Institute (IDIBELL) and performed in accordance with the guidelines of the International Guiding Principles for Biomedical Research Involving Animals, developed for the Council for International Organizations of Medical Sciences (CIOMS). The IDIBELL animal facility is accredited by the AAALAC (Association for Assessment and Accreditation of Laboratory Animal Care International, Unit 1155) since 2006 and works according to the European and National Legislation (CEE/86/609, RD1201/2005, RD214/1997). Our experimental procedure (9111) was revised and approved by local Government of Generalitat de Catalunya.

22. RNA Sequencing.

Total RNA from DMS-273 SCR and shTRIT1 cells was extracted using a Maxwell RSC device (Promega, Madison, WI, USA). Then, 5 µg of total RNA from three biological replicates from each sample were used for RNA sequencing (RNA-seq). The RNA-seq libraries were prepared from total RNA with TruSeq®Stranded mRNA LT Sample Prep Kit (Illumina, San Diego, CA, USA). Each library was sequenced using a TruSeq SBS Kit v4-HS, in paired-end mode with a read length of 2 × 76 + 8 + 8bp. We obtained ~500 million paired-end reads in a fraction of a sequencing lane on HiSeq2500 (Illumina, San Diego, CA, USA), following the manufacturer's protocol. Raw reads were quality assessed and pre-processed using FASTQC (version 0.11.7, Babraham Bioinformatics, Babraham Institute, Cambridge, UK) and Trimmomatic (version 0.36, The Usadel Lab, Aachen University, Aachen, Germany) software. Differential expression analysis was performed using DESeq2 Bioconductor package (v1.18.1), in R (v3.4.3). Gene annotations were extracted from GENECODE (v35). Gene ontology (GO) biological processes for the downregulated genes with a log2-fold change >|1| and a false discovery rate (FDR) adjusted p-value < 0.05 included in the GSEA signature database were used to perform an enrichment analysis.

23. Drug-Dose Response Assay.

After determining the optimal number, 20,000 cells were seeded onto 96-well plates. After overnight incubation, cells were treated with increasing concentrations of arsenic trioxide (A1010, Sigma-Aldrich) or cisplatin (P4394, cis-diammineplatinum(II)dichloride,

Sigma-Aldrich) in order to calculate the half-maximal inhibitory concentration (IC50). After 48 h, 10 µl of 5mg/ml MTT (3-(4,5-dimethyl-2-thiazolyl)-2,5-diphenyl-2H-tetrazolium bromide, M2128-10G, Sigma-Aldrich) reagent was added. After 3 h of incubation at 37°C, cells were lysed for about 20 h with MTT lysis buffer (50% N-N dimethylformamide, 20% sodium dodecyl sulphate, 2.5% glacial acetic acid, 2.1% 1 N HCl, at pH 4.7). Viable cells with active metabolism convert MTT into formazan leading to a colorimetric change from yellow to purple. Thus, the measured absorbance with an optical spectrometer at 560 nm is proportional to the number of viable cells. IC50 was determined with GraphPad Prism (Version 5 for Windows, GraphPad Software).

24. Statistical Analysis.

Statistical analyses were carried out with GraphPad Prism (Version 5 for Windows, GraphPad Software), using Student's t test or Wilcoxon rank sum test, as denoted in the results. Values of $p < 0.05$ were considered statistically significant (* $p < 0.05$; ** $p < 0.01$; *** $p < 0.001$). All statistical tests were two-sided. The values corresponding to TRIT1 copy number and expression in cell lines were obtained from the Broad Institute Cancer Cell Line Encyclopedia (CCLE) (https://depmap.org/portal/download/ Public Release 20Q4, accessed on 13 January 2021).

IV. RESULTS

IV. RESULTS

1. Identification of a genetic or epigenetic disruption of transfer RNA modifiers in human cancer cell lines.

Aimed to identify the presence of genetic and epigenetic alterations in tRNA modifiers described to date (**Table 2**), we performed an exhaustive analysis of multiomic data from about 1000 human cancer cell lines [258,259] including DNA methylation landscape, exome sequencing, and gene copy number information. One of the most interesting findings was the identification of an outstanding TRIT1 copy number amplification restricted only to small cell lung cancer (SCLC) cell lines (11 of 60) (**Figure 13**) For the complete data in the ~1000 cell lines see the Supplementary Materials Dataset S1 in the published manuscript at https://www.mdpi.com/article/10.3390/cancers13081869/s1.

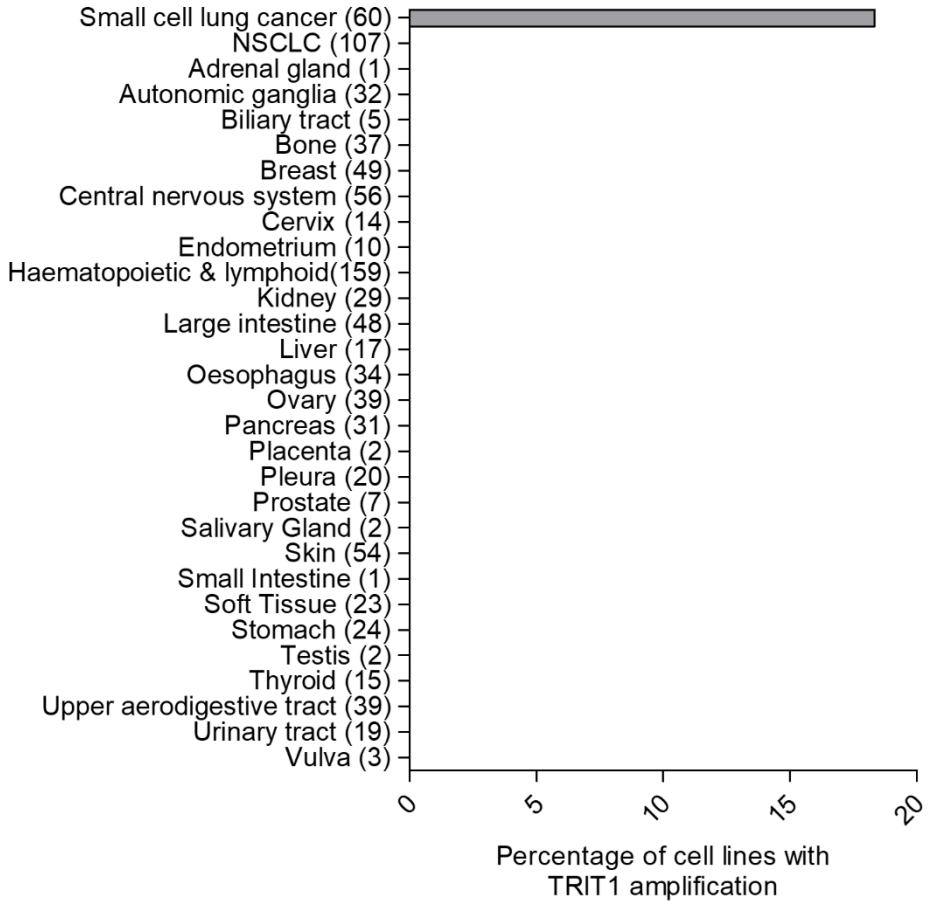

Figure 13. Frequency of the *TRIT1* gene amplification (copy number CN ≥ 8). Panel of human cancer cell lines from the dataset Iorio et al., Cell, 2016 [258]. The number of cell lines for each tumour type is shown in parenthesis.

Considering RB1 and TP53 are highly mutated genes in SCLC we first assessed the association of *TRIT1* amplification with these genetic alterations. With this goal, we datamined available data from 60 SCLC cell lines [258,259]. We observed that 82% (9 of 11) and 100% (11 of 11) of the *TRIT1* amplified cell lines showed *RB1* and *TP53* mutations, respectively; an identical distribution from that found in the 49 non-amplified cell lines (Fisher's exact test, *RB1* p = 0.4781 and *TP53* p = 1, respectively).

Next, we evaluated the effect of this amplification at the transcriptional level. We analysed the RNA expression profiles available for 36 SCLC cell lines from the described set [259] and found a significant increased expression in the *TRIT1*-amplified cell lines (**Figure 14A**). Furthermore, Oncomine (https://www.oncomine.org) analysis in Rohrbeck Lung published dataset for gene expression of 47 patient samples revealed the upregulation of *TRIT1* mRNA in SCLC in contrast to other lung cancer types and normal lung tissue (**Figure 14B**) [260].

Taking into account the elevated mortality of small cell lung cancer due to its aggressiveness and the lack of specific therapeutic targets, we decided to focus the study on the analysis of aberrant amplification of the *TRIT1* gene and the biological consequences of its associated increased expression in small cell lung cancer.

Considering the obtained results, we selected two cell lines featuring TRIT1 amplification (DMS-273 and HCC-33) and one cell line without amplification (NCI-H82), all cell lines included in the characterised set [258,259] and available in our laboratory. Accordingly, the whole exome sequencing (WES) data from dataset [258], the NCI-H82 cell line is reported to have two copies of the *TRIT1* gene; meanwhile, DMS-273 has 12 copies, and HCC-33 has 22 copies (https://www.mdpi.com/article/10.3390/cancers13081869/s1). First, these copy number patterns were validated using fluorescence *in situ* hybridisation (FISH) with a red-labelled probe targeting the region 39,695,285-39,879,670 of p-arm (short arm, 1p34.2) of chromosome 1 where *TRIT1* is situated. We included the D-5099-100-OG green probe targeting the chromosomal region 1p32.3 as control. As expected, NCI-H82 showed two copies of the TRIT1 gene, whereas DMS-273 and HCC-33 presented a clear amplification signal (**Figure 15A**). This result was confirmed by multiplex ligation-dependent probe amplification (MLPA) assay (**Figure 15B**).

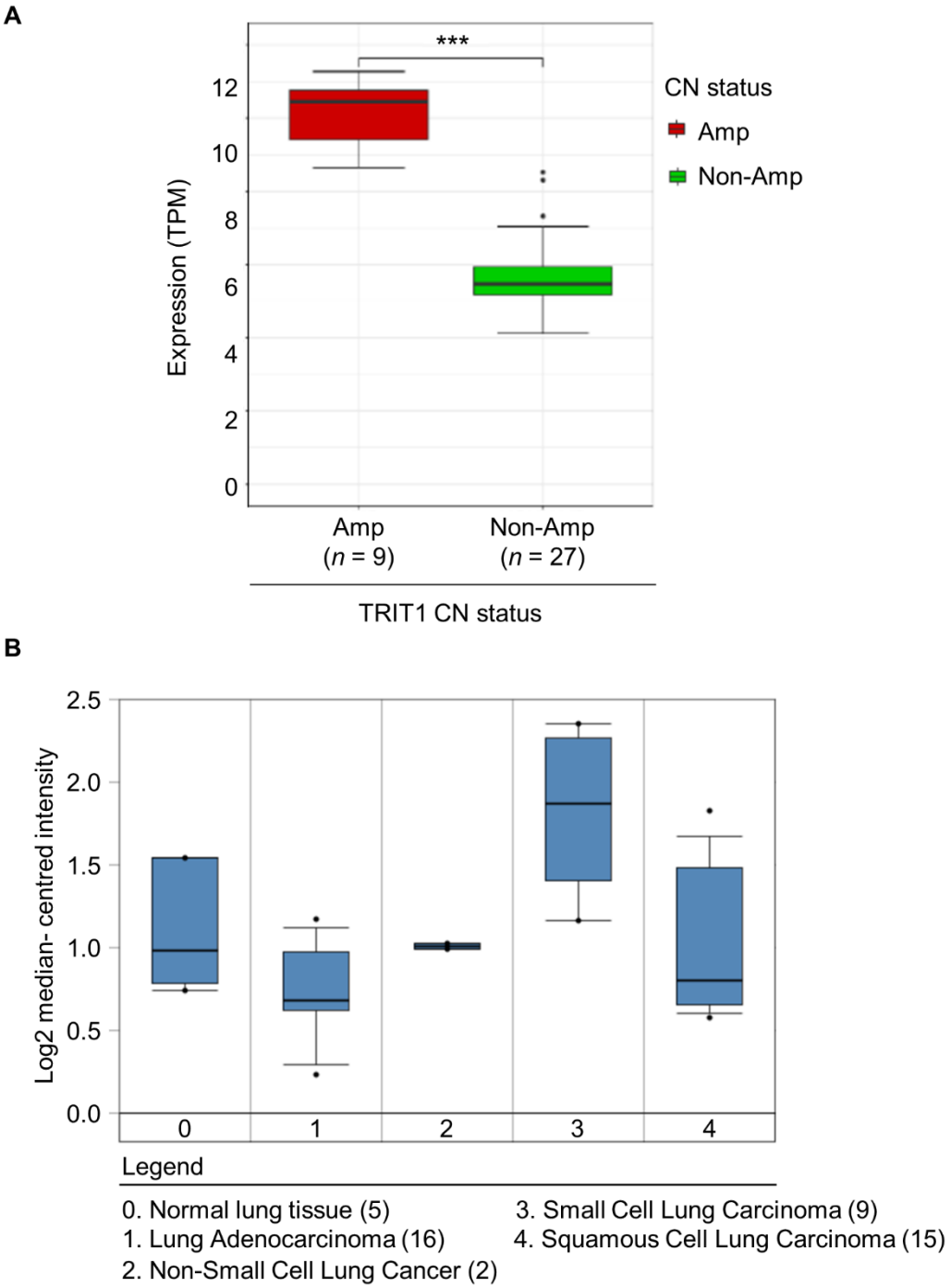

Figure 14. *TRIT1* expression in human cancer cell lines, normal lung samples and lung cancer patient samples. **(A)** *TRIT1* gene amplification was associated with high levels of the *TRIT1* transcript in SCLC cell lines with available expression data (n = 36). Non-Amp, non-amplified; Amp, amplified. TPM, transcripts per million. p-value obtained by Wilcoxon rank-sum test. *** $p < 0.001$. **(B)** Oncomine analysis. Comparison of *TRIT1* gene expression profiles of normal lung tissues, small cell lung cancers and non-small cell lung cancers (NSCLC, adenocarcinomas and squamous cell carcinomas) [260]. Small-cell lung cancers show the highest expression of *TRIT1* gene. Graphic obtained from Oncomine Platform (https://www.oncomine.org).

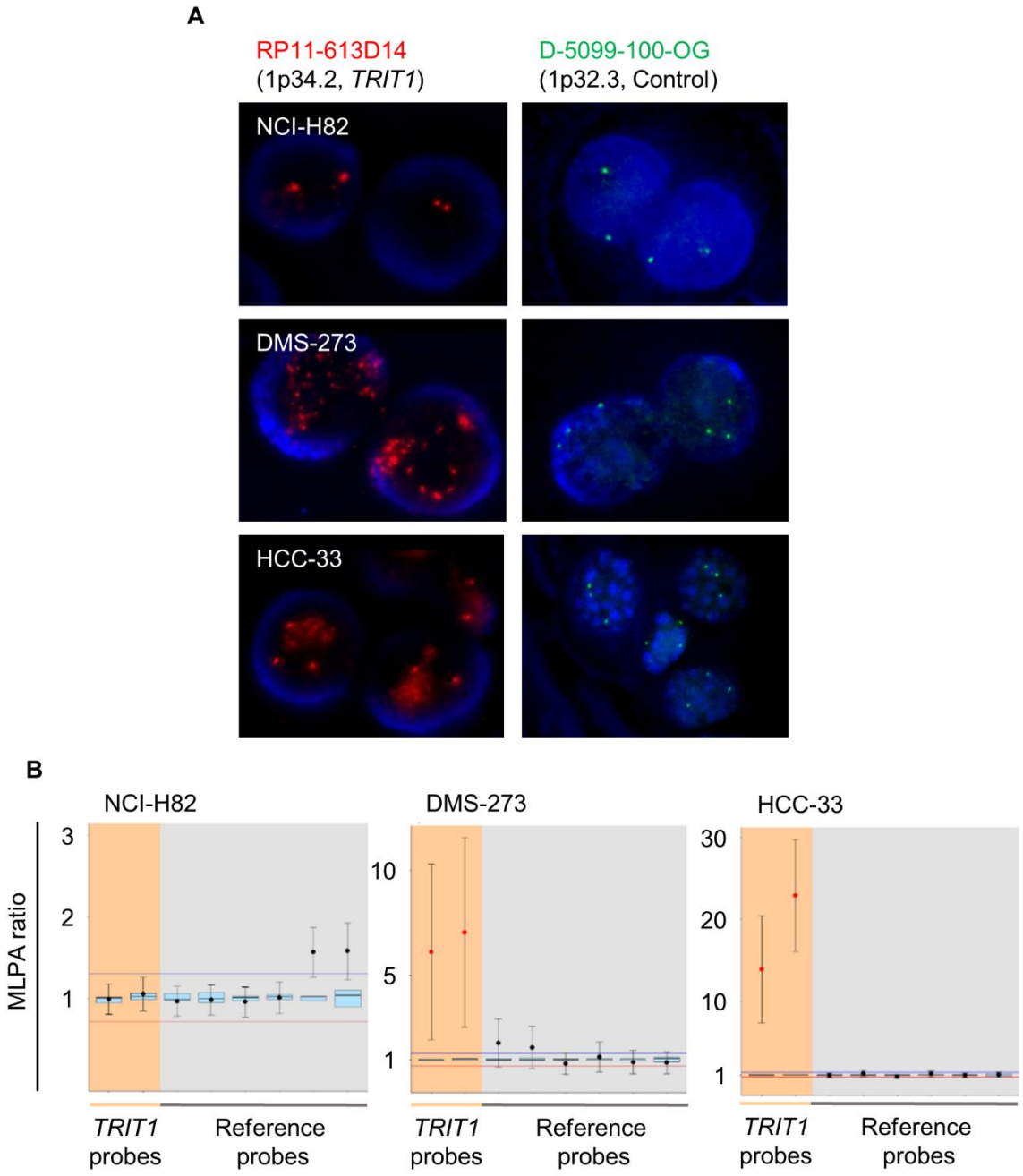

Figure 15. Determination of *TRIT1* gene amplification in SCLC cell lines. **(A)** Fluorescent *in situ* hybridization (FISH) for the *TRIT1* gene in the SCLC cell lines. The BAC clone RP11-613D14 spanning the 1p34.2 region for the *TRIT1* gene was labelled in red. The D-5099-100-OG green probe (1p32.3) was used as a control. The samples were counterstained with DAPI. Gene amplification was found in the DMS-273 and HCC-33 SCLC cell lines. **(B)** Multiplex ligation-dependent probe amplification (MLPA) assay. Probe mixes contained two probes for exons 4 and 9 of the TRIT1 gene (in orange). Six reference probes were also included (in grey). Values greater than 2 (two copies, corresponding to MLPA ratio of 1) were considered to indicate the presence of extra copies. DMS-273 and HCC-33 cell lines showed TRIT1 gene amplification, whilst NCI-H82 is shown as an example of TRIT1 two copy number cells.

Once confirmed the copy-number results obtained from the whole-exome sequencing data-mining (https://www.mdpi.com/article/10.3390/cancers13081869/s1) by FISH and MLPA, we wanted to assess if *TRIT1* gene amplification was associated with the overexpression of the TRIT1 messenger RNA and protein. Thus, we performed a real-time quantitative PCR (RT-qPCR) that showed higher *TRIT1* expression at the transcriptional level in the *TRIT1*-amplified DMS-273 and HCC-33 cell lines than in NCI-H82 (**Figure 16A**). Likewise, this significant increase in mRNA level led to an increased protein expression in *TRIT1* amplified SCLC cell lines, determined by western-blot (**Figure 16B**) and immunocytochemistry (**Figure 16C**).

2. Generation of TRIT1 loss-of-function cellular model.

After demonstrating the link between TRIT1 amplification and its overexpression, we assessed its biological effect in the context of small cell lung cancer generating loss-of-function cellular models. Four commercial short hairpin RNAs (shRNAs) were tested (shTRIT1.A, B, C and D). We first used the colon cancer cell line HCT-116 to assess the shRNAs efficiency. First, we expressed the full-length mRNA isoform of the *TRIT1* gene cloned in a pLVX-IRES-tdTomato plasmid and sorted the cells by tomato fluorescence. Next, transfected the four shRNAs individually, the scramble-shRNA (SCR) as a negative control and the shRNA against the tomato protein (shT1) as a positive control. Last, we sorted cells by green fluorescence and analysed the tomato signal of those cells.

As shown in **Figure 17A**, all shRNAs diminished tomato fluorescence except for the SCR (negative control). The shTRIT1.B and C curves were the ones that resembled the most the shT1 positive control. They were also the ones with the strongest inhibitory effect in TRIT1 expression (**Figure 17B**). Thus, we tested both, shTRIT1.B and shTRIT1.C to silence TRIT1in the DMS-273 SCLC cells. ShTRIT1.C (here after referred as shTRIT1) was the one that diminished the TRIT1 protein expression the most in this SCLC cell line (**Figure 17C**) and was then used for loss-of-function experiments.

Once we selected an efficient short hairpin RNA, we generated the loss-of-function (LOF) model by stable transfection in DMS-273 cell line. The capacity to significantly downregulate TRIT1 messenger RNA and protein expression was validated by RT-qPCR (**Figure 18A**) and western blot (**Figure 18B**), respectively.

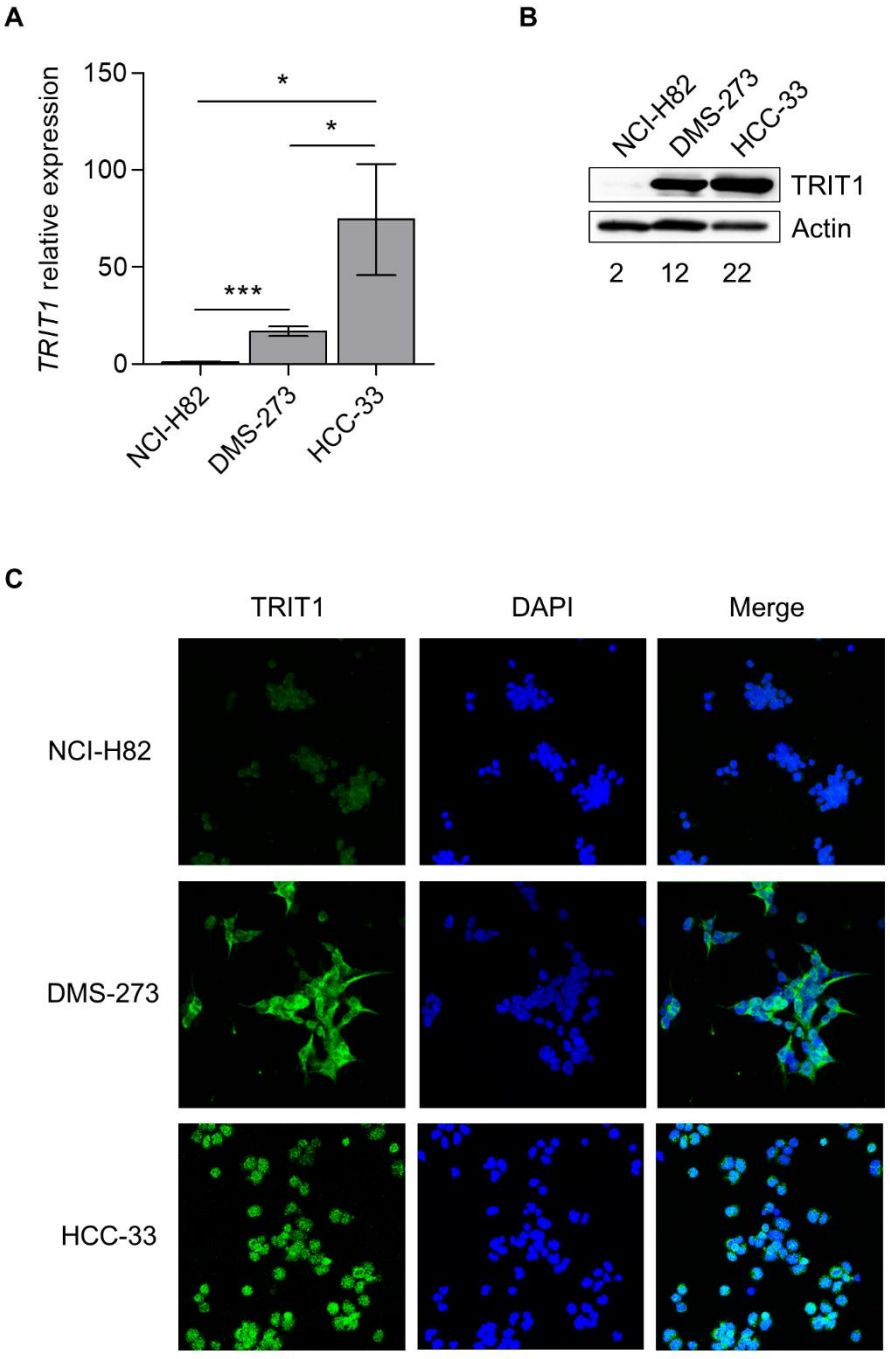

Figure 16. *TRIT1* amplification is associated with increased expression in SCLC cell lines. **(A)** RT-qPCR analysis of *TRIT1* expression. *TRIT1* gene amplification was significantly associated with high levels of the *TRIT1* transcript in the small-cell lung cancer cell lines DMS-273 and HCC-33. * $p < 0.05$; *** $p < 0.001$. **(B)** Western blot of TRIT1 protein expression levels in the non-amplified (NCI-H82) and amplified (DMS-273 and HCC-33) cancer cell lines analysed. Actin was used as the loading control. **(C)** TRIT1 protein expression in SCLC cell lines assessed by immunocytochemistry show the overexpression of TRIT1 protein in DMS-273 and HCC-33 cell lines. Cells were counterstained with DAPI.

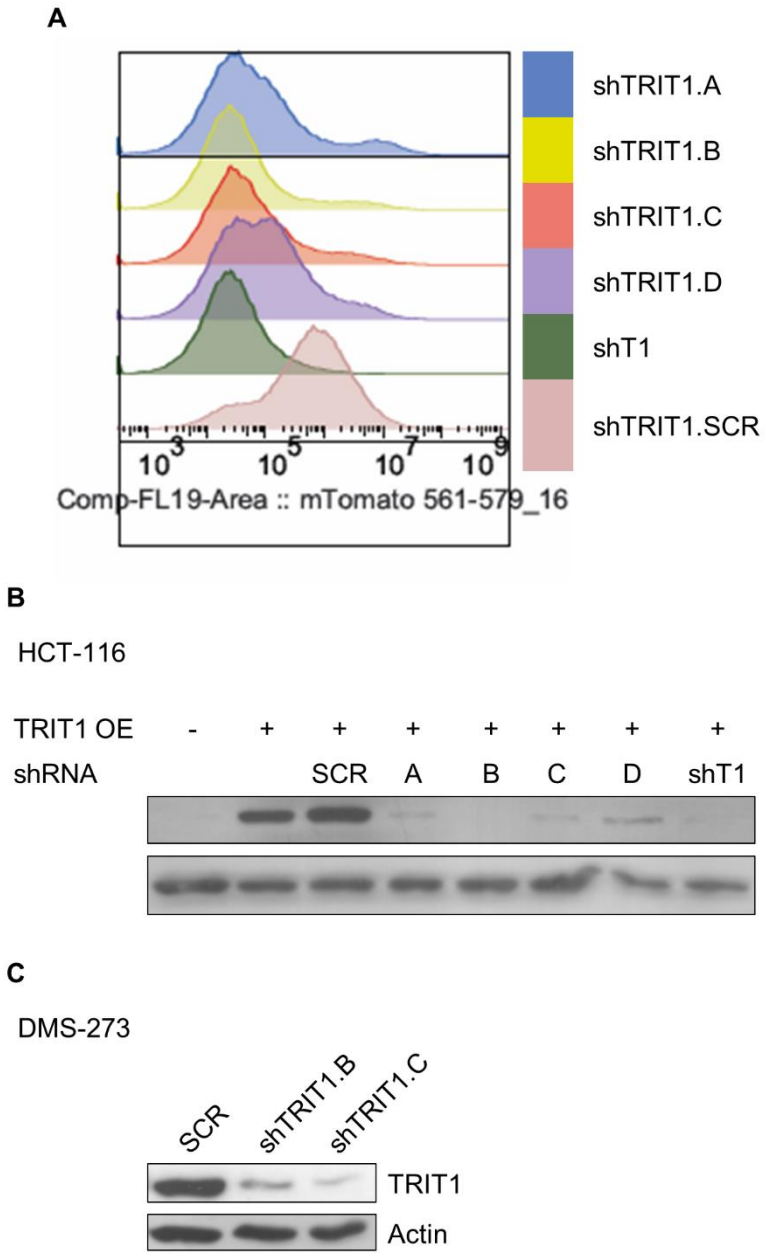

Figure 17. Validation of the inhibitory effect of TRIT1 shRNAs in TRIT1 expression. **(A)** Cytometry analysis of transfected HCT-116 to assess the shRNAs against *TRIT1*. *TRIT1* cloned in the plasmid pLVX-IRES-tdTomato was transfected in HCT-116 cell line (*TRIT1* CN = 2). Cells were sorted by tomato fluorescence. These selected cells were transfected with four shRNA against TRIT1 (shTRIT1.A, B, C or D), a scrambled shRNA (shTRIT1.SCR) as the negative control, or a shRNA against the fluorescent Tomato protein (shT1) as the positive control. Cells were sorted and analysed by green fluorescence. **(B)** Western blot of HCT-116 generated cell lines. TRIT1 was overexpressed upon transfection with TRIT1-pLVX-IRES-tdTomato, and its expression diminished upon shRNA.A, B, C, D and Tomato transfection. **(C)** Western blot analysis of *TRIT1* mRNA depletion in DMS-273 for shTRIT1.B and C.

Next, we assessed the cellular localisation of TRIT1. Although Mod5, the TRIT1 homologue in *Saccharomyces cerevisiae*, is described to have a tRNA gene-mediated transcriptional silencing function in the nucleus, we did not detect TRIT1 protein in the nucleus, even in the shRNA-scramble DMS-273 cells harbouring the amplified TRIT1 gene (**Figure 18C**). As previously reported, we confirmed that TRIT1 protein localises in the cytoplasm (**Figure 18C**) [216].

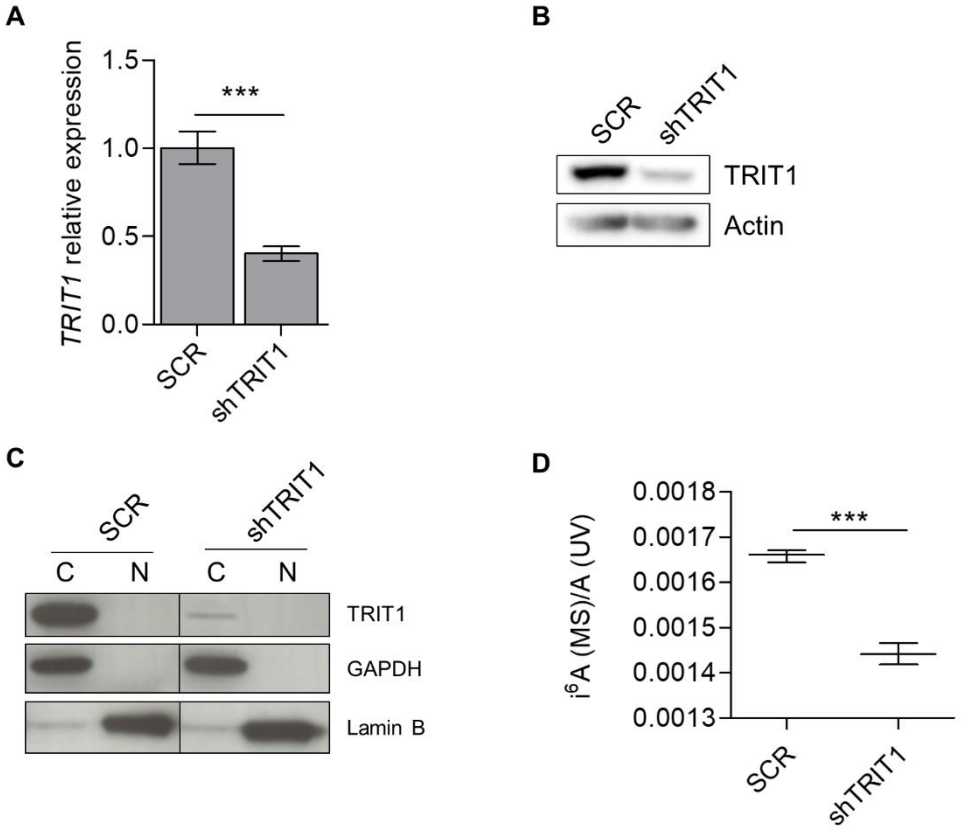

Figure 18. Generation of TRIT1 loss-of-function cellular model in DMS-273 SCLC cell line. **(A)** Stable downregulation of the *TRIT1* gene by short hairpin RNA in the SCLC cell line DMS-273 (shTRIT1) determined by RT-qPCR. SCR, scramble shRNA. *** $p < 0.001$. **(B)** TRIT1 protein decrease by short hairpin RNA in the SCLC cell line DMS-273 (shTRIT1) confirmed by western blot. SCR, scramble shRNA. Actin was used as loading control. **(C)** Subcellular fractionation of DMS-273 SCR and shTRIT1 cells shows TRIT1 expression restricted to the cytoplasm. GAPDH and Lamin B were used as cytoplasm and nuclear markers, respectively. **(D)** Nucleoside analysis of tRNAs by LC/MS showing that shRNA-mediated depletion of TRIT1 in DMS-273 cells induces the depletion of the i6A-modified nucleoside. Student's t-test, *** $p = 0.0002$.

Then, we interrogated the TRIT1 function as a tRNA modifier analysing the impact of TRIT1 loss on i^6A-tRNA-associated activity. We evaluated the chemical modification status of A37 using tRNA-associated liquid chromatography-mass spectrometry (LC-MS) [46]. As expected, TRIT1 shRNA-mediated downregulation of TRIT1 in DMS-273 cells induced a decrease in levels of the i^6A nucleoside (**Figure 18D**).

In addition, considering N^6-isopentenyladenosine is the preceding modification to ms^2i^6A, we looked for changes in the i^6A level by indirectly quantifying ms^2i^6A. For this aim, we used a protocol to measure the 2-Methylthio-N^6-isopentenyladenosine (ms^2i^6A) modification in mitochondrial tRNAs by reverse-transcription quantitative PCR [257]. We observed diminution of ms^2i^6A modification in serine, tryptophan, and tyrosine mitochondrial tRNAs in TRIT1 shRNA-depleted compared with scramble-shRNA DMS-273 cells, but not in the mitochondrial phenylalanine tRNA (**Figure 19**).

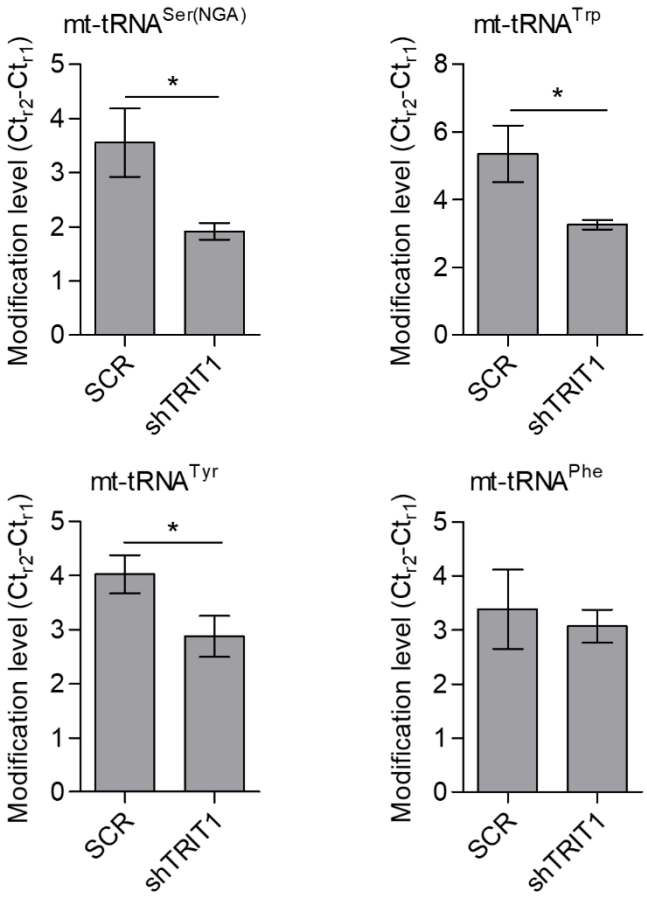

Figure 19. Ms^2i^6A modification levels. Measurement of 2-methylthio modification in mt-tRNA$^{Ser(NGA)}$, mt-tRNA^{Trp}, mt-tRNA^{Tyr} and mt-tRNA^{Phe} in scramble shRNA and TRIT1-depleted shRNA (shTRIT1) DMS-273 cells by RT-qPCR.

3. *In vitro* study of the biological function of TRIT1 using the cellular model of loss-of-function.

Once the *TRIT1* loss-of-function model was generated in the small cell lung cancer DMS-273 cell line, the possible biological functions of *TRIT1* amplification and the disruption of tRNA modification were evaluated.

First, we analysed the effect on cell proliferation. Upon transfection of shRNA against *TRIT1* in the *TRIT1*-amplified DMS-273 cell line, the cells did not show differences in proliferation in the 3-(4,5-dimethylthiazol-2-yl)-2,5-diphenyltetrazolium bromide (MTT) assay (**Figure 20A**) in comparison with the shRNA-scramble (SCR)-transfected cells. No differences were detected either between cells expressing shTRIT1 and those transduced with the shRNA-scramble (SCR) in the ability to form colonies, evaluated after seeding a low number of cells (**Figure 20B**).

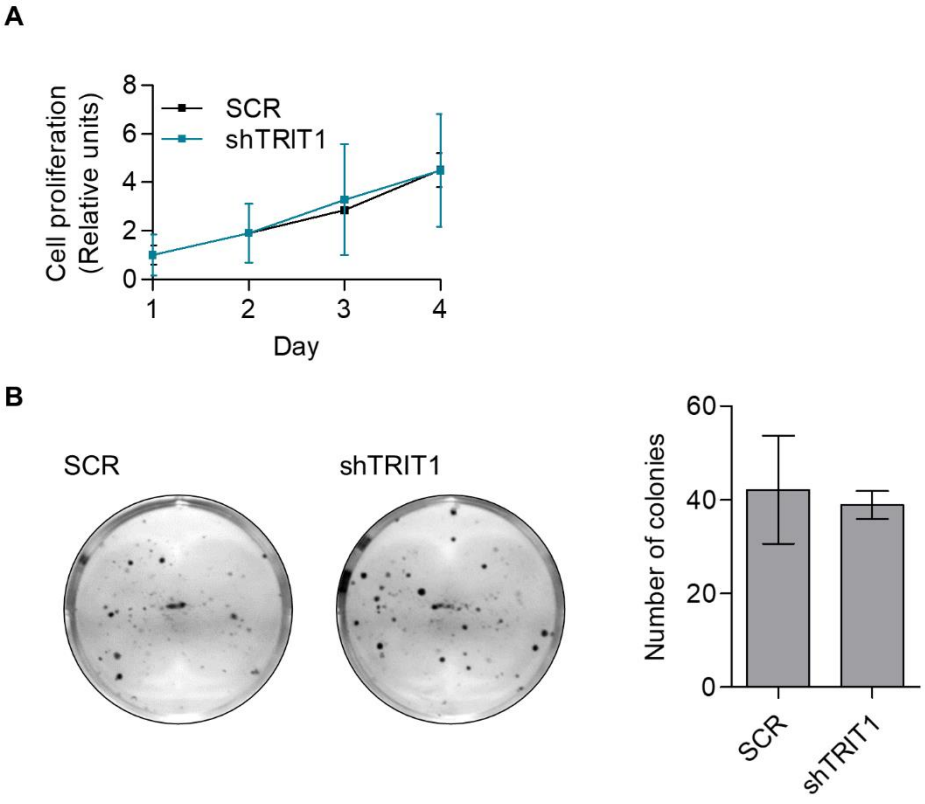

Figure 20. Effect of TRIT1 shRNA-mediated depletion on cell proliferation and colony formation in DMS-273 cells. **(A)** Effects on cell proliferation were determined by MTT assay. **(B)** Colony formation assay showed no significant differences upon TRIT1 depletion in DMS-273 cells. Left: Representative image of the colonies. Right: Statistical analysis of the colony number in each cellular model. Student's t-test, no significative (Mean ± SD, n = 3).

In addition, lack of changes were detected in the cell cycle profile upon TRIT1 depletion, as shown by the cell cycle analysis using flow cytometry after staining with the DNA intercalating agent propidium iodide (**Figure 21A**). We also assessed the amount of CDKN1A protein as an indicator of the blockage of the cell cycle in the G1/S and G2/M transition [261] and no differences were detected when comparing TRIT1-depleted and shRNA scramble-transfected cells (**Figure 21B**).

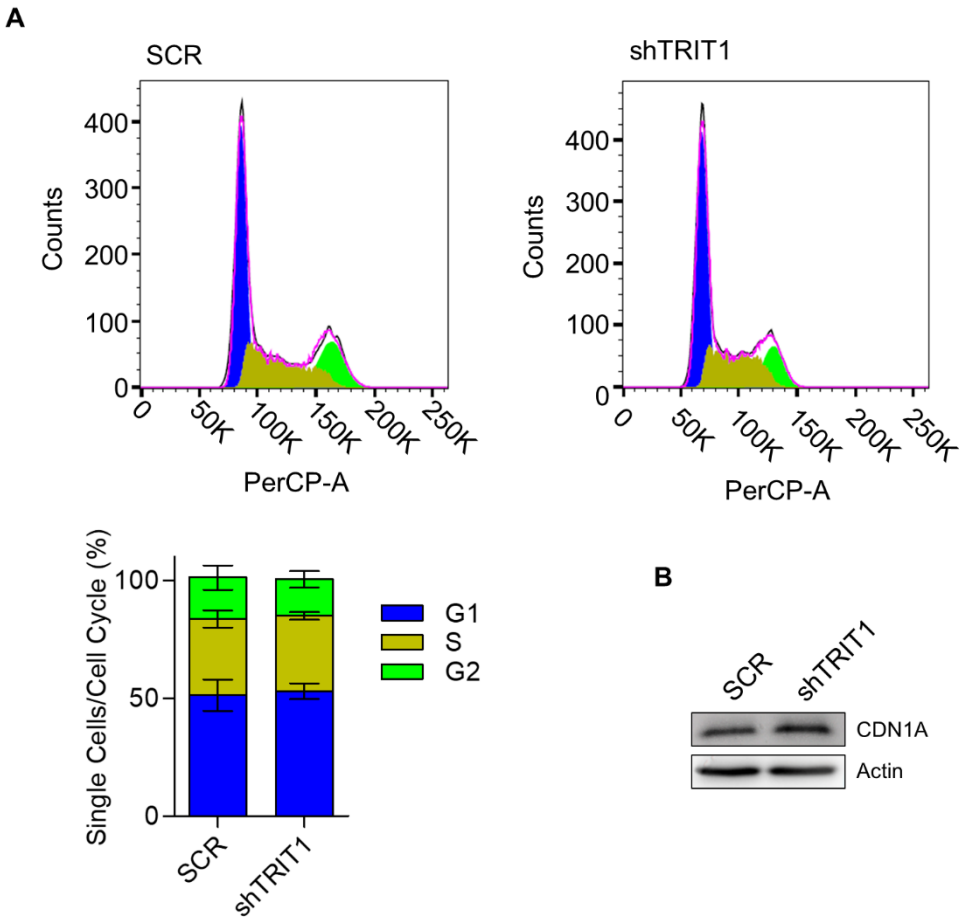

Figure 21. Effect of TRIT1 depletion in cell cycle. **(A)** Cell cycle analysis by DNA content estimation with flow cytometry. Top: Representative cell cycle distribution in scramble shRNA (SCR) and shRNA against TRIT1 (shTRIT1). Bottom: Distribution in the different phases of the cell cycle in the analysed cells. No differences between cell cycle phases were detected. **(B)** Expression of the cell cycle arrest marker CDKN1A assessed by Western blot. Actin was used as loading control.

Although we did not detected changes in cell cycle, we wondered if TRIT1 depletion could impair cell death. With this aim, we first calculated the proportion of alive to apoptotic cells by flow cytometry of AnnexinV/PI [262]. No differences were observed between DMS-273 cells transduced with the shRNA-scramble (SCR) and the TRIT1 shRNA-depleted (shTRIT1) in the proportion of total apoptotic and alive cells (**Figure 22**).

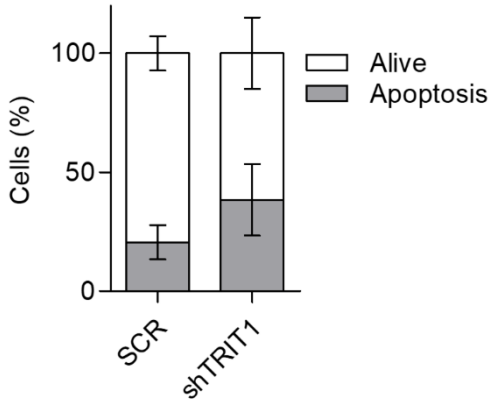

Figure 22. Apoptosis assay with Annexin V/PI. Quantification of the flow cytometry values of Annexin V/PI show the non-proapoptotic effect of TRIT1 knock-down in DMS-273. Student's t-test, no significative (Mean ± SD, n = 3).

Next, we evaluated differences in senescence through the senescence-associated β-galactosidase (SA-β-gal) assay [263] but senescent cells were not detected in SCR or shTRIT1 cells (**Figure 23**).

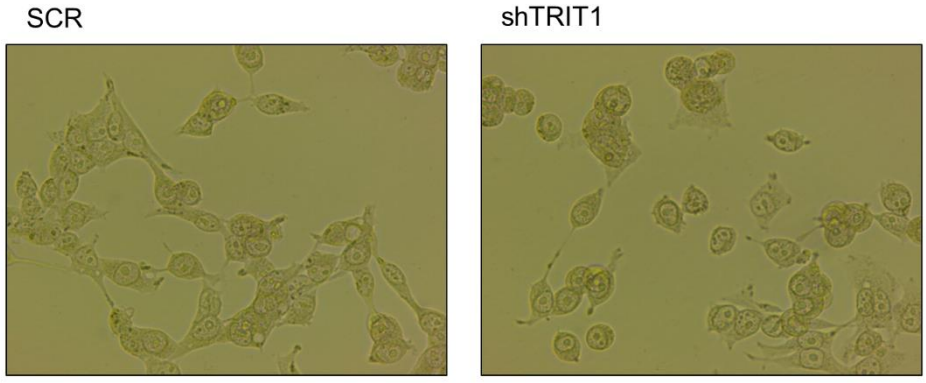

Figure 23. Senescence-associated β-galactosidase assay. No-senescent cells were detected in DMS-273 culture cell models through senescence-associated β-galactosidase (SA-β-gal) staining.

Then, the fact that several selenoproteins are described to be involved in endoplasmic reticulum stress [264], and TRIT1 modifies some mitochondrial tRNAs, encourage us to investigate possible effects of TRIT1 expression in unfolded protein response (UPR) and mitochondrial function. Taking advantage of the *XBP1* splicing during UPR [265], we analysed the expression pattern of the two *XBP1* isoforms by RT-PCR. As a positive control, we treated SCR and shTRIT1 DMS-273 cells with thapsigargin, a known inhibitor of the endoplasmic reticulum Ca^{2+} ATPase, that clearly showed an increase in the spliced isoform. TRIT1 cellular models expressed both *XBP1* mRNA transcripts but any change in the spliced form was detected upon TRIT1 depletion changes indicating no UPR (**Figure 24A**). These results were supported by the western blot analysis of the HSPA5 and EIF2AK3 proteins involved in the UPR [266], and ERO1A involved in protein folding [267] that did not show differences between the shRNA-scramble (SCR) and the TRIT1 shRNA-depleted (shTRIT1) DMS-273 cells (**Figure 24B**). Moreover, the Oxidative Phosphorylation System (OXPHOS) mitochondrial complexes exhibited no changes upon shRNA mediated TRIT1 depletion, which indicates no apparent issues in mitochondrial production of ATP [268] (**Figure 24C**).

4. *In vivo* study of the biological function of TRIT1 using the cellular model of loss-of-function.

Although *in vitro* assays in cultured cell lines could provide key information to elucidate biological functions, there are insurmountable limitations, mainly associated with the lack of interactions with the tumour microenvironment, as well as changes associated with adaptations to two-dimensional growth [269,270]. The tumour microenvironment is composed of stroma and inflammatory cells that, through cell-cell interactions and secreted factors, favour the development of the neoplasia contributing to the tumour progression and survival [271-273].

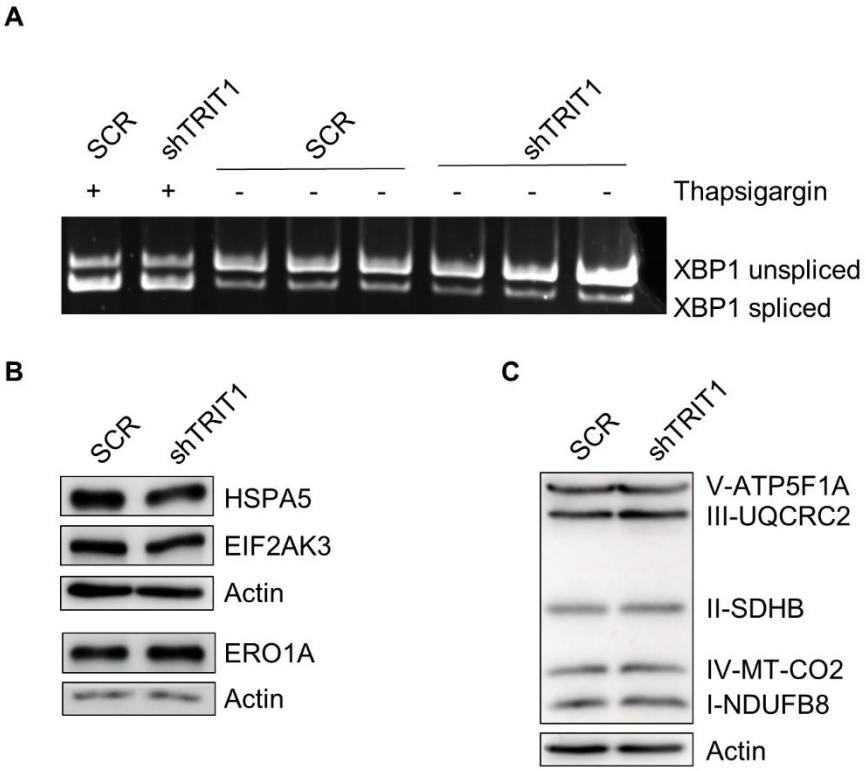

Figure 24. Endoplasmic reticulum and mitochondrial stress analysis. **(A)** *XBP1* splice assay to assess unfolded protein response (UPR) to endoplasmic reticulum stress in SCR and shTRIT1 DMS-273 cells. Electrophoresis of the RT-PCR shows the expression of two isoforms of *XBP1* transcripts. DMS-273 SCR and shTRIT1 cells were treated with Thapsigargin as a positive control. No changes in splicing were detected upon TRIT1 depletion. **(B)** Western blots of proteins associated with unfolded protein response pathway (HSPA5 and EIF2AK3) and protein folding assistance (ERO1A) in TRIT1 knock-down DMS-273 cell line show no differences in endoplasmic reticulum stress. **(C)** Western blot of Oxidative Phosphorylation System (OXPHOS) mitochondrial complexes. An antibody cocktail against proteins representing the five mitochondrial oxidative phosphorylation complexes was used to examine the expression of mitochondrial proteins in TRIT1 shRNA-mediated depleted DMS-273 cells.

Thus, in order to evaluate the functional consequences of the TRIT1 knockdown in a more physiological context, we characterised the capacity of shRNA-depleted TRIT1 (shTRIT1) and shRNA-scramble (SCR) DMS-273 cells to form tumours. With this aim, cells were subcutaneously injected in the flank of nude mice to assess tumour growth measuring the tumours every five days (**Figure 25A**). After 20 days of injection, mice were sacrificed, and tumours were weighed (**Figure 25B**). In the monitoring of tumour growth and the final tumour weight, a significant reduction in growth was detected in tumours derived from shTRIT1 DMS-273 cells compared with SCR-derived tumours

(**Figure 25A-C**). Knockdown of TRIT1 expression was maintained in the shTRIT1-derived tumours compared to SCR-derived tumours (**Figure 25D**).

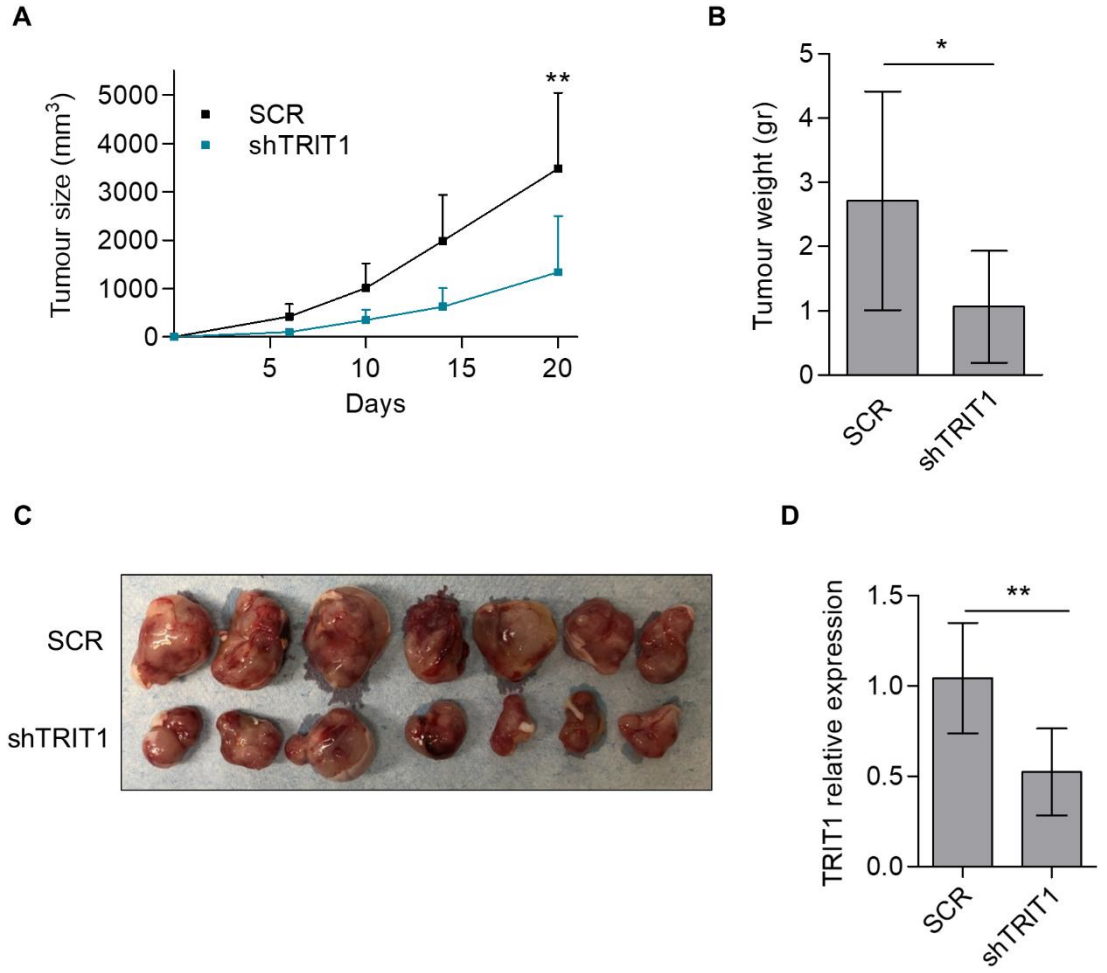

Figure 25. Effect of TRIT1 shRNA-mediated depletion on the growth of subcutaneous tumours in nude mice derived from DMS-273 cells (amplified and overexpressing TRIT1). **(A)** There was a significant reduction in tumour volume in the TRIT1 shRNA-depleted cells. Data are summarised as the mean and standard deviation (n = 9). Student's t-test, ** $p < 0.01$. **(B)** There was a significant reduction in tumour weight in the TRIT1 shRNA-depleted cells (n = 8) compared to scramble shRNA cells (n = 9). Data are summarised as the mean and standard deviation. Student's t-test, * $p < 0.05$. **(C)** Representative images of the tumours extracted after sacrifice. **(D)** TRIT1 gene downregulation by short hairpin RNA was maintained in DMS-273-shTRIT1-derived tumours in nude mice. Determined by RT-qPCR. ** $p < 0.01$.

5. Molecular effects of TRIT1 depletion in SCLC cells.

We next explored whether the decrease of i^6A modification in tRNAs of TRIT1 shRNA-downregulated cells had any impact on the transcriptome profile. We sequenced the transcriptome of the DMS-273 shRNA-scramble and shRNA TRIT1 cells and compared them (RNA-seq data deposited in the Sequence Read Archive repository (SRA) under the project code PRJNA692378. Data can be accessed through the following web address: https://www.ncbi.nlm.nih.gov/bioproject/PRJNA692378 (accessed on 27 October 2021)). The depletion of TRIT1 in the DMS-273 cells with gene amplification altered the levels of 4510 mRNAs (The entire list is available at https://www.mdpi.com/article/10.3390/cancers13081869/s1). Notably, 75.6% (3409 of 4510) of mRNAs were found downregulated upon TRIT1 depletion (**Figure 26**).

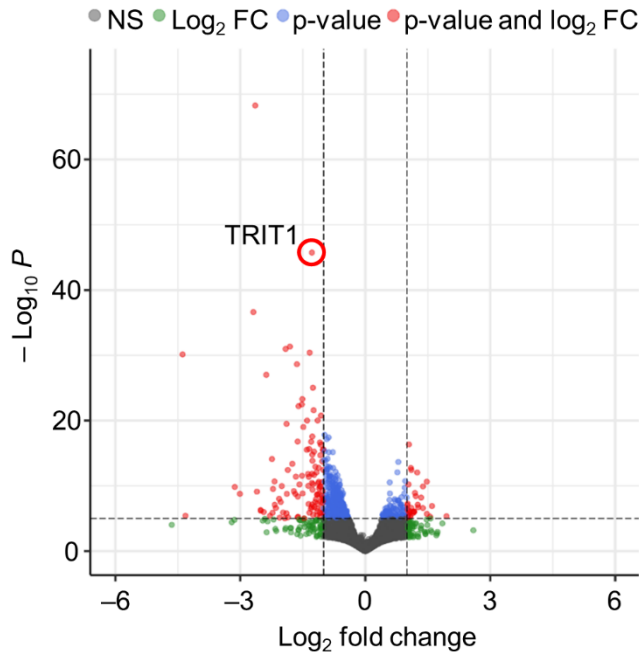

Figure 26. Transcriptional changes derived from TRIT1 shRNA-depletion. Volcano plot of the RNA-seq experiment showing mRNAs differentially expressed in TRIT1 shRNA-depleted DMS-273 cells compared with scramble-shRNA DMS-273 cells. Significant differences in fold change (FC), p-value, or both are denoted in green, blue, or red, respectively. TRIT1 is indicated. NS: no significant (grey).

Subsequently, a gene set enrichment analysis (GSEA), determined by gene ontology (GO), was carried out to investigate which biological aspects of the downregulated genes were overrepresented. The first ten categories of gene ontology from the downregulated genes in TRIT1 shRNA-depleted compared with scramble-shRNA DMS-273 cells are

shown in **Figure 27**. The first category overrepresented was the GO biological process "regulation of cell differentiation" (**Figure 27**).

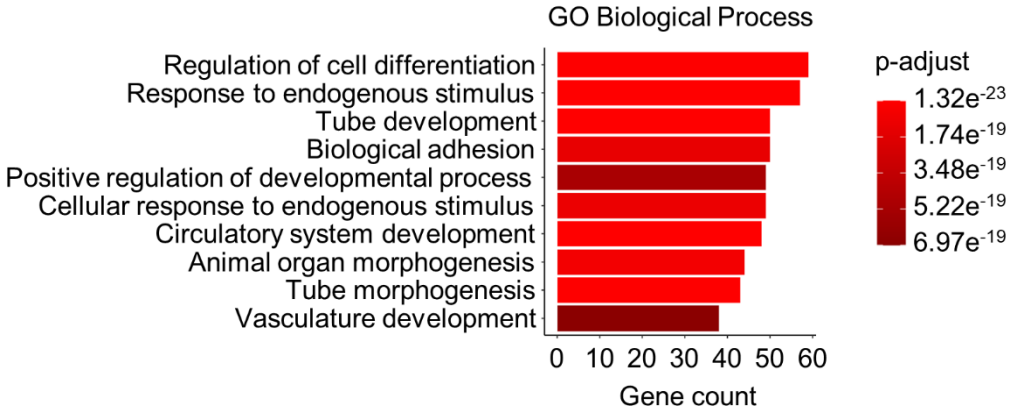

Figure 27. Functional enrichment upon depletion of TRIT1 in DMS-273 cells. Gene ontology (GO) analysis of Biological Process categories in the transcripts downregulated upon TRIT1 depletion in DMS-273 cells.

We next validated by qRT-PCR the downregulation upon TRIT1 depletion of some candidates with a well-recognised role in differentiation and carcinogenesis: *ID1* (Inhibitor Of DNA Binding 1, HLH Protein), *ID3* (Inhibitor Of DNA Binding 3, HLH Protein) [274-276], *COL3A1* (Collagen Type III Alpha 1 Chain) [277-279], *MT1X* (Metallothionein 1X) [280], *LAMA4* (Laminin Subunit Alpha 4) [281,282], *ANGPTL4* (Angiopoietin Like 4) [283,284], and *GPX4* (Glutathione Peroxidase 4) [285,286]. Gene expression of these genes was decreased upon TRIT1 depletion, confirming the results obtained by RNA sequencing (**Figure 28A**). Remarkably, one of these transcripts is GPX4, one of the 25 selenoproteins described in humans. As previously commented, selenocysteine tRNA was the first to be described to contain i^6A [222]. Further validation of the downregulation of GPX4 upon TRIT1 depletion by western blot (**Figure 28B**), reinforced the concept that defects in isopentenylated tRNAs can reduce the expression of selenoproteins.

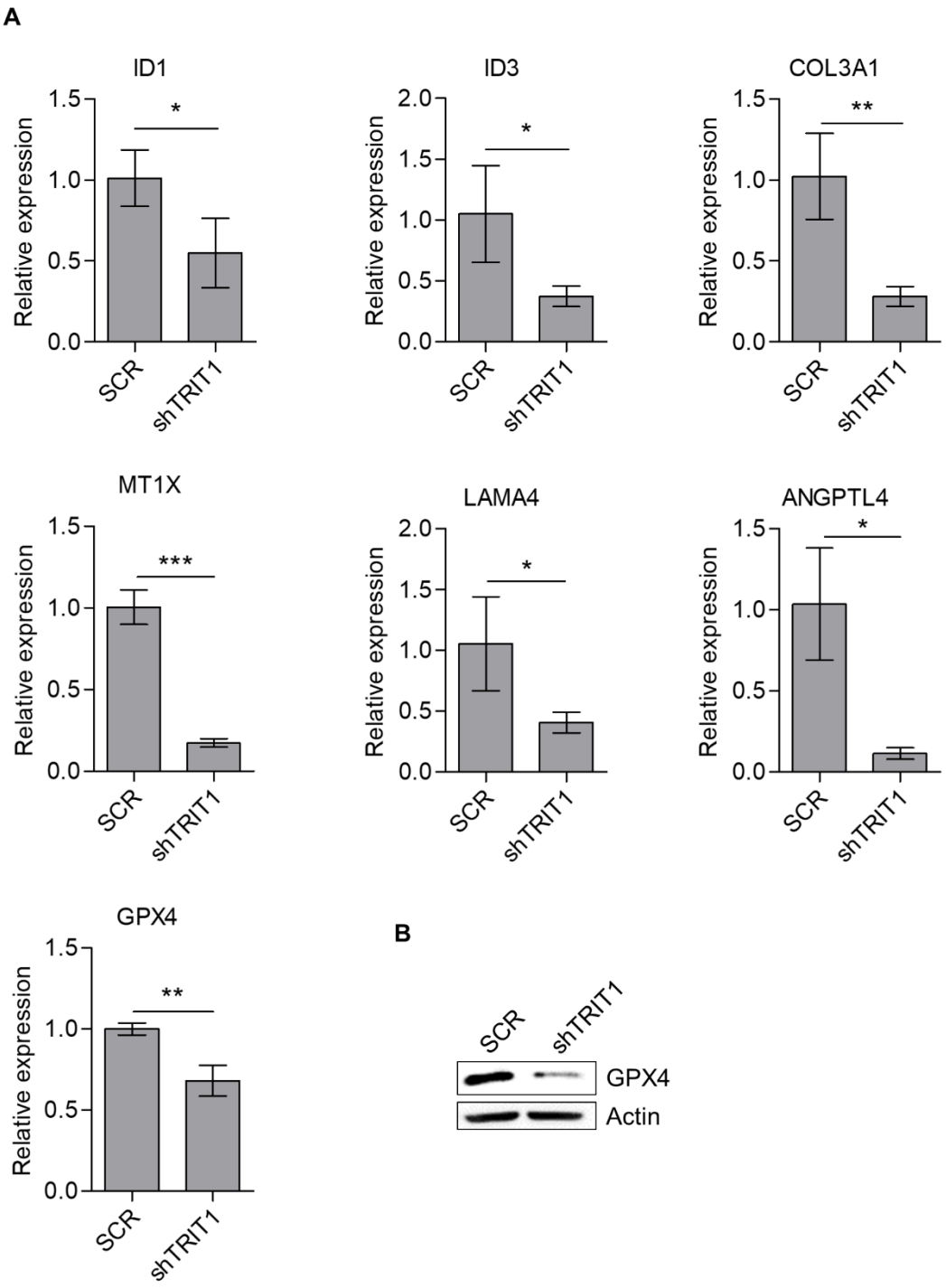

Figure 28. Validation of downregulation of expression in genes involved in cell differentiation upon TRIT1 depletion. **(A)** RT-qPCR of genes related to the regulation of cell differentiation. Short-hairpin RNA-mediated knockdown of *TRIT1* in DMS-273 cells caused a significant reduction in the expression of *ID1*, *ID3*, *COL3A1*, *MT1X*, *LAMA4*, *ANGPTL4* and *GPX4*. Student's t-test, *p < 0.05; **p < 0.01; ***p < 0.001. **(B)** Western blot analysis of GPX4 protein expression, which is downregulated upon TRIT1 depletion. Actin was used as loading control.

6. Drug sensitivity associated to TRIT1 gene amplification in SCLC cell lines.

Considering that therapeutic options in SCLC are limited, we wondered if TRIT1 amplification could confer sensitivity to some drug, particularly some already approved in other tumour type that could potentially be repurposed to treat *TRIT1*-amplified SCLC patients. With this goal, we performed an exhaustive revision of the literature to identify drugs affecting TRIT1-targeted proteins. The most relevant candidate was arsenic trioxide (As_2O_3), able to inhibit selenoprotein activity and synthesis [287,288]. Importantly, As_2O_3 has been successfully used in the treatment of acute promyelocytic leukaemia (APL), as shown in several clinical trials [289-291]. Also, recent studies highlight its therapeutical potential in other malignancies [292,293] including lung cancer [294]. In addition, the arsenic trioxide effect in APL has been related to induce the differentiation of the leukaemia cells [295], fact that could be linked to the GO biological process "regulation of cell differentiation" obtained in our RNA-seq analysis (**Figure 27A**). Altogether, we wondered if TRIT1 expression levels could be associated with arsenic trioxide sensitivity in SCLC cells.

We determined the half-maximal inhibitory concentration (IC50) by treating the cellular models of TRIT1 shRNA-mediated downregulation with increasing concentrations of arsenic trioxide. After 48 hours, the drug concentration at which cell viability was reduced by 50% was determined in triplicate through an assay with the MTT assay (**Figure 29A**). DMS-273 scramble shRNA cells overexpressing the TRIT1 gene were significantly more sensitive to the growth-inhibitory effect mediated by arsenic trioxide than were TRIT1-depleted cells (**Figure 29B**).

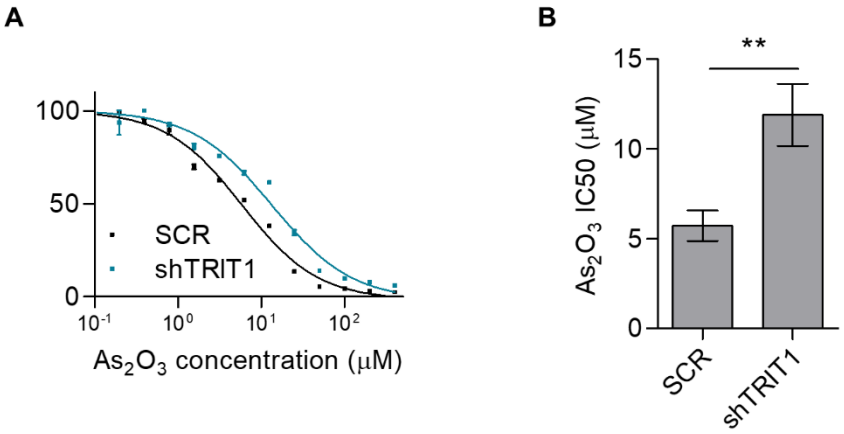

Figure 29. Sensitivity to arsenic trioxide upon modulation of TRIT1 expression in cultured cells. **(A)** Representative graphic of cell viability assessed by MTT assay of cell models treated with increasing concentrations of arsenic trioxide. **(B)** Data is summarised as the mean and standard

deviation. TRIT1 shRNA-depleted DMS-273 cells were significantly less sensitive to the antiproliferative effect of arsenic trioxide than were the shRNA scramble-transfected cells harbouring TRIT1 gene amplification-associated overexpression. Student's t-test, ** $p < 0.01$.

The positive result encouraged us to perform the assay *in vivo*. To this end, we injected the cells subcutaneously in the flanks of nude mice and started the treatment with arsenic trioxide on the tenth day. The DMS-273 scramble shRNA-derived tumours harbouring gene amplification-associated overexpression of TRIT1 were responders to arsenic trioxide administration. They showed decreased tumour size upon arsenic trioxide treatment compared with the lack of differences in the shTRIT1-derived tumours (**Figure 30**).

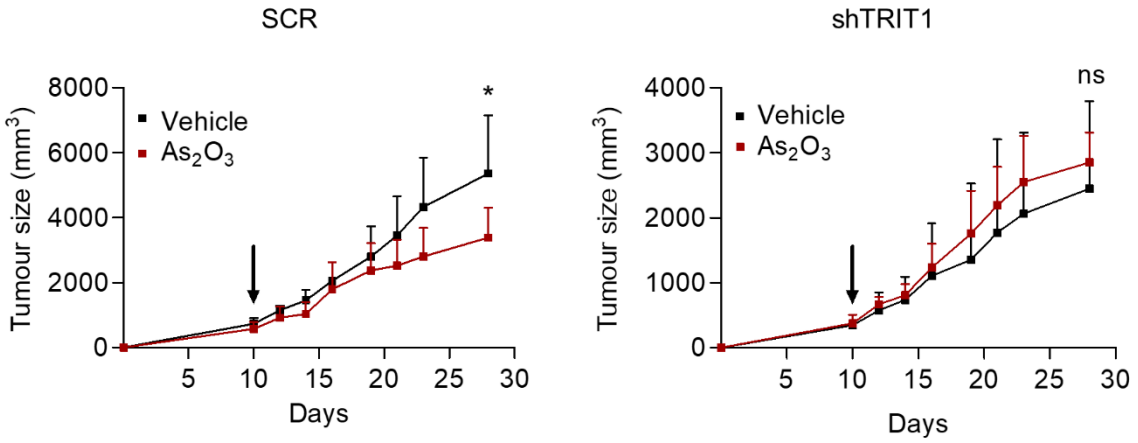

Figure 30. Arsenic trioxide sensitivity associated with *TRIT1* gene amplification in *in vivo* mouse model. *In vivo* response to arsenic trioxide in mice. shRNA scramble (SCR, left panel) and TRIT1 shRNA-depleted (shTRIT1, right panel) DMS-273 cells were injected into the flanks of nude mice to form subcutaneous tumours. Tumour volume over time according to treatment conditions, vehicle (black lines) vs arsenic trioxide-treated group (red lines) are shown. The black arrow indicates when the mice were randomised and started to be treated with arsenic trioxide or vehicle. Means and standard deviations (bars) are illustrated. Tumours derived from SCR DMS-273 cells were sensitive to the growth inhibitory effect of arsenic trioxide, while TRIT1 shRNA-mediated depletion eliminates the enhanced sensitivity to arsenic trioxide. Student's t-test, * $p < 0.05$; ns, non-significant.

In order to confirm the effect of TRIT1 expression in modulating the sensitivity to arsenic trioxide, we generated an additional depleted cellular model in the NCI-H1694 SCLC cell line. After validating the TRIT1 downregulation at mRNA (**Figure 31A**) and protein (**Figure 31B**) level, we established the IC50 concentration for arsenic trioxide for NCI-H1694 SCR and shTRIT1 cells. In agreement with the previous result in DMS-273 cells, scramble shRNA cells overexpressing the TRIT1 gene were significantly more sensitive to arsenic trioxide (**Figure 31C**).

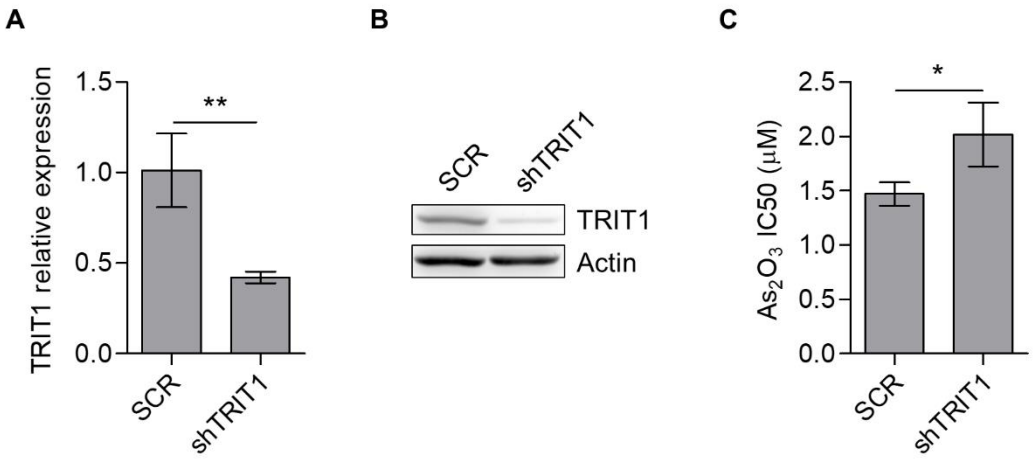

Figure 31. Validation of the effect of TRIT1 expression in modulating the sensitivity to arsenic trioxide in NCI-H1694 cells. **(A)** Stable downregulation of the TRIT1 gene by short hairpin RNA in the NCI-H1694 SCLC cell line (shTRIT1) determined by RT-qPCR. SCR, scramble shRNA. Student's t-test, ** $p < 0.01$. **(B)** TRIT1 protein underexpression by short hairpin RNA in the NCI-H1694 cell line (shTRIT1) determined by western blot analysis. SCR, scramble shRNA. Actin was used as loading control. **(C)** Arsenic trioxide IC50 of NCI-H1694 cell models assessed by MTT assay summarised as mean and standard deviation. TRIT1 shRNA-depleted NCI-H1694 cells were significantly less sensitive to the antiproliferative effect of arsenic trioxide than were the shRNA scramble-transfected cells harbouring TRIT1 gene amplification-associated overexpression. SCR, scramble shRNA. Student's t-test, * $p < 0.05$.

Once we demonstrated the sensitivity to arsenic trioxide, we then applied an additional approach to identify other compounds effective against small cell lung tumours harbouring TRIT1 gene amplification. We analysed the correlations between the IC50 values for 265 drugs in the SCLC cell lines from the Cancer Gene Project and the TRIT1 mRNA expression available from RNA sequencing [258]. The dimethyloxalylglycine (DMOG), a competitive inhibitor of the hypoxia-inducible factor prolyl hydroxylase, an antagonist of the α-ketoglutarate cofactor, and inductor of autophagy [296-298] displayed the best correlation with TRIT1 expression (Pearson correlation: -0.4735, p-value =

0.0008; **Figure 32A**). From those SCLC cell lines with available copy number status, we determined that *TRIT1*-amplified cell lines were significantly more sensitive to DMOG (**Figure 32B**). Next, we performed the MTT assay in triplicate to calculate the IC50 for DMOG in DMS-273 cellular models (**Figure 32C**). As *in silico* predicted, DMS-273 scramble shRNA cells overexpressing *TRIT1* were significantly more sensitive to DMOG than the TRIT1-depleted cells (**Figure 32D**).

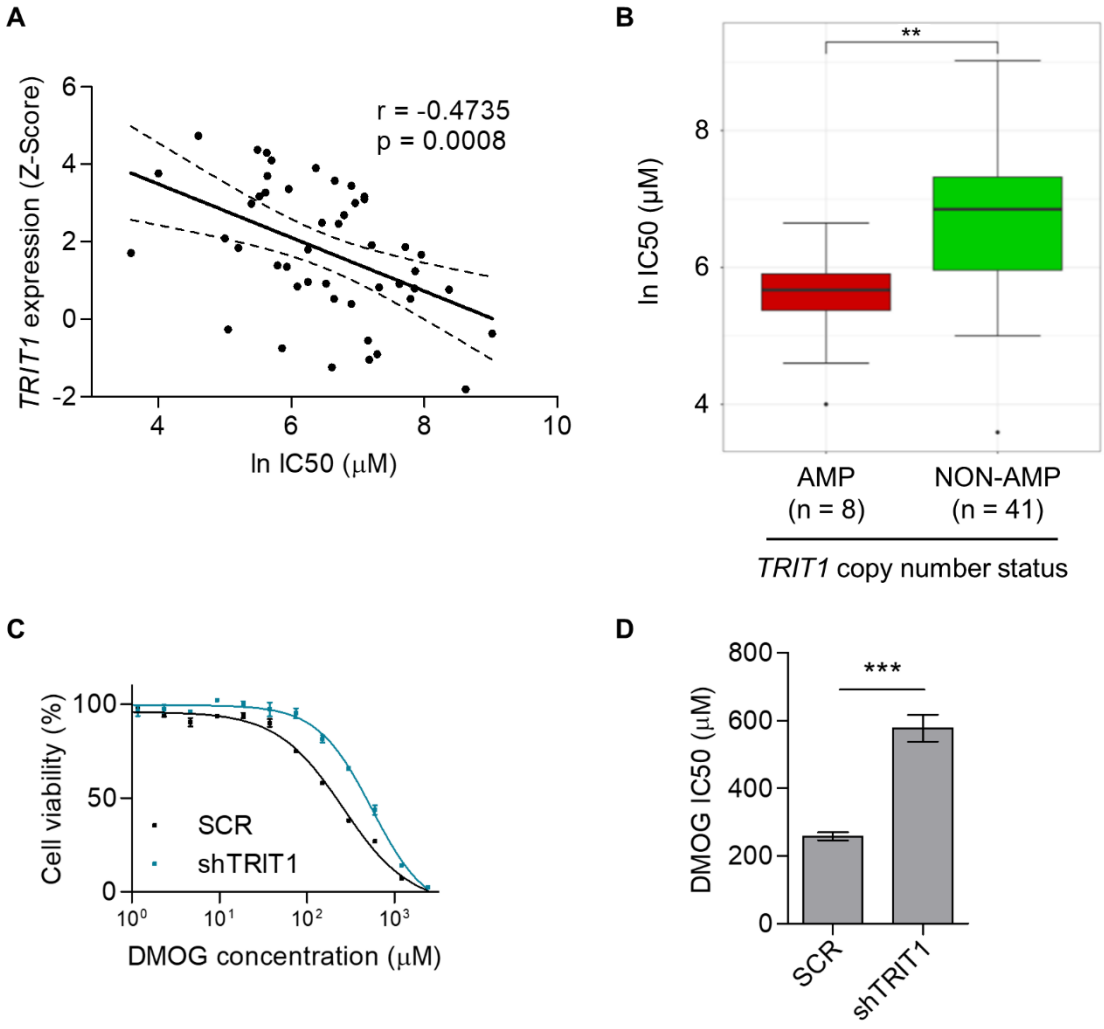

Figure 32. Effect of TRIT1 expression in sensitivity to dimethyloxalylglycine (DMOG). **(A)** Correlation between IC50 and TRIT1 mRNA expression in a panel of 47 SCLC cell lines. Data collected from Iorio et al. [258]. **(B)** Effect of TRIT1 copy number status in a panel of 49 SCLC cell lines from Iorio et al. [258]. Wilcoxon rank-sum test, ** p-value = 0.006. **(C)** Representative graph of cell viability assessed by MTT assay of SCR and shTRIT1 DMS-273 cells treated with increasing concentrations of DMOG. **(D)** Data is summarised as the mean and standard deviation. TRIT1 shRNA-depleted DMS-273 cells were significantly less sensitive to the effect of DMOG than the shRNA scramble-transfected cells harbouring TRIT1 gene amplification-associated overexpression. Student's t-test, *** $p < 0.001$.

Finally, considering cisplatin-based chemotherapy is extensively used in the first-line treatment of small cell lung cancer [299], we analysed the effect of TRIT1 modulation in cisplatin sensitivity. We carried out the three MTT assay replicates for DMS-273 SCR and shTRIT1 cell lines treated with cisplatin (**Figure 33A**) and, after analysing the IC50 mean, we found no difference in the sensitivity to cisplatin (**Figure 33B**).

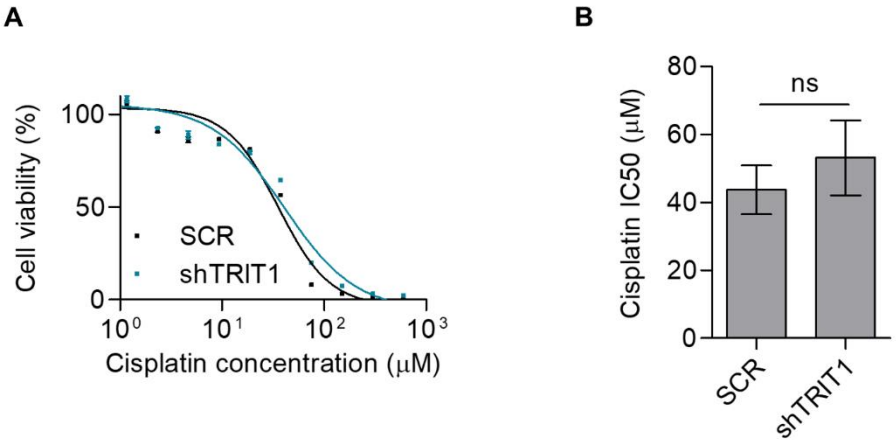

Figure 33. Effect of modulation of TRIT1 expression in cisplatin sensitivity in DMS-273 cells. **(A)** Representative graphic of cell viability assessed by MTT assay of DMS-273 SCR and shTRIT1 cells treated with increasing concentrations of cisplatin. **(B)** Data is summarised as the mean and standard deviation. TRIT1 shRNA-mediated depletion did not affect sensitivity to cisplatin. Student's t-test, ns, non-significant.

7. Occurrence of TRIT1 gene amplification in SCLC patients.

The outstanding results in SCLC cell lines prompted us to assess the occurrence of TRIT1 amplification in primary tumour samples from SCLC patients. We studied a cohort of 39 primary SCLC cases and found that 10.3% (4/39) harboured *TRIT1* gene amplification, analysing the samples by MLPA. **Figure 34A** shows representative examples of *TRIT1*-amplified and *TRIT1*- non amplified SCLC cases.

Clinicopathological features of the studied SCLC cohort are summarised in **Table 7**. Patient age, gender, smoking status, or clinical stage were not associated with TRIT1 amplification (**Table 7**). Moreover, no differences were detected in the distribution of *RB1* and *TP53* mutations [16] between *TRIT1* amplified and non-amplified cases (Fisher's exact test, p = 1). *TRIT1* gene amplification was not associated with overall survival (hazard ratio = 0.625; p = 0.449; 95% CI = 0.185–2.113; log-rank test, p = 0.445), although lack of association could be limited by the relatively low number of cases available for the analysis.

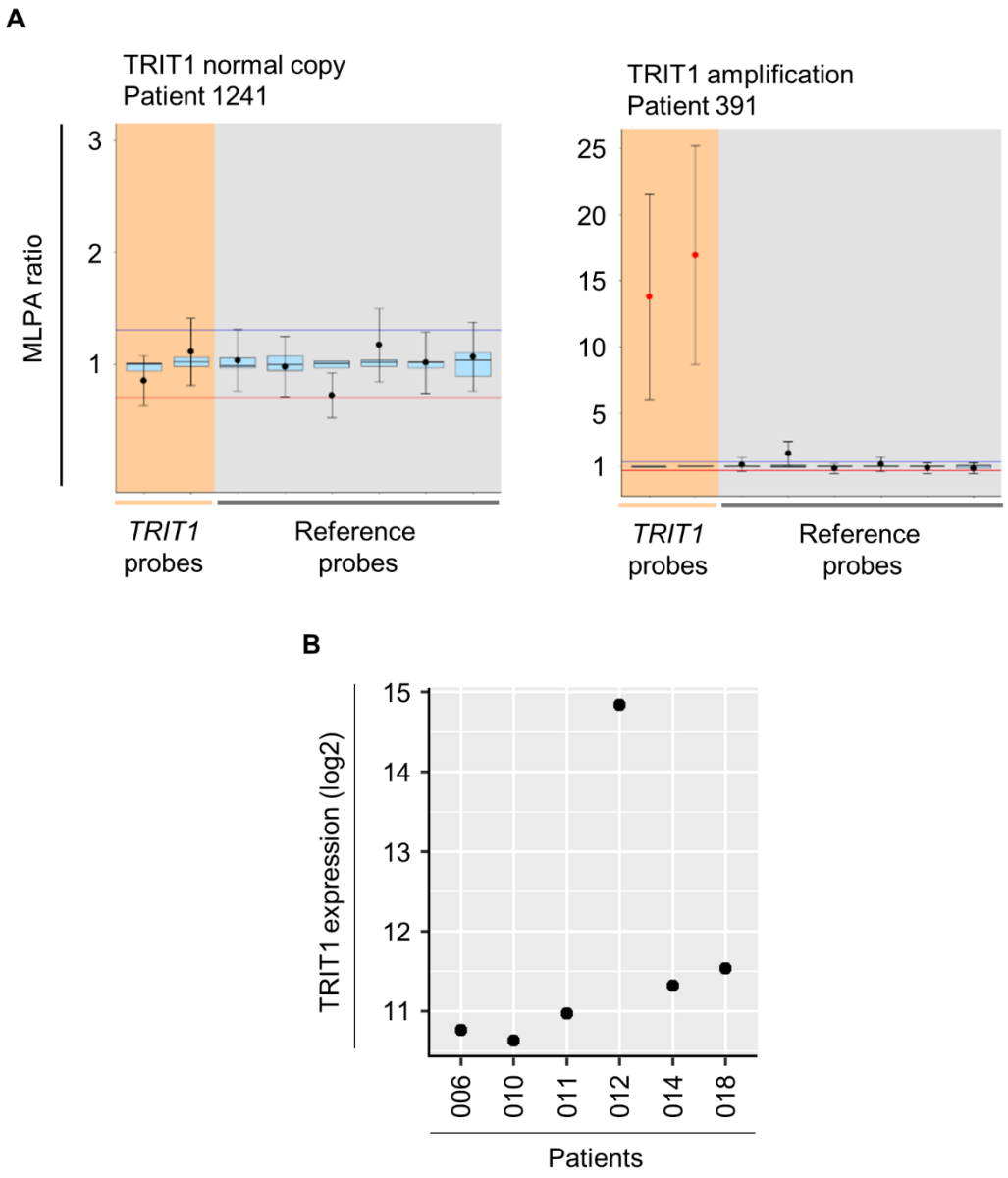

Figure 34. *TRIT1* amplification and expression in primary tumours of SCLC patients. **(A)** MLPA assay of primary small-cell lung cancer samples. Probe mixes contained two probes for exons 4 and 9 of the *TRIT1* gene (in orange). Six reference probes were also included (in grey). Values greater than 2 (two copies, corresponding to MLPA ratio of 1) were considered to indicate the presence of extra copies. Patient 1241 is shown as an example of a *TRIT1* two copy number case, whilst patient 391 shows *TRIT1* gene amplification. **(B)** *TRIT1* RNA expression levels were derived from Affymetrix U133Plus2.0 microarray data in six primary SCLC samples where the *TRIT1* copy number was determined.

Table 7. Clinicopathological features of the studied SCLC patients according to TRIT1 gene amplification status.

Clinical characteristics	Total (n=39)	TRIT1 Non-amplified (n=35)	TRIT1 Amplified (n=4)	p value*
Age years [median (range)]	65 (49-84)	65 (49-84)	65 (55-71)	
< 65	17 (43.6%)	15 (42.9%)	2 (50.0%)	1.000
≥ 65	22 (56.4%)	20 (57.1%)	2 (50.0%)	
Gender				
Female	8 (20.5%)	7 (20.0%)	1 (25.0%)	1.000
Male	31 (79.5%)	28 (80.0%)	3 (75.0%)	
Smoker				
Yes	33 (84.6%)	29 (82.9%)	4 (100.0%)	
No	3 (7.7%)	3 (8.6%)	0 (0.0%)	1.000
Unknown	3 (7.7%)	3 (8.6%)	0 (0.0%)	
Stage				
I	10 (25.6%)	7 (20.0%)	3 (75.0%)	
II	4 (10.3%)	4 (11.4%)	0 (0.0%)	0.098
III	11 (28.2%)	10 (28.6%)	1 (25.0%)	
IV	14 (35.9%)	14 (40.0%)	0 (0.0%)	

*p-value represents Fisher's exact test or X^2.

The expression microarray data was available for six of these SCLC cases [300]. The only patient that exhibited TRIT1 gene amplification (#012) showed the highest TRIT1 expression level. Two copies of TRIT1 were observed in the 006, 010, 011, 014 and 018 samples (**Figure 34B**).

We also datamined a set of 68 SCLC cases with available copy number information [301]. In this dataset, 14.7% (10/68) of primary SCLC cases showed *TRIT1* gene amplification. For the subset of 23 cases with available microarray expression data [301], *TRIT1* gene amplification (observed in three cases) was correlated with higher TRIT1 expression levels (Spearman's correlation test, p = 0.05). For these 23 cases, expression patterns of ASCL1, NEUROD1, POU2F3, and YAP1 were analysed to classify the tumours by the molecular subtypes [34] and assess the distribution of TRIT1 gene amplification. The three cases with *TRIT1* gene amplification corresponded with the ASCL1 subtype (**Figure 35**).

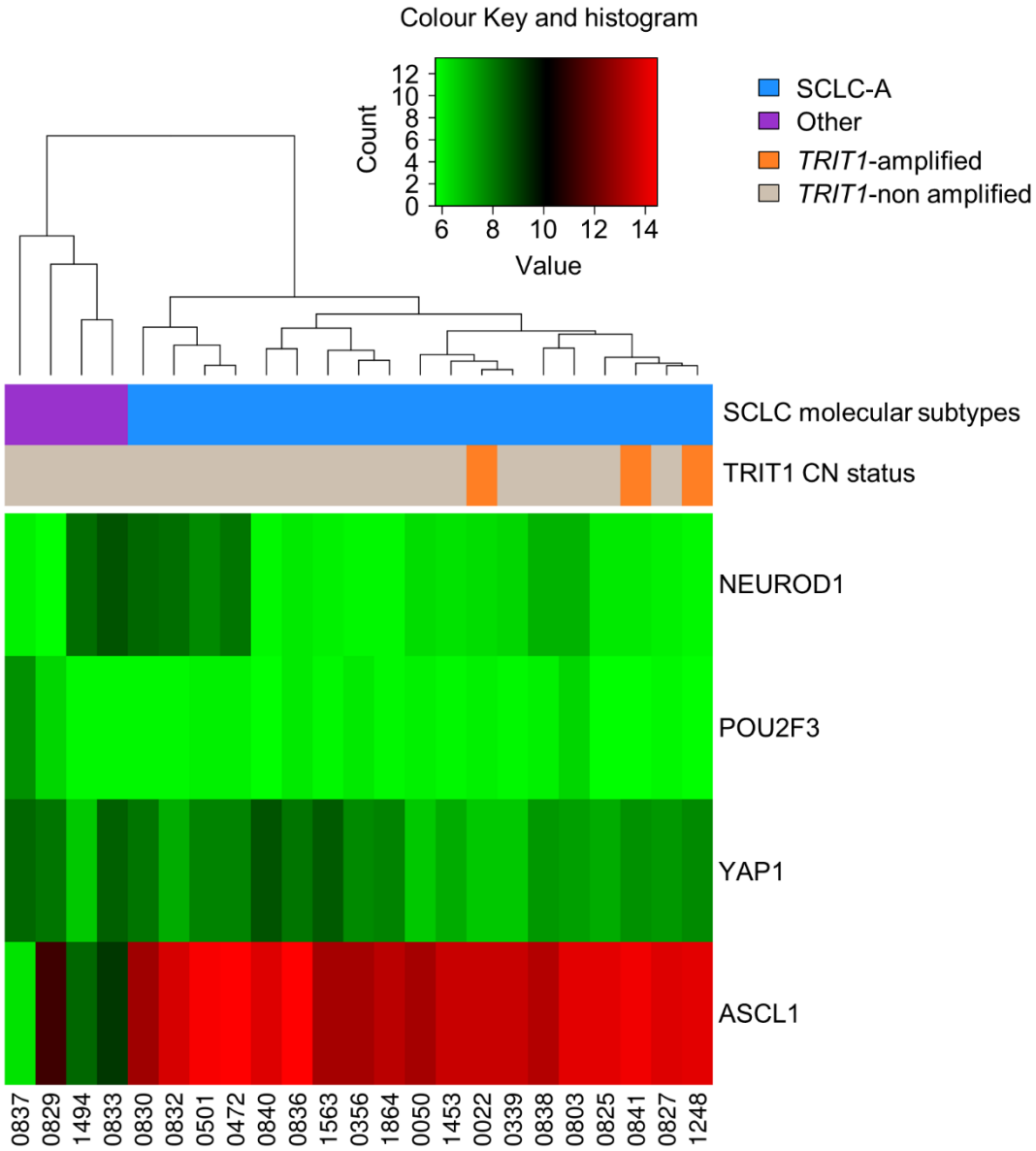

Figure 35. Molecular classification of SCLC tumour samples and *TRIT1* copy number (CN) status. The 23 samples with matched CN and gene expression data were used to perform a hierarchical clustering, and heatmap representation of the expression values of the four genes (*ASCL1*, *NEUROD1*, *POU2F3*, *YAP1*) used to classify SCLC samples as described by Rudin C.M et al. [34]. The vast majority of the samples (19 out of 23) can be classified as SCLC-A by showing significantly higher *ASCL1* expression (Wilcoxon rank-sum test p-value = 0.0023). *TRIT1* copy number status is also denoted.

The results derived from this study were published in *Cancers* journal (Coll-SaMartín et al., 2021), available at: https://www.mdpi.com/2072-6694/13/8/1869/htm. DOI: 10.3390/cancers13081869 [302].

For my experience in FISH, I also participated in another study which objective was to identify Cancer of Unknown Primary (CUP) patients with *FGFR2* rearrangements that could benefit from the treatment with pemigatinib, recently approved (2020) by the US Food and Drug Administration (FDA). This study is summarizedin the Annex section.

V. DISCUSSION

V. DISCUSSION

The epitranscriptomic field has experienced a development boost in the last few years, mainly associated to the technological advances. Previously unknown modifications have been discovered in all life domains as well as the enzymes that incorporate and detect them. Our group has already demonstrated key roles of epitranscriptomics players in colon cancer [187], glioma [303], and NSCLC [304] and we continue to explore this field to broad our knowledge about the impact of epitranscriptomics in cancer with the main goal of providing information that guide novel approaches to improve the clinical management of cancer patients.

RNA modifications have a crucial role in the RNA life cycle and functions. Disruptions in RNA modification patterns and enzymes have been associated with numerous diseases. In particular, the epitranscriptome has been described to participate in acquiring the different hallmarks of cancer, partially through alterations in the genes encoding the related enzymes [62].

This fact encouraged us to focus our research on the identification of alterations in key epitranscriptomic players occurring in cancer. Specifically, we investigated genetic and epigenetic alterations that would affect transfer RNAs modifications, which are the most tightly modified.

***TRIT1* gene is amplified in small cell lung cancer (SCLC).**

Transfer RNAs have a central role in translation, consequently impacting protein synthesis. Control of translation is readjusted in cancer to cope with the protein needs of the tumour, which triggers changes in cell proliferation and cell fate [85,305]. It is well known that genetic alterations are involved in malignancy transformation. Moreover, epigenetic effects through promoter CpG methylation and histone marks changes have been vastly described in cancer [306]. After data-mining the copy number and DNA methylation data for tRNA modifier enzymes in about 1000 cell lines, the frequency of *TRIT1* gene amplification in small cell lung cancer (SCLC) caught our attention (**Figure 13**). SCLC is characterised by rapid growth, aggressive invasion, and early metastasis. Patients usually have metastatic disease at the time of presentation and diagnosis. The first and second-line standard treatments have been barely changed for several decades. Although patients initially respond well to cytotoxic therapy, tumour recurrence

frequently occurs within the first 2 years after treatment with the development of acquired drug resistance. Due to the lack of effective drugs for second-line chemotherapy, the 5-year survival rate of SCLC patients is lower than 5% [307]. The lack of driver oncogenic-activating genetic events, in contrast to the common loss-of-function events, have seriously difficulted the identification of actionable targets that can be efficiently targeted by drugs. Almost all SCLC cell lines showed characteristic TP53 and RB1 loss-of-function events. For instance, RB1 inactivating mutations, even prevalent in SCLC, lack intrinsic factors that guide the design of small chemical inhibitors [308].

Thus, the identification of the cancer-specific amplification of *TRIT1* gene in SCLC was the starting point of an exhaustive study. We focused on evaluating the implication of this event in tumorigenesis, as well as its potential as a drug target candidate.

The *TRIT1* gene amplification in cancer cell lines (**Figures 13, 15**) and SCLC primary samples (**Figure 34**) was associated to a significant increase at transcriptional and protein levels (**Figures 14, 16, 34**).

In healthy cells, TRIT1 partially isopentenylates adenosine 37 [212], but amplification and tumoral conditions might increase the modification rate. The modification proportion deviation can change the translation process, as occurs with mcm^5s^2U34-related enzymes overexpression in $BRAF^{V600E}$ mutated melanoma cells that favour the hypoxia-induced factor 1α (HIF1α) translation promoting tumour progression [141].

In order to elucidate the functional role of TRIT1 amplification in SCLC in tumorigenesis, we assessed the consequences of decrease the expression of TRIT1 using the shRNA approach in the *TRIT1*-amplified DMS-273 SCLC cell line. In agreement with previous reports in the literature [212], the level of isopentenyladenosine decreased upon decreasing TRIT1 expression (**Figure 18**) and, so does the level of ms^2i^6A (**Figure 19**), the hypermodification introduced after i^6A in some mitochondrial tRNAs.

We first evaluated several processes frequently altered in cancer using classical *in vitro* assays of cell proliferation, colony formation capacity, cell cycle, apoptosis, senescence, and endoplasmic reticulum (ER) and mitochondrial stress; by comparing the results obtained in the parental DMS-273 *TRIT1*-amplified cell line vs. the knockdown (DMS-273 shTRIT1).

We speculated that changes in the tRNA modification level and, therefore, in translation might have affected the cellular division rate. Actually, it has been described that NSCLC

cell lines transfected with TRIT1 show a reduction in colony formation [211]. However, cell proliferation analysis using MTT and clonogenicity assays revealed no changes in cell proliferation or colony formation *in vitro* upon TRIT1 knockdown in the DMS-273 *TRIT1*-amplified SCLC cell line (**Figure 20**). We neither detected differences in cell cycle after TRIT1 knockdown, neither in the flow cytometry analysis by propidium iodide nor by the expression of CDN1A, involved in the mitotic arrest in G1 / S and G2 / M (**Figure 21**). Negative results were also obtained when we explored the role of TRIT1 in apoptosis and senescence, evaluated by Annexin V flow cytometry (**Figure 22**), and the activity of the enzyme β-galactosidase, respectively (**Figure 23**).

Considering the lack of effects of restoring the TRIT1 levels to basal-like conditions in the DMS-273 *TRIT1*-amplified SCLC cell line observed upon the analyses of the classical *in vitro* assays to study cancer-related features, we decided to investigate more specific processes related to the TRIT1 molecular functions.

Modifications in $tRNA^{[Ser]Sec}$ have been related to oxidative stress, as some selenoproteins have a role in reducing ROS [309]. Although oxidative stress can be toxic for the tumour for raising genomic instability and mutation, can also enhance tumorigenesis in some contexts [211,310]. Consequently, selenoproteins can have both positive and negative effects on the tumour. Also, it has been described that patients with mutations in *TRIT1* gene show combined oxidative phosphorylation deficiency 35 (COXPD 35), a combined OXPHOS deficiency [216,311] that could trigger mitochondrial stress. Apart from that, seven selenoproteins localise to the endoplasmic reticulum maintaining its homeostasis. Cancer cells might be dependent on the role of some selenoproteins in unfolded protein response [264,312] and being affected by the decrease in $tRNA^{[Ser]Sec}$ modification. Altogether encouraged us to study ER and mitochondrial stress, but we did not observe changes upon TRIT1 knockdown (**Figure 24**).

As *in vitro* assays did not provide keys to elucidate the role of TRIT1 in cancer, we decided to go one step further and perform *in vivo* assays in mice. In contrast with 2D cell cultures, murine models are able to provide the proper microenvironment to better recapitulate key molecular processes occurring in tumour cells. The interactions with the stroma, the activation of specific molecular pathways and the triggering of inflammatory responses could favour the tumour development [272] and provide the optimal scenario to unravel the functional effects of TRIT1 deregulation. In fact, after subcutaneous injection of parental *TRIT1*-amplified or shTRIT1-silenced cells in mice, we observed a

significant reduction in tumour growth upon TRIT1 knockdown, providing a robust evidence of the impact of *TRIT1* amplification in cancer (**Figure 25**).

Consequences of TRIT1 overexpression in transcription

Aimed to further identify specific molecular pathways and/or biological processes governing the TRIT1 cancer-related roles, as well as potential target genes whose expression could be modulated by i^6A modification levels in the context of SCLC, we carried out massive RNA sequencing of the loss-of-function model in the DMS-273 cell line. The capability to evaluate the entire transcriptome makes RNA sequencing an ideal strategy to study the ultimate transcriptional consequences. After computational analysis, 4510 differential expressed mRNA were identified. Notably, 3409 (75.9%) of these mRNAs were found downregulated upon TRIT1 depletion reflecting the significant impact of i^6A hypomodification (**Figure 26**).

We performed a gene set enrichment analysis (GSEA) from the downregulated genes and graphed the overrepresented GO biological processes. The most enriched process upon TRIT1 depletion was “regulation of cell differentiation”. Considering this interesting finding, from the genome-wide transcriptomic approach (RNAseq), we selected a set of genes with key roles in gene differentiation for further validation:

- Inhibitor Of DNA Binding 1, HLH Protein (ID1) and Inhibitor Of DNA Binding 3, HLH Protein (ID3) are basic helix-loop-helix (bHLH) proteins that lack a DNA binding domain. bHLH proteins form dimers or heterodimers that bind to DNA and activate gene transcription, but they cannot bind to DNA when the dimer contains an ID protein. Thus, ID proteins act as dominant-negative regulators of transcription [276,313]. ID proteins have been reported to be upregulated in cancer cells, more interestingly in SCLC the ID upregulation has been associated with the malignant phenotype [314]. ID1 has a role in regulating proliferation and differentiation, and is considered a tumour promoter [276]. Moreover, it has been described that the suppression of ID3 significantly suppressed tumorigenesis in nude mice [275].
- Collagen Type III Alpha 1 Chain (COL3A1) composes type III collagen, a major structural component usually found in extensible connective tissues such as skin, lung, uterus, intestine and the vascular system [315]. COL3A1 play roles in cell adhesion, migration, proliferation, and differentiation via interactions with cell-surface receptor integrins [316-318]. COL3A1 is upregulated in various cancers,

and its expression is correlated with the tumour immune microenvironment and pan-cancer prognosis [278,319]. Moreover, upregulation of COL3A1 expression has been associated to smoking-related NSCLC [320].

- Metallothionein 1X (MT1X) is a metallothionein (MT), a small cysteine-rich protein. Numerous studies have revealed a relationship between MT expression and tumour differentiation [280]. Moreover, MT1X was significantly overexpressed in highly metastatic NSCLC compared with weakly metastatic cells [321].
- Laminin Subunit Alpha 4 (LAMA4) belongs to the laminin family, extracellular glycoproteins that play essential roles in providing a microenvironment for cell functions through the regulation of cell differentiation, migration, and adhesion [322-324]. Furthermore, LAMA4 overexpression has been described in angiotropic melanoma areas [323].
- Angiopoietin Like 4 (ANGPTL4) protein belongs to a superfamily of secreted proteins. ANGPTL4 has a highly multifaceted roles in cell differentiation and tumorigenesis, among others [325-327]. ANGPLT expression has been found upregulated in several tumour types including breast tumours, basal cell carcinoma, melanoma, and gallbladder cancer [284,328-332].
- Glutathione Peroxidase 4 (GPX4) is a selenoprotein whose expression can be triggered by differentiation [333]. There is controversy about GPX4 role in carcinogenesis. It has been proved that GPX4 sustains detoxification and prevents the triggering of cell death programs like the recently described ferroptosis. Consequently, tumours require inhibition of ferroptosis to sustain proliferation [334-336]. However, some studies have determined that GPX4 may function as a tumour suppressor in some contexts [337-339].

The downregulation of these genes upon TRIT1 knockdown identified by RNAseq, was successfully validated by RT-qPCR (**Figure 28A**). From the selected candidates, GPX4 is, in our TRIT1 context, the most interesting gene because it is a selenoprotein that depends on the $tRNA^{[Ser]Sec}$ to be translated, directly linking the finding with the molecular role of TRIT1. Moreover, we observed a reduction in GPX4 protein expression upon shTRIT1 (**Figure 28B**).

TRIT1 amplification is a sensitivity marker for arsenic trioxide (As_2O_3) and dimethyloxalylglycine (DMOG).

The identification of cell differentiation as a key biological process affected by the deregulation of TRIT1 provided clues about how *TRIT1* amplification could be a realistic drug-targeting candidate, a crucial aspect considering the limited potentially targetable molecular lesions in SCLC. Some drugs have been proved to affect differentiation in a variety of primary tumour cells [295]. Remarkably, it has been shown that arsenic trioxide (As_2O_3) can induce differentiation in patients with acute promyelocytic leukaemia (APL) [340,341]. Furthermore, in our TRIT1-related context, As_2O_3 is an interesting drug for its described interaction with selenium and selenoproteins [150,287,342]. In addition, Sobh et al. observed that disruption of enzymes involved in selenocysteine metabolism and, therefore, selenoprotein synthesis results in a decreased tolerance to As_2O_3 [343]. *In vitro* studies showed that As_2O_3 also induces cell death, DNA damage and changes in levels of stress-related proteins in lung cell lines [344].

Arsenic compounds have been used for more than 2000 years for different cultures as Chinese, Greek and Indian [292]. First, well-known as a poison, its virtue as a medicine to successfully treat several diseases including syphilis became As_2O_3 an attractive therapeutic agent. Importantly, As_2O_3 can not only be administrated by intravenous infusion, but also by oral routes, simplifying its use in the clinical practice [292,345,346]. In 2000, the FDA approved the use of As_2O_3 for the treatment of APL [347]. As_2O_3 has demonstrated strong clinical benefits as a single agent in APL, with a 5-year disease-free survival rate around 70% [348]. Moreover, As_2O_3 has shown to decrease the incidence of relapse in *de novo* APL [349]. The success of As_2O_3 in APL treatment has encouraged to test its use in other haematological malignancies and, also solid tumours including glioma, hepatocellular carcinoma and, bladder, cervical, colorectal, liver and lung cancers [345,349,350].

Remarkably, previous *in vitro* and *in vivo* studies support the anti-tumour benefits of (As_2O_3) in SCLC [351]. When we tested As_2O_3 in our cells, we observed sensitivity to this drug in the TRIT1-amplified cell lines that was significantly decreased upon TRIT1 depletion (**Figures 29, 31**). More relevant, *in vivo* experiment reinforced our findings with the decreased tumour burden observed in the As_2O_3-treated DMS-273-derived tumours, in comparison with the ones with vehicle (**Figure 30**), an effect abolished in the TRIT1-depleted DMS-273 cells. Altogether, *in vitro* and *in vivo* analyses confirmed the potential of TRIT1 amplification as a master of sensitivity to arsenic trioxide.

We also followed a computational approach to widen the drug candidates to treat small cell lung tumours harbouring TRIT1 gene amplification. Our group participated in a multiomic study to identify genomic and epigenomic alterations associated to drug sensitivity [258], findings summarized in the Genomics of Drug Sensitivity in Cancer Web portal of the Welcome Sanger Institute that holds the IC50 values for more than 200 compounds for 1000 human cancer cell lines [258]. These pharmacogenomic screens in SCLC cell lines revealed a negative correlation between TRIT1 overexpression and resistance to dimethyloxalylglycine (DMOG), and our *in vitro* studies confirmed this finding (**Figure 32**). DMOG is a synthetic analogue of α-ketoglutarate that acts as a competitive inhibitor of prolyl-4-hydroxylase domain protein used for hypoxia-inducible factors (HIFs) stabilisation [352,353]. HIFs regulates more than 150 genes involved in tumour metastasis, angiogenesis, energy metabolism, cell differentiation, and apoptosis [354-356], highlighting the potential of this drug.

Although the addition of the immune checkpoint blockade to the therapeutic arsenal against SCLC was a significant improvement after several decades of standard chemotherapy treatment [30,35], the FDA approved use of the anti-PD-L1 inhibitor atezolizumab in combination with carboplatin plus etoposide chemotherapy to treat extensive-stage disease, has shown only a modest clinical effect [31]. Thus, one of our more relevant findings in this study has been to identify a novel actionable alteration, that could provide novel therapeutic opportunities for SCLC patients. Although further validation in larger cohorts of patients is needed, we propose the gene amplification-associated overexpression of the tRNA modifier TRIT1 in SCLC as an optimal *bona fide* target candidate that points out sensitivity towards arsenic trioxide and DMOG treatments.

TRIT1 amplification in SCLC patients

Despite SCLC and NSCLC presenting similar diagnostic symptoms, the fastest-spreading is of SCLC, and consequent usual diagnosis at already metastatic stages entails a poor survival [357]. This fact also affects the availability of primary tumour samples for research. For this study, we were able to analyse 39 primary tumour samples, as well as a collection of 68 cases with available SNP array data [301].

More than a tenth of the analysed cases with SCLC cancer showed amplification of the *TRIT1* gene: 4 of 39 from the first cohort (10.3%, **Table 7),** and 10 of 68 from the second cohort (14.7%). The analysis of these two sets of SCLC patients was key to demonstrate

that *TRIT1* gene amplification in SCLC is not only limited to cell lines, but it happens in primary tumour samples.

Our results show the relevance of an epitranscriptomic alteration in cancer and widen the current knowledge about TRIT1 enzyme and i^6A modification roles in malignancy progression. We detected *TRIT1* gene amplification both in cancer cell lines and primary tumour samples. *In vivo* analysis demonstrated the impact of TRIT1 amplification in tumorigenesis. The identification of cell differentiation as a key biological process affected by the TRIT1 deregulation leads us to discover the sensitivity of *TRIT1*-amplified cells to arsenic trioxide, a finding complemented with the identification of DMOG by the computational approach. Our work also highlights the need to further explore the molecular mechanisms involved in SCLC tumorigenesis to provide new therapeutic opportunities to better tailor treatment decisions in the precise medicine era. Finally, it is also essential to potentiate all the strategies to eradicate tobacco consumption in the population, the leading cause of SCLC as well as a vast range of cancers and diseases.

VI. CONCLUSIONS

VI. CONCLUSIONS

1. The tRNA modifier *TRIT1* gene is amplified in 18.3% of small cell lung cancer (SCLC) cell lines, the most lethal and aggressive subtype of lung cancer.
2. *TRIT1* gene amplification occurs in about 10-15% of SCLC patients.
3. *TRIT1* amplification leads to an increase of its expression at the transcriptional and translational levels.
4. The depletion of TRIT1 expression decreases the levels of i^6A-modified nucleoside, as shown in the loss-of-function model generated in DMS-273 *TRIT1*-amplified SCLC cell line.
5. The reduction of i^6A-modified nucleoside leads to a reduction of ms^2i^6A in some mitochondrial tRNAs, including mt-$tRNA^{Ser(NGA)}$, mt-$tRNA^{Trp}$ and mt-$tRNA^{Tyr}$.
6. *TRIT1* gene amplification increases the tumorigenic potential, as evidenced by the decreased tumour growth achieved by the tumours derived from *TRIT1*-depleted cells, in comparison with those derived from *TRIT1*-amplified cells, in murine models.
7. The shRNA-based TRIT1 depletion in the DMS-273 cells with gene amplification altered the levels of 4510 mRNAs, decreasing the expression of 75.6% of them, including genes related to differentiation.
8. The gene amplification-associated overexpression of *TRIT1* confers sensitivity to arsenic trioxide and dimethyloxalylglycine (DMOG), as shown *in vitro* cellular assays and *in vivo* experiments in mice.

VII. ANNEX

VIII. ANNEX: Detecting FGFR2 rearrangements in Cancer of Unknown Primary as a potential therapeutic target.

I. Introduction

1. FGFR2 fusion proteins in intrahepatic cholangiocarcinoma.

Fibroblast Growth Factor Receptor 2 (FGFR2) is a cell-surface receptor tyrosine kinase (RTK) for fibroblast growth factors. FGFR2 plays a key function in regulating development, and other cellular functions such as proliferation and apoptosis. FGFR2, in association with heparin sulphate proteoglycans, dimerises and autophosphorylates. Then, FGFR2 can phosphorylate downstream adaptor proteins [358,359].

FGFR2 gene, located in 10q26.13, is often disrupted by chromosomal translocations during tumour initiation and progression, that can result in oncogenic fusion proteins. The resulting in-frame fusion proteins usually are composed of an N-terminal FGFR2 moiety retaining an intact kinase domain fused and a C-terminal partner gene which contains a dimerisation/oligomerisation domain. These fusion proteins lack the FGFR2 regulation becoming constitutively dimerised and, hence, constitutively activated. In turn, they activate several oncogenic downstream pathways. There are more than 150 known FGFR2 fusion partners such as Periphilin 1 (PPHLN1), Adenosylhomocysteinase Like 1 (AHCYL1), Bicaudal family RNA binding protein 1 (BICC1), Transforming Acidic Coiled-Coil Containing Protein 3 (TACC3), Meningioma Expressed Antigen 5 (Hyaluronidase) (MGEA5), and Shootin 1 (KIAA1598) [358,360]. Moreover, a single tumour can carry more than one FGFR2 fusion [358,361,362]. FGFR2 fusions can be found in different cancer types, but the highest frequency (15%) is found in intrahepatic cholangiocarcinoma (ICC) [359,361,363-365].

ICC is a subtype of cholangiocarcinoma, cancer that originates from the cells of the biliary tract. It represents 10-20% of all primary liver cancer [366], and is one of the most fatal malignancies with very limited treatment options that is usually diagnosed at an advanced unresectable stage [367-369].

Pemigatinib (INCB054828) is a highly selective FGFR-inhibitor that has been recently approved (2020) by the US Food and Drug Administration (FDA) for the treatment of cholangiocarcinoma patients harbouring FGFR2 fusions or rearrangements [370,371]. This approval was based on the FIGHT-202 open-label single-arm phase II study that demonstrated a survival benefit of pemigatinib on patients with FGFR2 fusions [372]. Pemigatinib binding to FGFR1/2/3 results in the inhibition of the downstream signal pathways, and consequently inhibits proliferation on FGFR1/2/3-overexpressing tumour cells.

2. Cancer of Unknown Primary (CUP).

Cancer of Unknown Primary (CUP) is a heterogeneous group of confirmed metastatic tumours that lack an identifiable primary tumour, despite a standardized diagnosis work-up [373]. They account for 3–5% of all human cancers [374,375]. Most of CUP patients (80-85%) have an unfavourable prognosis with a dismal survival of 3-6 months, despite empirical chemotherapy treatments. CUPs present a higher chromosomal instability compared to metastasis of known origin [376].

CUP aggressiveness and the limited treatment options result in poor outcomes [377,378]. Currently, treatment for CUPs mainly depends on clinical presentation as there is no existing standard chemotherapy, neither prognostic and predictive biomarkers [378,379]. Our laboratory developed EPICUP, a DNA methylation-based assay that allows us to identify the primary tumour site in CUPs [380]. Our and other studies have shown that the use of tumour-type specific therapies leads to improved outcomes. However, the occurrence of shared molecular alterations in different tumour types has supposed the emergence of tissue-agnostic approaches and basket trials which eligibility is based on the presence of specific genetic alterations, irrespective of histology. Identification of actionable alterations in CUP patients could improve the dismal outcome.

II. Objective

Identify CUP patients with *FGFR2* rearrangements that could benefit from the treatment with pemigatinib.

III. Material and Methods

1. Cell Lines.

The HUT-78 cutaneous cell-lymphoma cell line (American Type Culture Collection, ATCC), and the SNU16 gastric adenocarcinoma and NCI-H716 colorectal adenocarcinoma cell lines (kindly provided by Dr Diego Arango, Institut de Recerca Hospital Vall d'Hebron) were used for this study. Cells lines were cultured according to the supplier's indications. HUT-78 was cultured with Iscove's Modified Dulbecco's Medium (IMDM, Gibco). SNU16 and NCI-H716 were cultured with Roswell Park Memorial Institute (RPMI1640, Gibco). Culture medium was completed with 10% foetal bovine serum (FBS, Gibco, Waltham, MA, USA) and 1% penicillin/streptomycin (Invitrogen, Carlsbad, CA, USA). Cells were cultured at 37°C with 5% (v/v) of CO2. All cell lines tested negative for mycoplasma.

Cells were centrifugated and preserved in formalin-fixed, paraffin-embedded (FFPE) blocks in order to mimic a tumour tissue, as usually preserved in the clinical practice, to optimize the experimental approaches to assess CUP samples.

2. Human Biological Samples.

We analysed 52 CUP samples collected through collaborations with hospitals and health institutions. Samples derived from surplus of biological material used for diagnostic tests. Patient informed consents were signed, according to Biomedical Research law 14/2007. Comprehensive clinical information was collected, processed, and stored under confidentiality policies, following current legislation regarding personal data protection. Biological samples were identified with a code that was used by the researchers.

Tumour samples preserved in FFPE tissue blocks were cut in 5 µm thick slices and placed on glass slides.

Haematoxylin and eosin (H&E) stained slides were used to identify the optimal region of the tumour to perform the Fluorescence *in situ* hybridisation (FISH).

3. Fluorescence *in situ* hybridisation (FISH) on Formalin-Fixed Paraffin-Embedded (FFPE) tissues.

FFPE sections were incubated at 65ºC for 25 min and deparaffinised with xylene. Later, the slides were dehydrated in absolute ethanol and immersed in 1X SSC at 86ºC for 30 min. After a water cleaning, the samples were digested with Pepsin (01N31-005, Abbott, Lake County, Illinois, USA) at 37ºC, and next, dehydrated in absolute ethanol. Then, samples were hybridised overnight with the probe Vysis 10q26 FGFR2 Break Apart FISH Probe Kit (09N23-060, Abbott) according to the manufacturer’s instructions. Before

microscope analysis, slides were washed with 2X SSC/0.3% Tween at 73ºC and stained with DAPI.

Cell line images were acquired in the Cytogenetics Platform of the Institut Català d'Oncologia (ICO)-Hospital Germans Trias i Pujol (IGTP) (Barcelona, Spain). Tumour sample images were acquired by Atrys Health (Barcelona, Spain).

IV. Results

1. Detection of *FGFR2* rearrangement in control cell lines.

In order to optimise the FISH assay to detect *FGFR2* rearrangements, we used previously characterised cell lines. To mimic a sample tissue, pelleted cells were fixed with formalin and embedded in paraffin. Then, samples were hybridized with the FGFR2 Break Apart FISH Probe (Abbott). In this break apart design, the red probe targets the 3' region of the *FGFR2* gene while the green probe targets the 5' region of the *FGFR2* gene and the Arginyltransferase 1 (*ATE1*) neighbour gene (**Annexed Figure 1**). When there are no signals of the split, two pairs of closely approximated or fused signals (yellow) are observed; meanwhile, if there is a *FGFR2* rearrangement, the two colours are clearly distinguished.

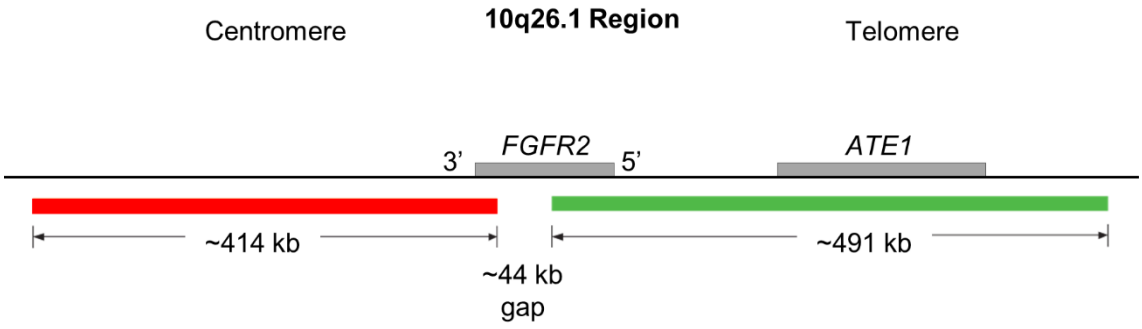

Annexed Figure 1. *FGFR2* break-apart FISH probe (Abbott). Dual colour probe involving the chromosomal region 10q26.1. Red probe targets the 3' region of the *FGFR2* gene and green probe targets the 5' region of the *FGFR2* gene and the *ATE1* gene.

We selected three previously characterised cell lines, the SNU16 and NCI-H71 harbouring *FGFR2* rearrangements, and the HUT-78 cell line as a negative control. HUT-78 was karyotyped by Chen T. R. in 1992, showing that this cell line presents a hypodiploidy affecting chromosome 10 [381]. Also, the patient from which HUT-78 was

derived had mycosis fungoides and Sezary syndrome that has been associated with deletions in chromosome 10q [382]. In agreement, we observed the described hypodiploidy upon FISH assay. HUT-78 cells present nucleus with 1 or 2 copies of *FGFR2* and *ATE1* genes without rearrangements (**Annexed Figure 2A**).

In the SNU16 cell line, the *FGFR2* rearrangement involves the 5' region of the *APIP* gene (11p13) and the 3' region of the *FGFR2* gene. In addition, a high level of amplification of this rearrangement has been reported [383]. In the FISH assay, we observed that some nucleus present *FGFR2* and *ATE1* co-amplification, the two genes covered by the probe in red (3' region) and green (5' region), and others amplification and rearrangement (break-apart) (**Annexed Figure 2B**).

In the NCI-H716 colorectal cancer cell line, the previously reported *FGFR2* amplification [384,385] seriously hindered the detection of the previously described FGFR2-COL14A1 fusion [384,386] and it was difficult to define if the red and green-probes co-localised or there break-apart (**Annexed Figure 2C**).

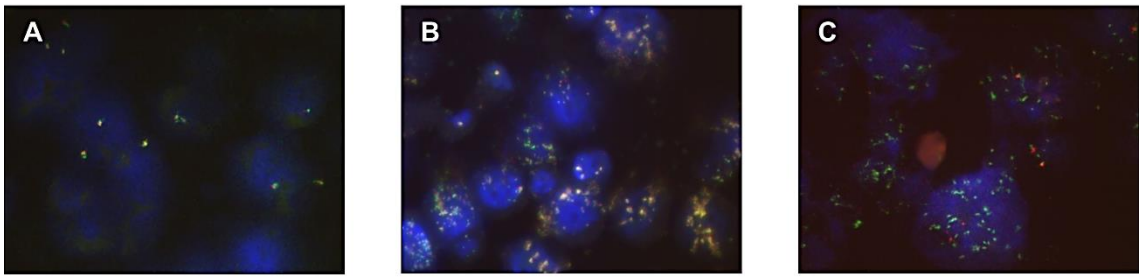

Annexed Figure 2. *FGFR2* break-apart FISH analysis of control cell lines. **(A)** HUT-78 cells present nucleus with 1 or 2 copies of *FGFR2* and *ATE1* genes without rearrangement. **(B)** In SNU16 cells some nucleus present co-amplification of *FGFR2* and *ATE1* genes, others amplification and rearrangement (break-apart). **(C)** NCI-H716 cells present an amplification that includes *FGFR2* gene (5' region) and *ATE1* gene.

2. Detection of FGFR2 rearrangement in CUP samples.

We performed a histopathological analysis of 52 CUP samples previously stained with haematoxylin and eosin to define the proper region for FISH. In preliminary analysis, four samples were discarded due to the lack of tumoral tissue. Once selected the optimal tumoral region, we hybridised the sample with the FGFR2 Break Apart FISH Probe (**Annexed Figure 1**).

After excluding 8 cases due to failed probe hybridisation, we analysed 40 samples. From them, we were able to identify a *FGFR2* rearrangement in one CUP case (CGC-43, **Annexed Figure 3**); meanwhile, 39 cases were negative for FGFR2 break-apart. The 26% of the analysed nucleus of the CGC-43 case were positives for the *FGFR2* split. The positive sample was resected from the peritoneum, the serous membrane that lines the abdominal cavity.

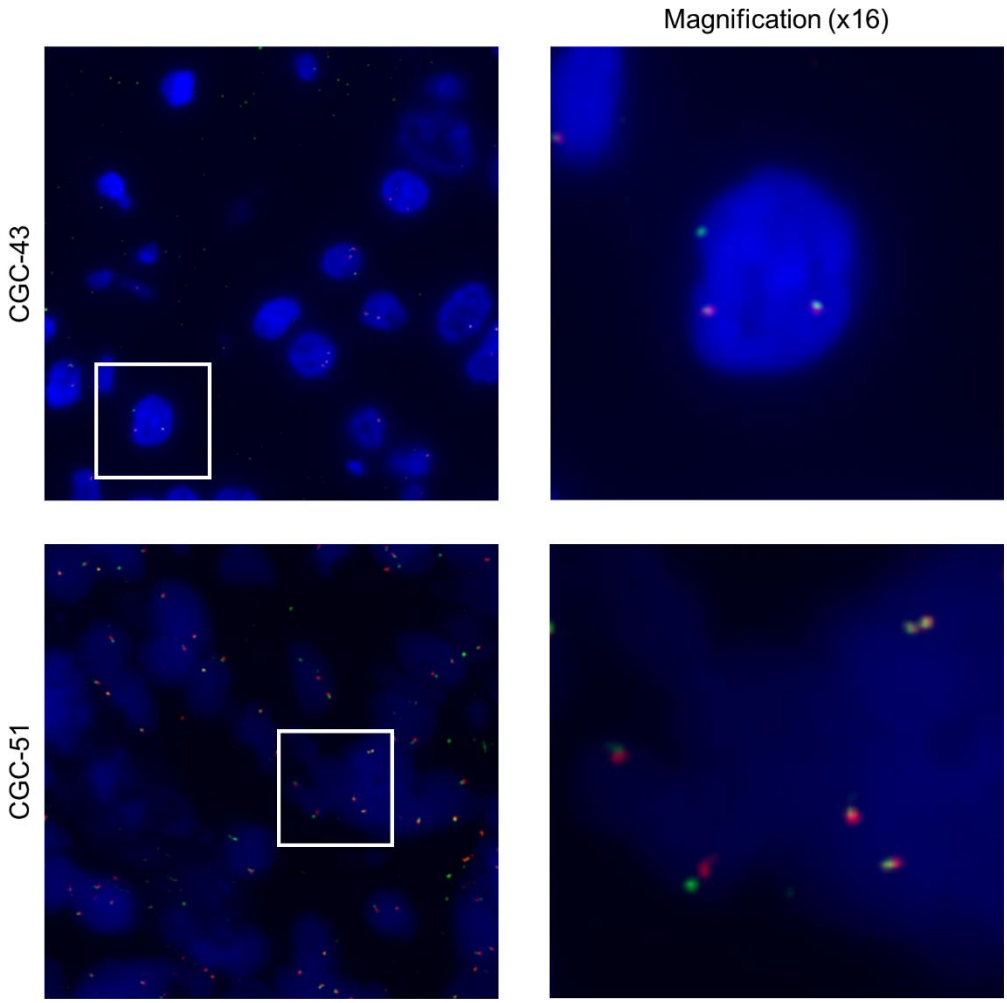

Annexed Figure 3. *FGFR2* break-apart FISH analysis in Cancer of Unknown Primary (CUP) patient samples. FGFR2 rearrangement was detected in the CGC-43 case (upper panel). A negative representative example without FGFR2 rearrangement (CGC-51) is shown in the lower panel.

V. Discussion and Conclusions

Genomic characterization of tumours and emergence of target therapies and personalized medicine have changed the panorama of clinical management in several cancer types. Moreover, novel precision oncology trial designs, such as basket trials, which eligibility is based on the presence of a specific genomic alteration, irrespective of histology, are an efficient strategy for patients with tumours harbouring actionable alterations.

However, the relatively low incidence of CUPs could be one of the reasons why this orphan disease does not significantly benefit from the progress of precision oncology. The recently demonstrated efficacy of pemigatinib in cholangiocarcinomas with FGFR2 fusions or rearrangements encouraged us to evaluate the presence of *FGFR2* rearrangements in CUP cases, to assess the potential of pemigatinib as therapeutic strategy for this orphan disease.

The identification of an *FGFR2* rearrangement in one of the 39 CUP cases assessed in this study is a *proof-of-concept* that the identification of the status of actionable targets for existing drugs could open new therapeutic opportunities for CUP patients.

Considering the clinical challenge of diagnosing a CUP, the identified *FGFR2*-rearranged CUP case could be an intrahepatic cholangiocarcinoma (ICC) misdiagnosed as CUP. Remarkably, the peritoneum, the anatomic site of the analysed tissue, is one of the most common metastasis sites of cholangiocarcinoma [387,388]. Our results encourage to study additional cohorts of patients, as the identification of *FGFR2* rearrangements in a subset of CUP patients would represent a great milestone for management of this disease guiding treatment decision towards a more effective tailored therapy, as the use of pemigatinib.

Moreover, the break-apart FISH assay, commonly used to identify gene translocations events on formalin-fixed, paraffin-embedded (FFPE) material [389], is an easy-to-use technique and also relatively inexpensive, both key features in the clinical practice. Considering the dismal prognosis of CUP patients, with a 1-year survival rate that hardly reaches 25%, we need to increase our efforts to expand the therapeutic alternatives beyond the empirical chemotherapy.

VIII. REFERENCES

VII. REFERENCES

1. Ferlay, J.; Laversanne, M.; Ervik, M.; Lam, F.; Colombet, M.; Mery, L.; Piñeros, M.; Znaor, A.; Soerjomataram, I.; Bray, F. Global Cancer Observatory: Cancer Today. Available online: https://gco.iarc.fr/today (accessed on 3 May).
2. Siegel, R.; Miller, K.; Fuchs, H.; Jemal, A. Cancer Statistics, 2021. *CA: a cancer journal for clinicians* **2021**, *71*, doi:10.3322/caac.21654.
3. Esteller, M.; Pandolfi, P. The Epitranscriptome of Noncoding RNAs in Cancer. *Cancer discovery* **2017**, *7*, doi:10.1158/2159-8290.CD-16-1292.
4. Llinàs-Arias, P.; Esteller, M. Epigenetic inactivation of tumour suppressor coding and non-coding genes in human cancer: an update. *Open biology* **2017**, *7*, doi:10.1098/rsob.170152.
5. Hanahan, D.; Weinberg, R. The hallmarks of cancer. *Cell* **2000**, *100*, doi:10.1016/s0092-8674(00)81683-9.
6. Hanahan, D.; Weinberg, R. Hallmarks of cancer: the next generation. *Cell* **2011**, *144*, doi:10.1016/j.cell.2011.02.013.
7. *World Cancer Report 2014*; Stewart, B., Wild, C., Eds.; IARC: Lyon, France, 2014.
8. Hecht, S. Lung carcinogenesis by tobacco smoke. *International journal of cancer* **2012**, *131*, doi:10.1002/ijc.27816.
9. SEER Cancer Stat Facts: Lung and Bronchus Cancer. Available online: https://seer.cancer.gov/statfacts/html/lungb.html (accessed on June).
10. Hirsch, F.; Scagliotti, G.; Mulshine, J.; Kwon, R.; Curran Jr, W.; Wu , Y.; Paz-Ares, L. Lung cancer: current therapies and new targeted treatments. *Lancet (London, England)* **2017**, *389*, doi:10.1016/S0140-6736(16)30958-8.
11. Nasim, F.; Sabath, B.; Eapen, G. Lung Cancer. *The Medical clinics of North America* **2019**, *103*, doi:10.1016/j.mcna.2018.12.006.
12. Travis, W.; Brambilla, E.; Nicholson, A.; Yatabe, Y.; Austin, J.; Beasley, M.; Chirieac, L.; Dacic, S.; Duhig, E.; Flieder, D.; et al. The 2015 World Health Organization Classification of Lung Tumors: Impact of Genetic, Clinical and Radiologic Advances Since the 2004 Classification. *Journal of thoracic oncology : official publication of the International Association for the Study of Lung Cancer* **2015**, *10*, doi:10.1097/JTO.0000000000000630.
13. Herbst, R.; Morgensztern, D.; Boshoff, C. The biology and management of non-small cell lung cancer. *Nature* **2018**, *553*, doi:10.1038/nature25183.
14. *WHO Classification of Tumours of the Lung, Pleura, Thymus and Heart.*, 4t Edition ed.; Travis, W., Brambilla, E., Burke, A.P., Marx, A., Nicholson, A.G., Eds.; IARC: Lyon, 2015; Volume 7.
15. Bernhardt, E.; Jalal, S. Small Cell Lung Cancer. *Cancer treatment and research* **2016**, *170*, doi:10.1007/978-3-319-40389-2_14.
16. Iwakawa, R.; Kohno, T.; Totoki, Y.; Shibata, T.; Tsuchihara, K.; Mimaki, S.; Tsuta, K.; Narita, Y.; Nishikawa, R.; Noguchi, M.; et al. Expression and clinical significance of genes frequently mutated in small cell lung cancers defined by whole exome/RNA sequencing. *Carcinogenesis* **2015**, *36*, doi:10.1093/carcin/bgv026.
17. George, J.; Lim, J.; Jang, S.; Cun, Y.; Ozretić, L.; Kong, G.; Leenders, F.; Lu, X.; Fernández-Cuesta, L.; Bosco, G.; et al. Comprehensive genomic profiles of small cell lung cancer. *Nature* **2015**, *524*, doi:10.1038/nature14664.
18. Liu, J.; Zhang, C.; Hu, W.; Feng, Z. Tumor suppressor p53 and its mutants in cancer metabolism. *Cancer letters* **2015**, *356*, doi:10.1016/j.canlet.2013.12.025.

19. Berry, J.; Polski, A.; Cavenee, W.; Dryja, T.; Murphree, A.; Gallie, B. The RB1 Story: Characterization and Cloning of the First Tumor Suppressor Gene. *Genes* **2019**, *10*, doi:10.3390/genes10110879.
20. Lacroix, M.; Riscal, R.; Arena, G.; Linares, L.; Le Cam, L. Metabolic functions of the tumor suppressor p53: Implications in normal physiology, metabolic disorders, and cancer. *Molecular metabolism* **2020**, *33*, doi:10.1016/j.molmet.2019.10.002.
21. Woodard, G.; Jones, K.; Jablons, D. Lung Cancer Staging and Prognosis. *Cancer treatment and research* **2016**, *170*, doi:10.1007/978-3-319-40389-2_3.
22. *Cancer Principles & Practice of Oncology* 11th edition ed.; DeVita, J.V., Lawrence, T., Rosenberg, S., Eds.; Lippincott Williams & Wilkins (LWW): 2018.
23. Glisson, B. Recurrent small cell lung cancer: update. *Seminars in oncology* **2003**, *30*, doi:10.1053/sonc.2003.50014.
24. Rudin, C.; Brambilla, E.; Faivre-Finn, C.; Sage, J. Small-cell lung cancer. *Nature reviews. Disease primers* **2021**, *7*, doi:10.1038/s41572-020-00235-0.
25. Putora, P.; Glatzer, M.; Belderbos, J.; Besse, B.; Blackhall, F.; Califano, R.; Cappuzzo, F.; de Marinis, F.; Dziadziuszko, R.; Felip, E.; et al. Prophylactic cranial irradiation in stage IV small cell lung cancer: Selection of patients amongst European IASLC and ESTRO experts. *Radiotherapy and oncology : journal of the European Society for Therapeutic Radiology and Oncology* **2019**, *133*, doi:10.1016/j.radonc.2018.12.014.
26. Paz-Ares, L.; Dvorkin, M.; Chen, Y.; Reinmuth, N.; Hotta, K.; Trukhin, D.; Statsenko, G.; Hochmair, M.; Özgüroğlu, M.; Ji, J.; et al. Durvalumab plus platinum-etoposide versus platinum-etoposide in first-line treatment of extensive-stage small-cell lung cancer (CASPIAN): a randomised, controlled, open-label, phase 3 trial. *Lancet (London, England)* **2019**, *394*, doi:10.1016/S0140-6736(19)32222-6.
27. Farago, A.; Keane, F. Current standards for clinical management of small cell lung cancer. *Translational lung cancer research* **2018**, *7*, doi:10.21037/tlcr.2018.01.16.
28. O'Brien, M.; Ciuleanu, T.; Tsekov, H.; Shparyk, Y.; Cuceviá, B.; Juhasz, G.; Thatcher, N.; Ross, G.; Dane, G.; Crofts, T. Phase III trial comparing supportive care alone with supportive care with oral topotecan in patients with relapsed small-cell lung cancer. *Journal of clinical oncology : official journal of the American Society of Clinical Oncology* **2006**, *24*, doi:10.1200/JCO.2006.06.5821.
29. Schulze, A.; Evers, G.; Kerkhoff, A.; Mohr, M.; Schliemann, C.; Berdel, W.; Schmidt, L. Future Options of Molecular-Targeted Therapy in Small Cell Lung Cancer. *Cancers* **2019**, *11*, doi:10.3390/cancers11050690.
30. Taniguchi, H.; Sen, T.; Rudin, C. Targeted Therapies and Biomarkers in Small Cell Lung Cancer. *Frontiers in oncology* **2020**, *10*, doi:10.3389/fonc.2020.00741.
31. Horn, L.; Mansfield, A.; Szczęsna, A.; Havel, L.; Krzakowski, M.; Hochmair, M.; Huemer, F.; Losonczy, G.; Johnson, M.; Nishio, M.; et al. First-Line Atezolizumab plus Chemotherapy in Extensive-Stage Small-Cell Lung Cancer. *The New England journal of medicine* **2018**, *379*, doi:10.1056/NEJMoa1809064.
32. Goldman, J.; Dvorkin, M.; Chen, Y.; Reinmuth, N.; Hotta, K.; Trukhin, D.; Statsenko, G.; Hochmair, M.; Özgüroğlu, M.; Ji, J.; et al. Durvalumab, with or without tremelimumab, plus platinum-etoposide versus platinum-etoposide alone in first-line treatment of extensive-stage small-cell lung cancer (CASPIAN): updated results from a randomised, controlled, open-label, phase 3 trial. *The Lancet. Oncology* **2021**, *22*, doi:10.1016/S1470-2045(20)30539-8.
33. Iams, W.; Porter, J.; Horn, L. Immunotherapeutic approaches for small-cell lung cancer. *Nature reviews. Clinical oncology* **2020**, *17*, doi:10.1038/s41571-019-0316-z.

34. Rudin, C.; Poirier, J.; Byers, L.; Dive, C.; Dowlati, A.; George, J.; Heymach, J.; Johnson, J.; Lehman, J.; MacPherson, D.; et al. Molecular subtypes of small cell lung cancer: a synthesis of human and mouse model data. *Nature reviews. Cancer* **2019**, *19*, doi:10.1038/s41568-019-0133-9.
35. Poirier, J.; George, J.; Owonikoko, T.; Berns, A.; Brambilla, E.; Byers, L.; Carbone, D.; Chen, H.; Christensen, C.; Dive, C.; et al. New Approaches to SCLC Therapy: From the Laboratory to the Clinic. *Journal of thoracic oncology : official publication of the International Association for the Study of Lung Cancer* **2020**, *15*, doi:10.1016/j.jtho.2020.01.016.
36. Hiddinga, B.; Kok, K. Small-Cell Lung Cancer: Is the Black Box Finally Opening Up? *Cancers* **2021**, *13*, doi:10.3390/cancers13020236.
37. Baine, M.; Hsieh, M.; Lai, W.; Egger, J.; Jungbluth, A.; Daneshbod, Y.; Beras, A.; Spencer, R.; Lopardo, J.; Bodd, F.; et al. SCLC Subtypes Defined by ASCL1, NEUROD1, POU2F3, and YAP1: A Comprehensive Immunohistochemical and Histopathologic Characterization. *Journal of thoracic oncology : official publication of the International Association for the Study of Lung Cancer* **2020**, *15*, doi:10.1016/j.jtho.2020.09.009.
38. Gay, C.; Stewart, C.; Park, E.; Diao, L.; Groves, S.; Heeke, S.; Nabet, B.; Fujimoto, J.; Solis, L.; Lu, W.; et al. Patterns of transcription factor programs and immune pathway activation define four major subtypes of SCLC with distinct therapeutic vulnerabilities. *Cancer cell* **2021**, *39*, doi:10.1016/j.ccell.2020.12.014.
39. Cohn, W.; Volkin, E. Nucleoside-5′-Phosphates from Ribonucleic Acid. *Nature* **1951**, *167*, 483-484, doi:doi:10.1038/167483a0.
40. Saletore, Y.; Meyer, K.; Korlach, J.; Vilfan, I.; Jaffrey, S.; Mason, C. The birth of the Epitranscriptome: deciphering the function of RNA modifications. *Genome biology* **2012**, *13*, doi:10.1186/gb-2012-13-10-175.
41. Keith, G. Mobilities of modified ribonucleotides on two-dimensional cellulose thin-layer chromatography. *Biochimie* **1995**, *77*, doi:10.1016/0300-9084(96)88118-1.
42. Zhao, X.; Yu, Y. Detection and quantitation of RNA base modifications. *RNA (New York, N.Y.)* **2004**, *10*, doi:10.1261/rna.7110804.
43. Grosjean, H.; Droogmans, L.; Roovers, M.; Keith, G. Detection of enzymatic activity of transfer RNA modification enzymes using radiolabeled tRNA substrates. *Methods in enzymology* **2007**, *425*, doi:10.1016/S0076-6879(07)25003-7.
44. Chan, C.; Dyavaiah, M.; DeMott, M.; Taghizadeh, K.; Dedon, P.; Begley, T. A quantitative systems approach reveals dynamic control of tRNA modifications during cellular stress. *PLoS genetics* **2010**, *6*, doi:10.1371/journal.pgen.1001247.
45. Addepalli, B.; Limbach, P. Mass spectrometry-based quantification of pseudouridine in RNA. *Journal of the American Society for Mass Spectrometry* **2011**, *22*, doi:10.1007/s13361-011-0137-5.
46. Su, D.; Chan, C.; Gu, C.; Lim, K.; Chionh, Y.; McBee, M.; Russell, B.; Babu, I.; Begley, T.; Dedon, P. Quantitative analysis of ribonucleoside modifications in tRNA by HPLC-coupled mass spectrometry. *Nature protocols* **2014**, *9*, doi:10.1038/nprot.2014.047.
47. Holley, R.; Apgar, J.; Everett, G.; Madison, J.; Marquisee, M.; Merrill, S.; Penswick, J.; Zamir, A. Structure of a Ribonucleic Acid. *Science (New York, N.Y.)* **1965**, *147*, doi:10.1126/science.147.3664.1462.
48. Helm, M.; Motorin, Y. Detecting RNA modifications in the epitranscriptome: predict and validate. *Nature reviews. Genetics* **2017**, *18*, doi:10.1038/nrg.2016.169.
49. Novoa, E.; Mason, C.; Mattick, J. Charting the unknown epitranscriptome. *Nature reviews. Molecular cell biology* **2017**, *18*, doi:10.1038/nrm.2017.49.

50. Jonkhout, N.; Tran, J.; Smith, M.; Schonrock, N.; Mattick, J.; Novoa, E. The RNA modification landscape in human disease. *RNA (New York, N.Y.)* **2017**, *23*, doi:10.1261/rna.063503.117.
51. Motorin, Y.; Helm, M. Methods for RNA Modification Mapping Using Deep Sequencing: Established and New Emerging Technologies. *Genes* **2019**, *10*, doi:10.3390/genes10010035.
52. Chen, D.; Patton, J. Reverse transcriptase adds nontemplated nucleotides to cDNAs during 5'-RACE and primer extension. *BioTechniques* **2001**, *30*, doi:10.2144/01303rr02.
53. van Dijk, E.; Jaszczyszyn, Y.; Naquin, D.; Thermes, C. The Third Revolution in Sequencing Technology. *Trends in genetics : TIG* **2018**, *34*, doi:10.1016/j.tig.2018.05.008.
54. Garalde, D.; Snell, E.; Jachimowicz, D.; Sipos, B.; Lloyd, J.; Bruce, M.; Pantic, N.; Admassu, T.; James, P.; Warland, A.; et al. Highly parallel direct RNA sequencing on an array of nanopores. *Nature methods* **2018**, *15*, doi:10.1038/nmeth.4577.
55. Liu, H.; Begik, O.; Lucas, M.; Ramirez, J.; Mason, C.; Wiener, D.; Schwartz, S.; Mattick, J.; Smith, M.; Novoa, E. Accurate detection of m 6 A RNA modifications in native RNA sequences. *Nature communications* **2019**, *10*, doi:10.1038/s41467-019-11713-9.
56. Smith, A.; Jain, M.; Mulroney, L.; Garalde, D.; Akeson, M. Reading canonical and modified nucleobases in 16S ribosomal RNA using nanopore native RNA sequencing. *PloS one* **2019**, *14*, doi:10.1371/journal.pone.0216709.
57. Cantara, W.; Crain, P.; Rozenski, J.; McCloskey, J.; Harris, K.; Zhang, X.; Vendeix, F.; Fabris, D.; Agris, P. The RNA Modification Database, RNAMDB: 2011 update. *Nucleic acids research* **2011**, *39*, doi:10.1093/nar/gkq1028.
58. Boccaletto, P.; Machnicka, M.; Purta, E.; Piatkowski, P.; Baginski, B.; Wirecki, T.; de Crécy-Lagard, V.; Ross, R.; Limbach, P.; Kotter, A.; et al. MODOMICS: a database of RNA modification pathways. 2017 update. *Nucleic acids research* **2018**, *46*, doi:10.1093/nar/gkx1030.
59. Pan, T. Modifications and functional genomics of human transfer RNA. *Cell research* **2018**, *28*, doi:10.1038/s41422-018-0013-y.
60. Sarkar, A.; Gasperi, W.; Begley, U.; Nevins, S.; Huber, S.; Dedon, P.; Begley, T. Detecting the epitranscriptome. *Wiley interdisciplinary reviews. RNA* **2021**, doi:10.1002/wrna.1663.
61. Suzuki, T.; Suzuki, T. A complete landscape of post-transcriptional modifications in mammalian mitochondrial tRNAs. *Nucleic acids research* **2014**, *42*, doi:10.1093/nar/gku390.
62. Barbieri, I.; Kouzarides, T. Role of RNA modifications in cancer. *Nature reviews. Cancer* **2020**, *20*, doi:10.1038/s41568-020-0253-2.
63. Lorenz, C.; Lünse, C.; Mörl, M. tRNA Modifications: Impact on Structure and Thermal Adaptation. *Biomolecules* **2017**, *7*, doi:10.3390/biom7020035.
64. Duechler, M.; Leszczyńska, G.; Sochacka, E.; Nawrot, B. Nucleoside modifications in the regulation of gene expression: focus on tRNA. *Cellular and molecular life sciences : CMLS* **2016**, *73*, doi:10.1007/s00018-016-2217-y.
65. Raina, M.; Ibba, M. tRNAs as regulators of biological processes. *Frontiers in genetics* **2014**, *5*, doi:10.3389/fgene.2014.00171.
66. Jühling, F.; Mörl, M.; Hartmann, R.; Sprinzl, M.; Stadler, P.; Pütz, J. tRNAdb 2009: compilation of tRNA sequences and tRNA genes. *Nucleic acids research* **2009**, *37*, doi:10.1093/nar/gkn772.
67. Chan, P.; Lowe, T. GtRNAdb 2.0: an expanded database of transfer RNA genes identified in complete and draft genomes. *Nucleic acids research* **2016**, *44*, doi:10.1093/nar/gkv1309.

68. Ramsay, E.; Abascal-Palacios, G.; Daiß, J.; King, H.; Gouge, J.; Pilsl, M.; Beuron, F.; Morris, E.; Gunkel, P.; Engel, C.; et al. Structure of human RNA polymerase III. *Nature communications* **2020**, *11*, doi:10.1038/s41467-020-20262-5.
69. Hillen, H.; Morozov, Y.; Sarfallah, A.; Temiakov, D.; Cramer, P. Structural Basis of Mitochondrial Transcription Initiation. *Cell* **2017**, *171*, doi:10.1016/j.cell.2017.10.036.
70. Lyons, S.; Fay, M.; Ivanov, P. The role of RNA modifications in the regulation of tRNA cleavage. *FEBS letters* **2018**, *592*, doi:10.1002/1873-3468.13205.
71. Hanada, T.; Suzuki, T.; Yokogawa, T.; Takemoto-Hori, C.; Sprinzl, M.; Watanabe, K. Translation ability of mitochondrial $tRNAs^{Ser}$ with unusual secondary structures in an in vitro translation system of bovine mitochondria. *Genes to cells : devoted to molecular & cellular mechanisms* **2001**, *6*, doi:10.1046/j.1365-2443.2001.00491.x.
72. Ohtsuki, T.; Kawai, G.; Watanabe, K. The minimal tRNA: unique structure of Ascaris suum mitochondrial $tRNA^{(Ser)(UCU)}$ having a short T arm and lacking the entire D arm. *FEBS letters* **2002**, *514*, doi:10.1016/s0014-5793(02)02328-1.
73. Jühling, T.; Duchardt-Ferner, E.; Bonin, S.; Wöhnert, J.; Pütz, J.; Florentz, C.; Betat, H.; Sauter, C.; Mörl, M. Small but large enough: structural properties of armless mitochondrial tRNAs from the nematode Romanomermis culicivorax. *Nucleic acids research* **2018**, *46*, doi:10.1093/nar/gky593.
74. Helm, M.; Giegé, R.; Florentz, C. A Watson-Crick base-pair-disrupting methyl group (m^1A9) is sufficient for cloverleaf folding of human mitochondrial $tRNA^{Lys}$. *Biochemistry* **1999**, *38*, doi:10.1021/bi991061g.
75. Sakurai, M.; Ohtsuki, T.; Watanabe, K. Modification at position 9 with 1-methyladenosine is crucial for structure and function of nematode mitochondrial tRNAs lacking the entire T-arm. *Nucleic acids research* **2005**, *33*, doi:10.1093/nar/gki309.
76. Grosjean, H.; Edqvist, J.; Stråby, K.; Giegé, R. Enzymatic formation of modified nucleosides in tRNA: dependence on tRNA architecture. *Journal of molecular biology* **1996**, *255*, doi:10.1006/jmbi.1996.0007.
77. Salinas-Giegé, T.; Giegé, R.; Giegé, P. tRNA biology in mitochondria. *International journal of molecular sciences* **2015**, *16*, doi:10.3390/ijms16034518.
78. *Molecular Cell Biology*, 4th Edition ed.; Lodish, H., Berk, A., Zipursky, L., Matsudaira, P., Baltimore , D., Darnell, J., Eds.; Freema, WH: New York, USA, 2000.
79. Rajendran, V.; Kalita, P.; Shukla, H.; Kumar, A.; Tripathi, T. Aminoacyl-tRNA synthetases: Structure, function, and drug discovery. *International journal of biological macromolecules* **2018**, *111*, doi:10.1016/j.ijbiomac.2017.12.157.
80. Rubio Gomez, M.; Ibba, M. Aminoacyl-tRNA synthetases. *RNA (New York, N.Y.)* **2020**, *26*, doi:10.1261/rna.071720.119.
81. *Molecular Biology of the Cell.*, 6th Edition ed.; Alberts, B., Johnson, A., Lewis, J., Morgan, D., Raff, M., Roberts, K., Walter, P., Eds.; Garland Science: New York and Abingdon, UK., 2014.
82. Berg, M.; Brandl, C. Transfer RNAs: diversity in form and function. *RNA biology* **2021**, *18*, doi:10.1080/15476286.2020.1809197.
83. *The Cell: A Molecular Approach*, 8th Edition ed.; Cooper, G., Ed.; Oxford University Press: New York, USA, 2018.
84. El Yacoubi, B.; Bailly, M.; de Crécy-Lagard, V. Biosynthesis and function of posttranscriptional modifications of transfer RNAs. *Annual review of genetics* **2012**, *46*, doi:10.1146/annurev-genet-110711-155641.
85. Janin, M.; Coll-SanMartin, L.; Esteller, M. Disruption of the RNA modifications that target the ribosome translation machinery in human cancer. *Molecular cancer* **2020**, *19*, doi:10.1186/s12943-020-01192-8.

86. Arcari, P.; Brownlee, G. The nucleotide sequence of a small (3S) seryl-tRNA (anticodon GCU) from beef heart mitochondria. *Nucleic acids research* **1980**, *8*, doi:10.1093/nar/8.22.5207.
87. de Bruijn, M.; Schreier, P.; Eperon, I.; Barrell, B.; Chen, E.; Armstrong, P.; Wong, J.; Roe, B. A mammalian mitochondrial serine transfer RNA lacking the dihydrouridine loop and stem. *Nucleic acids research* **1980**, *8*, doi:10.1093/nar/8.22.5213.
88. Helm, M.; Alfonzo, J. Posttranscriptional RNA Modifications: playing metabolic games in a cell's chemical Legoland. *Chemistry & biology* **2014**, *21*, doi:10.1016/j.chembiol.2013.10.015.
89. Barraud, P.; Tisné, C. To be or not to be modified: Miscellaneous aspects influencing nucleotide modifications in tRNAs. *IUBMB life* **2019**, *71*, doi:10.1002/iub.2041.
90. Knight, J.; Garland, G.; Pöyry, T.; Mead, E.; Vlahov, N.; Sfakianos, A.; Grosso, S.; De-Lima-Hedayioglu, F.; Mallucci, G.; von der Haar, T.; et al. Control of translation elongation in health and disease. *Disease models & mechanisms* **2020**, *13*, doi:10.1242/dmm.043208.
91. Delaunay, S.; Frye, M. RNA modifications regulating cell fate in cancer. *Nature cell biology* **2019**, *21*, doi:10.1038/s41556-019-0319-0.
92. Ranjan, N.; Leidel, S. The epitranscriptome in translation regulation: mRNA and tRNA modifications as the two sides of the same coin? *FEBS letters* **2019**, *593*, doi:10.1002/1873-3468.13491.
93. Lamichhane, T.; Blewett, N.; Maraia, R. Plasticity and diversity of tRNA anticodon determinants of substrate recognition by eukaryotic A37 isopentenyltransferases. *RNA (New York, N.Y.)* **2011**, *17*, doi:10.1261/rna.2628611.
94. Endres, L.; Fasullo, M.; Rose, R. tRNA modification and cancer: potential for therapeutic prevention and intervention. *Future medicinal chemistry* **2019**, *11*, doi:10.4155/fmc-2018-0404.
95. Krutyhołowa, R.; Zakrzewski, K.; Glatt, S. Charging the code - tRNA modification complexes. *Current opinion in structural biology* **2019**, *55*, doi:10.1016/j.sbi.2019.03.014.
96. Crick, F. Codon--anticodon pairing: the wobble hypothesis. *Journal of molecular biology* **1966**, *19*, doi:10.1016/s0022-2836(66)80022-0.
97. Ontiveros, R.; Stoute, J.; Liu, K. The chemical diversity of RNA modifications. *The Biochemical journal* **2019**, *476*, doi:10.1042/BCJ20180445.
98. Rafels-Ybern, À.; Torres, A.; Grau-Bove, X.; Ruiz-Trillo, I.; Ribas de Pouplana, L. Codon adaptation to tRNAs with Inosine modification at position 34 is widespread among Eukaryotes and present in two Bacterial phyla. *RNA biology* **2018**, *15*, doi:10.1080/15476286.2017.1358348.
99. Brule, C.; Grayhack, E. Synonymous Codons: Choose Wisely for Expression. *Trends in genetics : TIG* **2017**, *33*, doi:10.1016/j.tig.2017.02.001.
100. Rafels-Ybern, À.; Torres, A.; Camacho, N.; Herencia-Ropero, A.; Roura Frigolé, H.; Wulff, T.; Raboteg, M.; Bordons, A.; Grau-Bove, X.; Ruiz-Trillo, I.; et al. The Expansion of Inosine at the Wobble Position of tRNAs, and Its Role in the Evolution of Proteomes. *Molecular biology and evolution* **2019**, *36*, doi:10.1093/molbev/msy245.
101. Endres, L.; Dedon, P.; Begley, T. Codon-biased translation can be regulated by wobble-base tRNA modification systems during cellular stress responses. *RNA biology* **2015**, *12*, doi:10.1080/15476286.2015.1031947.
102. Yarus, M. Translational efficiency of transfer RNA's: uses of an extended anticodon. *Science (New York, N.Y.)* **1982**, *218*, doi:10.1126/science.6753149.
103. Arimbasseri, A.; Iben, J.; Wei, F.; Rijal, K.; Tomizawa, K.; Hafner, M.; Maraia, R. Evolving specificity of tRNA 3-methyl-cytidine-32 (m^3C32) modification: a subset

of tRNAsSer requires N^6-isopentenylation of A37. *RNA (New York, N.Y.)* **2016**, *22*, doi:10.1261/rna.056259.116.
104. Schweizer, U.; Bohleber, S.; Fradejas-Villar, N. The modified base isopentenyladenosine and its derivatives in tRNA. *RNA biology* **2017**, *14*, doi:10.1080/15476286.2017.1294309.
105. Han, L.; Phizicky, E. A rationale for tRNA modification circuits in the anticodon loop. *RNA (New York, N.Y.)* **2018**, *24*, doi:10.1261/rna.067736.118.
106. Edvardson, S.; Elbaz-Alon, Y.; Jalas, C.; Matlock, A.; Patel, K.; Labbé, K.; Shaag, A.; Jackman, J.; Elpeleg, O. A mutation in the THG1L gene in a family with cerebellar ataxia and developmental delay. *Neurogenetics* **2016**, *17*, doi:10.1007/s10048-016-0487-z.
107. Nakamura, A.; Wang, D.; Komatsu, Y. Biochemical analysis of human tRNA His guanylyltransferase in mitochondrial tRNA His maturation. *Biochemical and biophysical research communications* **2018**, *503*, doi:10.1016/j.bbrc.2018.07.150.
108. Matlock, A.; Smith, B.; Jackman, J. Chemical footprinting and kinetic assays reveal dual functions for highly conserved eukaryotic tRNA His guanylyltransferase residues. *The Journal of biological chemistry* **2019**, *294*, doi:10.1074/jbc.RA119.007939.
109. Martinez, A.; Yamashita, S.; Nagaike, T.; Sakaguchi, Y.; Suzuki, T.; Tomita, K. Human BCDIN3D monomethylates cytoplasmic histidine transfer RNA. *Nucleic acids research* **2017**, *45*, doi:10.1093/nar/gkx051.
110. Igoillo-Esteve, M.; Genin, A.; Lambert, N.; Désir, J.; Pirson, I.; Abdulkarim, B.; Simonis, N.; Drielsma, A.; Marselli, L.; Marchetti, P.; et al. tRNA methyltransferase homolog gene TRMT10A mutation in young onset diabetes and primary microcephaly in humans. *PLoS genetics* **2013**, *9*, doi:10.1371/journal.pgen.1003888.
111. Vilardo, E.; Amman, F.; Toth, U.; Kotter, A.; Helm, M.; Rossmanith, W. Functional characterization of the human tRNA methyltransferases TRMT10A and TRMT10B. *Nucleic acids research* **2020**, *48*, doi:10.1093/nar/gkaa353.
112. Vilardo, E.; Nachbagauer, C.; Buzet, A.; Taschner, A.; Holzmann, J.; Rossmanith, W. A subcomplex of human mitochondrial RNase P is a bifunctional methyltransferase--extensive moonlighting in mitochondrial tRNA biogenesis. *Nucleic acids research* **2012**, *40*, doi:10.1093/nar/gks910.
113. Reinhard, L.; Sridhara, S.; Hällberg, B. The MRPP1/MRPP2 complex is a tRNA-maturation platform in human mitochondria. *Nucleic acids research* **2017**, *45*, doi:10.1093/nar/gkx902.
114. Shaheen, R.; Tasak, M.; Maddirevula, S.; Abdel-Salam, G.; Sayed, I.; Alazami, A.; Al-Sheddi, T.; Alobeid, E.; Phizicky, E.; Alkuraya, F. PUS7 mutations impair pseudouridylation in humans and cause intellectual disability and microcephaly. *Human genetics* **2019**, *138*, doi:10.1007/s00439-019-01980-3.
115. Takakura, M.; Ishiguro, K.; Akichika, S.; Miyauchi, K.; Suzuki, T. Biogenesis and functions of aminocarboxypropyluridine in tRNA. *Nature communications* **2019**, *10*, doi:10.1038/s41467-019-13525-3.
116. Kato, T.; Daigo, Y.; Hayama, S.; Ishikawa, N.; Yamabuki, T.; Ito, T.; Miyamoto, M.; Kondo, S.; Nakamura, Y. A novel human tRNA-dihydrouridine synthase involved in pulmonary carcinogenesis. *Cancer research* **2005**, *65*, doi:10.1158/0008-5472.CAN-05-0600.
117. Bou-Nader, C.; Pecqueur, L.; Bregeon, D.; Kamah, A.; Guérineau, V.; Golinelli-Pimpaneau, B.; Guimarães, B.; Fontecave, M.; Hamdane, D. An extended dsRBD is required for post-transcriptional modification in human tRNAs. *Nucleic acids research* **2015**, *43*, doi:10.1093/nar/gkv989.

118. Bou-Nader, C.; Barraud, P.; Pecqueur, L.; Pérez, J.; Velours, C.; Shepard, W.; Fontecave, M.; Tisné, C.; Hamdane, D. Molecular basis for transfer RNA recognition by the double-stranded RNA-binding domain of human dihydrouridine synthase 2. *Nucleic acids research* **2019**, *47*, doi:10.1093/nar/gky1302.
119. Liu, J.; Strâby, K. The human tRNA(m(2)(2)G(26))dimethyltransferase: functional expression and characterization of a cloned hTRM1 gene. *Nucleic acids research* **2000**, *28*, doi:10.1093/nar/28.18.3445.
120. Dewe, J.; Fuller, B.; Lentini, J.; Kellner, S.; Fu, D. TRMT1-Catalyzed tRNA Modifications Are Required for Redox Homeostasis To Ensure Proper Cellular Proliferation and Oxidative Stress Survival. *Molecular and cellular biology* **2017**, *37*, doi:10.1128/MCB.00214-17.
121. Jonkhout, N.; Cruciani, S.; Santos Vieira, H.; Tran, J.; Liu, H.; Liu, G.; Pickford, R.; Kaczorowski, D.; Franco, G.; Vauti, F.; et al. Subcellular relocalization and nuclear redistribution of the RNA methyltransferases TRMT1 and TRMT1L upon neuronal activation. *RNA biology* **2021**, doi:10.1080/15476286.2021.1881291.
122. Sibert, B.; Patton, J. Pseudouridine synthase 1: a site-specific synthase without strict sequence recognition requirements. *Nucleic acids research* **2012**, *40*, doi:10.1093/nar/gkr1017.
123. Xu, L.; Liu, X.; Sheng, N.; Oo, K.; Liang, J.; Chionh, Y.; Xu, J.; Ye, F.; Gao, Y.; Dedon, P.; et al. Three distinct 3-methylcytidine (m 3 C) methyltransferases modify tRNA and mRNA in mice and humans. *The Journal of biological chemistry* **2017**, *292*, doi:10.1074/jbc.M117.798298.
124. Lentini, J.; Alsaif, H.; Faqeih, E.; Alkuraya, F.; Fu, D. DALRD3 encodes a protein mutated in epileptic encephalopathy that targets arginine tRNAs for 3-methylcytosine modification. *Nature communications* **2020**, *11*, doi:10.1038/s41467-020-16321-6.
125. Ignatova, V.; Kaiser, S.; Ho, J.; Bing, X.; Stolz, P.; Tan, Y.; Lee, C.; Gay, F.; Lastres, P.; Gerlini, R.; et al. METTL6 is a tRNA m 3 C methyltransferase that regulates pluripotency and tumor cell growth. *Science advances* **2020**, *6*, doi:10.1126/sciadv.aaz4551.
126. Guy, M.; Shaw, M.; Weiner, C.; Hobson, L.; Stark, Z.; Rose, K.; Kalscheuer, V.; Gecz, J.; Phizicky, E. Defects in tRNA Anticodon Loop 2'-O-Methylation Are Implicated in Nonsyndromic X-Linked Intellectual Disability due to Mutations in FTSJ1. *Human mutation* **2015**, *36*, doi:10.1002/humu.22897.
127. Li, J.; Wang, Y.; Xu, B.; Liu, Y.; Zhou, M.; Long, T.; Li, H.; Dong, H.; Nie, Y.; Chen, P.; et al. Intellectual disability-associated gene ftsj1 is responsible for 2'-O-methylation of specific tRNAs. *EMBO reports* **2020**, *21*, doi:10.15252/embr.202050095.
128. Brzezicha, B.; Schmidt, M.; Makalowska, I.; Jarmolowski, A.; Pienkowska, J.; Szweykowska-Kulinska, Z. Identification of human tRNA:m5C methyltransferase catalysing intron-dependent m5C formation in the first position of the anticodon of the pre-tRNA Leu (CAA). *Nucleic acids research* **2006**, *34*, doi:10.1093/nar/gkl765.
129. Tuorto, F.; Liebers, R.; Musch, T.; Schaefer, M.; Hofmann, S.; Kellner, S.; Frye, M.; Helm, M.; Stoecklin, G.; Lyko, F. RNA cytosine methylation by Dnmt2 and NSun2 promotes tRNA stability and protein synthesis. *Nature structural & molecular biology* **2012**, *19*, doi:10.1038/nsmb.2357.
130. Auxilien, S.; Guérineau, V.; Szweykowska-Kulińska, Z.; Golinelli-Pimpaneau, B. The human tRNA m (5) C methyltransferase Misu is multisite-specific. *RNA biology* **2012**, *9*, doi:10.4161/rna.22180.
131. Kawarada, L.; Suzuki, T.; Ohira, T.; Hirata, S.; Miyauchi, K.; Suzuki, T. ALKBH1 is an RNA dioxygenase responsible for cytoplasmic and mitochondrial tRNA modifications. *Nucleic acids research* **2017**, *45*, doi:10.1093/nar/gkx354.

132. Nakano, S.; Suzuki, T.; Kawarada, L.; Iwata, H.; Asano, K.; Suzuki, T. NSUN3 methylase initiates 5-formylcytidine biogenesis in human mitochondrial tRNA(Met). *Nature chemical biology* **2016**, *12*, doi:10.1038/nchembio.2099.
133. Haag, S.; Sloan, K.; Ranjan, N.; Warda, A.; Kretschmer, J.; Blessing, C.; Hübner, B.; Seikowski, J.; Dennerlein, S.; Rehling, P.; et al. NSUN3 and ABH1 modify the wobble position of mt-tRNAMet to expand codon recognition in mitochondrial translation. *The EMBO journal* **2016**, *35*, doi:10.15252/embj.201694885.
134. Van Haute, L.; Powell, C.; Minczuk, M. Dealing with an Unconventional Genetic Code in Mitochondria: The Biogenesis and Pathogenic Defects of the 5-Formylcytosine Modification in Mitochondrial tRNA Met. *Biomolecules* **2017**, *7*, doi:10.3390/biom7010024.
135. Van Haute, L.; Lee, S.; McCann, B.; Powell, C.; Bansal, D.; Vasiliauskaitė, L.; Garone, C.; Shin, S.; Kim, J.; Frye, M.; et al. NSUN2 introduces 5-methylcytosines in mammalian mitochondrial tRNAs. *Nucleic acids research* **2019**, *47*, doi:10.1093/nar/gkz559.
136. Shen, H.; Ontiveros, R.; Owens, M.; Liu, M.; Ghanty, U.; Kohli, R.; Liu, K. TET-mediated 5-methylcytosine oxidation in tRNA promotes translation. *The Journal of biological chemistry* **2021**, *296*, doi:10.1074/jbc.RA120.014226.
137. Takemoto, C.; Spremulli, L.; Benkowski, L.; Ueda, T.; Yokogawa, T.; Watanabe, K. Unconventional decoding of the AUA codon as methionine by mitochondrial tRNAMet with the anticodon f5CAU as revealed with a mitochondrial in vitro translation system. *Nucleic acids research* **2009**, *37*, doi:10.1093/nar/gkp001.
138. Lin, F.; Shen, L.; Jang, C.; Falnes, P.; Zhang, Y. Ikbkap/Elp1 deficiency causes male infertility by disrupting meiotic progression. *PLoS genetics* **2013**, *9*, doi:10.1371/journal.pgen.1003516.
139. Karlsborn, T.; Tükenmez, H.; Chen, C.; Byström, A. Familial dysautonomia (FD) patients have reduced levels of the modified wobble nucleoside mcm(5)s(2)U in tRNA. *Biochemical and biophysical research communications* **2014**, *454*, doi:10.1016/j.bbrc.2014.10.116.
140. Rapino, F.; Delaunay, S.; Zhou, Z.; Chariot, A.; Close, P. tRNA Modification: Is Cancer Having a Wobble? *Trends in cancer* **2017**, *3*, doi:10.1016/j.trecan.2017.02.004.
141. Rapino, F.; Delaunay, S.; Rambow, F.; Zhou, Z.; Tharun, L.; De Tullio, P.; Sin, O.; Shostak, K.; Schmitz, S.; Piepers, J.; et al. Codon-specific translation reprogramming promotes resistance to targeted therapy. *Nature* **2018**, *558*, doi:10.1038/s41586-018-0243-7.
142. Songe-Møller, L.; van den Born, E.; Leihne, V.; Vågbø, C.; Kristoffersen, T.; Krokan, H.; Kirpekar, F.; Falnes, P.; Klungland, A. Mammalian ALKBH8 possesses tRNA methyltransferase activity required for the biogenesis of multiple wobble uridine modifications implicated in translational decoding. *Molecular and cellular biology* **2010**, *30*, doi:10.1128/MCB.01602-09.
143. Flanagan, J.; Healey, S.; Young, J.; Whitehall, V.; Trott, D.; Newbold, R.; Chenevix-Trench, G. Mapping of a candidate colorectal cancer tumor-suppressor gene to a 900-kilobase region on the short arm of chromosome 8. *Genes, chromosomes & cancer* **2004**, *40*, doi:10.1002/gcc.20039.
144. Fu, D.; Brophy, J.; Chan, C.; Atmore, K.; Begley, U.; Paules, R.; Dedon, P.; Begley, T.; Samson, L. Human AlkB homolog ABH8 Is a tRNA methyltransferase required for wobble uridine modification and DNA damage survival. *Molecular and cellular biology* **2010**, *30*, doi:10.1128/MCB.01604-09.
145. Fu, Y.; Dai, Q.; Zhang, W.; Ren, J.; Pan, T.; He, C. The AlkB domain of mammalian ABH8 catalyzes hydroxylation of 5-methoxycarbonylmethyluridine at the wobble position of tRNA. *Angewandte Chemie (International ed. in English)* **2010**, *49*, doi:10.1002/anie.201001242.

146. van den Born, E.; Vågbø, C.; Songe-Møller, L.; Leihne, V.; Lien, G.; Leszczynska, G.; Malkiewicz, A.; Krokan, H.; Kirpekar, F.; Klungland, A.; et al. ALKBH8-mediated formation of a novel diastereomeric pair of wobble nucleosides in mammalian tRNA. *Nature communications* **2011**, *2*, doi:10.1038/ncomms1173.
147. Pastore, C.; Topalidou, I.; Forouhar, F.; Yan, A.; Levy, M.; Hunt, J. Crystal structure and RNA binding properties of the RNA recognition motif (RRM) and AlkB domains in human AlkB homolog 8 (ABH8), an enzyme catalyzing tRNA hypermodification. *The Journal of biological chemistry* **2012**, *287*, doi:10.1074/jbc.M111.286187.
148. Begley, U.; Sosa, M.; Avivar-Valderas, A.; Patil, A.; Endres, L.; Estrada, Y.; Chan, C.; Su, D.; Dedon, P.; Aguirre-Ghiso, J.; et al. A human tRNA methyltransferase 9-like protein prevents tumour growth by regulating LIN9 and HIF1-α. *EMBO molecular medicine* **2013**, *5*, doi:10.1002/emmm.201201161.
149. Endres, L.; Begley, U.; Clark, R.; Gu, C.; Dziergowska, A.; Małkiewicz, A.; Melendez, J.; Dedon, P.; Begley, T. Alkbh8 Regulates Selenocysteine-Protein Expression to Protect against Reactive Oxygen Species Damage. *PloS one* **2015**, *10*, doi:10.1371/journal.pone.0131335.
150. Lee, M.; Leonardi, A.; Begley, T.; Melendez, J. Loss of epitranscriptomic control of selenocysteine utilization engages senescence and mitochondrial reprogramming ☆. *Redox biology* **2020**, *28*, doi:10.1016/j.redox.2019.101375.
151. Van der Veen, A.; Schorpp, K.; Schlieker, C.; Buti, L.; Damon, J.; Spooner, E.; Ploegh, H.; Jentsch, S. Role of the ubiquitin-like protein Urm1 as a noncanonical lysine-directed protein modifier. *Proceedings of the National Academy of Sciences of the United States of America* **2011**, *108*, doi:10.1073/pnas.1014402108.
152. Fräsdorf, B.; Radon, C.; Leimkühler, S. Characterization and interaction studies of two isoforms of the dual localized 3-mercaptopyruvate sulfurtransferase TUM1 from humans. *The Journal of biological chemistry* **2014**, *289*, doi:10.1074/jbc.M114.605733.
153. Delaunay, S.; Rapino, F.; Tharun, L.; Zhou, Z.; Heukamp, L.; Termathe, M.; Shostak, K.; Klevernic, I.; Florin, A.; Desmecht, H.; et al. Elp3 links tRNA modification to IRES-dependent translation of LEF1 to sustain metastasis in breast cancer. *The Journal of experimental medicine* **2016**, *213*, doi:10.1084/jem.20160397.
154. Zhang, X.; Chen, X. The emerging roles of ubiquitin-like protein Urm1 in eukaryotes. *Cellular signalling* **2021**, *81*, doi:10.1016/j.cellsig.2021.109946.
155. Li, X.; Guan, M. A human mitochondrial GTP binding protein related to tRNA modification may modulate phenotypic expression of the deafness-associated mitochondrial 12S rRNA mutation. *Molecular and cellular biology* **2002**, *22*, doi:10.1128/MCB.22.21.7701-7711.2002.
156. Umeda, N.; Suzuki, T.; Yukawa, M.; Ohya, Y.; Shindo, H.; Watanabe, K.; Suzuki, T. Mitochondria-specific RNA-modifying enzymes responsible for the biosynthesis of the wobble base in mitochondrial tRNAs. Implications for the molecular pathogenesis of human mitochondrial diseases. *The Journal of biological chemistry* **2005**, *280*, doi:10.1074/jbc.M409306200.
157. Asano, K.; Suzuki, T.; Saito, A.; Wei, F.; Ikeuchi, Y.; Numata, T.; Tanaka, R.; Yamane, Y.; Yamamoto, T.; Goto, T.; et al. Metabolic and chemical regulation of tRNA modification associated with taurine deficiency and human disease. *Nucleic acids research* **2018**, *46*, doi:10.1093/nar/gky068.
158. Guan, M.; Yan, Q.; Li, X.; Bykhovskaya, Y.; Gallo-Teran, J.; Hajek, P.; Umeda, N.; Zhao, H.; Garrido, G.; Mengesha, E.; et al. Mutation in TRMU related to transfer RNA modification modulates the phenotypic expression of the deafness-

associated mitochondrial 12S ribosomal RNA mutations. *American journal of human genetics* **2006**, *79*, doi:10.1086/506389.
159. Boczonadi, V.; Smith, P.; Pyle, A.; Gomez-Duran, A.; Schara, U.; Tulinius, M.; Chinnery, P.; Horvath, R. Altered 2-thiouridylation impairs mitochondrial translation in reversible infantile respiratory chain deficiency. *Human molecular genetics* **2013**, *22*, doi:10.1093/hmg/ddt309.
160. Vitali, P.; Kiss, T. Cooperative 2'-O-methylation of the wobble cytidine of human elongator tRNA Met(CAT) by a nucleolar and a Cajal body-specific box C/D RNP. *Genes & development* **2019**, *33*, doi:10.1101/gad.326363.119.
161. Torres, A.; Piñeyro, D.; Rodríguez-Escribà, M.; Camacho, N.; Reina, O.; Saint-Léger, A.; Filonava, L.; Batlle, E.; Ribas de Pouplana, L. Inosine modifications in human tRNAs are incorporated at the precursor tRNA level. *Nucleic acids research* **2015**, *43*, doi:10.1093/nar/gkv277.
162. Rafels-Ybern, À.; Attolini, C.; Ribas de Pouplana, L. Distribution of ADAT-Dependent Codons in the Human Transcriptome. *International journal of molecular sciences* **2015**, *16*, doi:10.3390/ijms160817303.
163. Behrens, C.; Biela, I.; Petiot-Bécard, S.; Botzanowski, T.; Cianférani, S.; Sager, C.; Klebe, G.; Heine, A.; Reuter, K. Homodimer Architecture of QTRT2, the Noncatalytic Subunit of the Eukaryotic tRNA-Guanine Transglycosylase. *Biochemistry* **2018**, *57*, doi:10.1021/acs.biochem.8b00294.
164. Wang, X.; Matuszek, Z.; Huang, Y.; Parisien, M.; Dai, Q.; Clark, W.; Schwartz, M.; Pan, T. Queuosine modification protects cognate tRNAs against ribonuclease cleavage. *RNA (New York, N.Y.)* **2018**, *24*, doi:10.1261/rna.067033.118.
165. Tuorto, F.; Legrand, C.; Cirzi, C.; Federico, G.; Liebers, R.; Müller, M.; Ehrenhofer-Murray, A.; Dittmar, G.; Gröne, H.; Lyko, F. Queuosine-modified tRNAs confer nutritional control of protein translation. *The EMBO journal* **2018**, *37*, doi:10.15252/embj.201899777.
166. Johannsson, S.; Neumann, P.; Ficner, R. Crystal Structure of the Human tRNA Guanine Transglycosylase Catalytic Subunit QTRT1. *Biomolecules* **2018**, *8*, doi:10.3390/biom8030081.
167. Müller, M.; Legrand, C.; Tuorto, F.; Kelly, V.; Atlasi, Y.; Lyko, F.; Ehrenhofer-Murray, A. Queuine links translational control in eukaryotes to a micronutrient from bacteria. *Nucleic acids research* **2019**, *47*, doi:10.1093/nar/gkz063.
168. Golovko, A.; Hjälm, G.; Sitbon, F.; Nicander, B. Cloning of a human tRNA isopentenyl transferase. *Gene* **2000**, *258*, doi:10.1016/s0378-1119(00)00421-2.
169. Fradejas, N.; Carlson, B.; Rijntjes, E.; Becker, N.; Tobe, R.; Schweizer, U. Mammalian Trit1 is a tRNA(Ser Sec)-isopentenyl transferase required for full selenoprotein expression. *The Biochemical journal* **2013**, *450*, doi:10.1042/BJ20121713.
170. Khalique, A.; Mattijssen, S.; Haddad, A.; Chaudhry, S.; Maraia, R. Targeting mitochondrial and cytosolic substrates of TRIT1 isopentenyltransferase: Specificity determinants and tRNA-i^6A37 profiles. *PLoS genetics* **2020**, *16*, doi:10.1371/journal.pgen.1008330.
171. Reiter, V.; Matschkal, D.; Wagner, M.; Globisch, D.; Kneuttinger, A.; Müller, M.; Carell, T. The CDK5 repressor CDK5RAP1 is a methylthiotransferase acting on nuclear and mitochondrial RNA. *Nucleic acids research* **2012**, *40*, doi:10.1093/nar/gks240.
172. Wei, F.; Zhou, B.; Suzuki, T.; Miyata, K.; Ujihara, Y.; Horiguchi, H.; Takahashi, N.; Xie, P.; Michiue, H.; Fujimura, A.; et al. Cdk5rap1-mediated 2-methylthio modification of mitochondrial tRNAs governs protein translation and contributes to myopathy in mice and humans. *Cell metabolism* **2015**, *21*, doi:10.1016/j.cmet.2015.01.019.

173. Fakruddin, M.; Wei, F.; Emura, S.; Matsuda, S.; Yasukawa, T.; Kang, D.; Tomizawa, K. Cdk5rap1-mediated 2-methylthio-N6-isopentenyladenosine modification is absent from nuclear-derived RNA species. *Nucleic acids research* **2017**, *45*, doi:10.1093/nar/gkx819.
174. Mao, D.; Neculai, D.; Downey, M.; Orlicky, S.; Haffani, Y.; Ceccarelli, D.; Ho, J.; Szilard, R.; Zhang, W.; Ho, C.; et al. Atomic structure of the KEOPS complex: an ancient protein kinase-containing molecular machine. *Molecular cell* **2008**, *32*, doi:10.1016/j.molcel.2008.10.002.
175. Wan, L.; Maisonneuve, P.; Szilard, R.; Lambert, J.; Ng, T.; Manczyk, N.; Huang, H.; Laister, R.; Caudy, A.; Gingras, A.; et al. Proteomic analysis of the human KEOPS complex identifies C14ORF142 as a core subunit homologous to yeast Gon7. *Nucleic acids research* **2017**, *45*, doi:10.1093/nar/gkw1181.
176. Braun, D.; Rao, J.; Mollet, G.; Schapiro, D.; Daugeron, M.; Tan, W.; Gribouval, O.; Boyer, O.; Revy, P.; Jobst-Schwan, T.; et al. Mutations in KEOPS-complex genes cause nephrotic syndrome with primary microcephaly. *Nature genetics* **2017**, *49*, doi:10.1038/ng.3933.
177. Lin, H.; Miyauchi, K.; Harada, T.; Okita, R.; Takeshita, E.; Komaki, H.; Fujioka, K.; Yagasaki, H.; Goto, Y.; Yanaka, K.; et al. CO 2-sensitive tRNA modification associated with human mitochondrial disease. *Nature communications* **2018**, *9*, doi:10.1038/s41467-018-04250-4.
178. Kimura, S.; Miyauchi, K.; Ikeuchi, Y.; Thiaville, P.; Crécy-Lagard, V.; Suzuki, T. Discovery of the β-barrel-type RNA methyltransferase responsible for N6-methylation of N6-threonylcarbamoyladenosine in tRNAs. *Nucleic acids research* **2014**, *42*, doi:10.1093/nar/gku618.
179. Wei, F.; Suzuki, T.; Watanabe, S.; Kimura, S.; Kaitsuka, T.; Fujimura, A.; Matsui, H.; Atta, M.; Michiue, H.; Fontecave, M.; et al. Deficit of tRNA(Lys) modification by Cdkal1 causes the development of type 2 diabetes in mice. *The Journal of clinical investigation* **2011**, *121*, doi:10.1172/JCI58056.
180. Xie, P.; Wei, F.; Hirata, S.; Kaitsuka, T.; Suzuki, T.; Suzuki, T.; Tomizawa, K. Quantitative PCR measurement of tRNA 2-methylthio modification for assessing type 2 diabetes risk. *Clinical chemistry* **2013**, *59*, doi:10.1373/clinchem.2013.210401.
181. Wei, F.; Tomizawa, K. tRNA modifications and islet function. *Diabetes, obesity & metabolism* **2018**, *20 Suppl 2*, doi:10.1111/dom.13405.
182. Narendran, A.; Vangaveti, S.; Ranganathan, S.; Eruysal, E.; Craft, M.; Alrifai, O.; Chua, F.; Sarachan, K.; Litwa, B.; Ramachandran, S.; et al. Silencing of the tRNA Modification Enzyme Cdkal1 Effects Functional Insulin Synthesis in NIT-1 Cells: tRNA Lys3 Lacking ms 2- (ms 2 t 6 A 37) is Unable to Establish Sufficient Anticodon:Codon Interactions to Decode the Wobble Codon AAG. *Frontiers in molecular biosciences* **2021**, *7*, doi:10.3389/fmolb.2020.584228.
183. Brulé, H.; Elliott, M.; Redlak, M.; Zehner, Z.; Holmes, W. Isolation and characterization of the human tRNA-(N1G37) methyltransferase (TRM5) and comparison to the Escherichia coli TrmD protein. *Biochemistry* **2004**, *43*, doi:10.1021/bi049671q.
184. Noma, A.; Ishitani, R.; Kato, M.; Nagao, A.; Nureki, O.; Suzuki, T. Expanding role of the jumonji C domain as an RNA hydroxylase. *The Journal of biological chemistry* **2010**, *285*, doi:10.1074/jbc.M110.156398.
185. Powell, C.; Kopajtich, R.; D'Souza, A.; Rorbach, J.; Kremer, L.; Husain, R.; Dallabona, C.; Donnini, C.; Alston, C.; Griffin, H.; et al. TRMT5 Mutations Cause a Defect in Post-transcriptional Modification of Mitochondrial tRNA Associated with Multiple Respiratory-Chain Deficiencies. *American journal of human genetics* **2015**, *97*, doi:10.1016/j.ajhg.2015.06.011.

186. Zhou, M.; Xue, L.; Chen, Y.; Li, H.; He, Q.; Wang, B.; Meng, F.; Wang, M.; Guan, M. A hypertension-associated mitochondrial DNA mutation introduces an m 1 G37 modification into tRNA Met, altering its structure and function. *The Journal of biological chemistry* **2018**, *293*, doi:10.1074/jbc.RA117.000317.
187. Rosselló-Tortella, M.; Llinàs-Arias, P.; Sakaguchi, Y.; Miyauchi, K.; Davalos, V.; Setien, F.; Calleja-Cervantes, M.; Piñeyro, D.; Martínez-Gómez, J.; Guil, S.; et al. Epigenetic loss of the transfer RNA-modifying enzyme TYW2 induces ribosome frameshifts in colon cancer. *Proceedings of the National Academy of Sciences of the United States of America* **2020**, *117*, doi:10.1073/pnas.2003358117.
188. Maas, S.; Gerber, A.; Rich, A. Identification and characterization of a human tRNA-specific adenosine deaminase related to the ADAR family of pre-mRNA editing enzymes. *Proceedings of the National Academy of Sciences of the United States of America* **1999**, *96*, doi:10.1073/pnas.96.16.8895.
189. Goll, M.; Kirpekar, F.; Maggert, K.; Yoder, J.; Hsieh, C.; Zhang, X.; Golic, K.; Jacobsen, S.; Bestor, T. Methylation of tRNAAsp by the DNA methyltransferase homolog Dnmt2. *Science (New York, N.Y.)* **2006**, *311*, doi:10.1126/science.1120976.
190. Chen, J.; Patton, J. Pseudouridine synthase 3 from mouse modifies the anticodon loop of tRNA. *Biochemistry* **2000**, *39*, doi:10.1021/bi001109m.
191. Bekaert, M.; Rousset, J. An extended signal involved in eukaryotic -1 frameshifting operates through modification of the E site tRNA. *Molecular cell* **2005**, *17*, doi:10.1016/j.molcel.2004.12.009.
192. Shaheen, R.; Han, L.; Faqeih, E.; Ewida, N.; Alobeid, E.; Phizicky, E.; Alkuraya, F. A homozygous truncating mutation in PUS3 expands the role of tRNA modification in normal cognition. *Human genetics* **2016**, *135*, doi:10.1007/s00439-016-1665-7.
193. Cartlidge, R.; Knebel, A.; Peggie, M.; Alexandrov, A.; Phizicky, E.; Cohen, P. The tRNA methylase METTL1 is phosphorylated and inactivated by PKB and RSK in vitro and in cells. *The EMBO journal* **2005**, *24*, doi:10.1038/sj.emboj.7600648.
194. Lin, S.; Liu, Q.; Lelyveld, V.; Choe, J.; Szostak, J.; Gregory, R. Mettl1/Wdr4-Mediated m 7 G tRNA Methylome Is Required for Normal mRNA Translation and Embryonic Stem Cell Self-Renewal and Differentiation. *Molecular cell* **2018**, *71*, doi:10.1016/j.molcel.2018.06.001.
195. Zhang, L.; Liu, C.; Ma, H.; Dai, Q.; Sun, H.; Luo, G.; Zhang, Z.; Zhang, L.; Hu, L.; Dong, X.; et al. Transcriptome-wide Mapping of Internal N 7-Methylguanosine Methylome in Mammalian mRNA. *Molecular cell* **2019**, *74*, doi:10.1016/j.molcel.2019.03.036.
196. Blanco, S.; Dietmann, S.; Flores, J.; Hussain, S.; Kutter, C.; Humphreys, P.; Lukk, M.; Lombard, P.; Treps, L.; Popis, M.; et al. Aberrant methylation of tRNAs links cellular stress to neuro-developmental disorders. *The EMBO journal* **2014**, *33*, doi:10.15252/embj.201489282.
197. de Crécy-Lagard, V.; Boccaletto, P.; Mangleburg, C.; Sharma, P.; Lowe, T.; Leidel, S.; Bujnicki, J. Matching tRNA modifications in humans to their known and predicted enzymes. *Nucleic acids research* **2019**, *47*, doi:10.1093/nar/gkz011.
198. Powell, C.; Minczuk, M. TRMT2B is responsible for both tRNA and rRNA m 5 U-methylation in human mitochondria. *RNA biology* **2020**, *17*, doi:10.1080/15476286.2020.1712544.
199. Zucchini, C.; Strippoli, P.; Biolchi, A.; Solmi, R.; Lenzi, L.; D'Addabbo, P.; Carinci, P.; Valvassori, L. The human TruB family of pseudouridine synthase genes, including the Dyskeratosis Congenita 1 gene and the novel member TRUB1. *International journal of molecular medicine* **2003**, *11*.
200. Mukhopadhyay, S.; Deogharia, M.; Gupta, R. Mammalian nuclear TRUB1, mitochondrial TRUB2, and cytoplasmic PUS10 produce conserved

pseudouridine 55 in different sets of tRNA. *RNA (New York, N.Y.)* **2021**, *27*, doi:10.1261/rna.076810.120.
201. Suzuki, T.; Yashiro, Y.; Kikuchi, I.; Ishigami, Y.; Saito, H.; Matsuzawa, I.; Okada, S.; Mito, M.; Iwasaki, S.; Ma, D.; et al. Complete chemical structures of human mitochondrial tRNAs. *Nature communications* **2020**, *11*, doi:10.1038/s41467-020-18068-6.
202. Deogharia, M.; Mukhopadhyay, S.; Joardar, A.; Gupta, R. The human ortholog of archaeal Pus10 produces pseudouridine 54 in select tRNAs where its recognition sequence contains a modified residue. *RNA (New York, N.Y.)* **2019**, *25*, doi:10.1261/rna.068114.118.
203. Song, J.; Zhuang, Y.; Zhu, C.; Meng, H.; Lu, B.; Xie, B.; Peng, J.; Li, M.; Yi, C. Differential roles of human PUS10 in miRNA processing and tRNA pseudouridylation. *Nature chemical biology* **2020**, *16*, doi:10.1038/s41589-019-0420-5.
204. Finer-Moore, J.; Czudnochowski, N.; O'Connell, J.; Wang, A.; Stroud, R. Crystal Structure of the Human tRNA m(1)A58 Methyltransferase-tRNA(3)(Lys) Complex: Refolding of Substrate tRNA Allows Access to the Methylation Target. *Journal of molecular biology* **2015**, *427*, doi:10.1016/j.jmb.2015.10.005.
205. Chujo, T.; Suzuki, T. Trmt61B is a methyltransferase responsible for 1-methyladenosine at position 58 of human mitochondrial tRNAs. *RNA (New York, N.Y.)* **2012**, *18*, doi:10.1261/rna.035600.112.
206. Zhang, Y.; Xiao, Q.; Lei, G.; Li, Z. An investigation of a novel MnO_2 network-Ni/PVDF double shell/core membrane as an anode for lithium ion batteries. *Physical chemistry chemical physics : PCCP* **2015**, *17*, doi:10.1039/c5cp02753e.
207. Pisanti, S.; Picardi, P.; Ciaglia, E.; Margarucci, L.; Ronca, R.; Giacomini, A.; Malfitano, A.; Casapullo, A.; Laezza, C.; Gazzerro, P.; et al. Antiangiogenic effects of N6-isopentenyladenosine, an endogenous isoprenoid end product, mediated by AMPK activation. *FASEB journal : official publication of the Federation of American Societies for Experimental Biology* **2014**, *28*, doi:10.1096/fj.13-238238.
208. McCown, P.J.; Ruszkowska, A.; Kunkler, C.N.; Breger, K.; Hulewicz, J.P.; Wang, M.C.; Springer, N.A.; Brown, J.A. Naturally occurring modified ribonucleosides. *Wiley interdisciplinary reviews. RNA* **2020**, *11*, doi:10.1002/wrna.1595.
209. Robins, M.J.; Hall, R.H.; Thedford, R. N-6-(delta-3-isopentenyl) adenosine. A component of the transfer ribonucleic acid of yeast and of mammalian tissue, methods of isolation, and characterization. *Biochemistry* **1967**, *6*, doi:10.1021/bi00858a035.
210. Fittler, F.; Hall, R. Selective modification of yeast seryl-t-RNA and its effect on the acceptance and binding functions. *Biochemical and biophysical research communications* **1966**, *25*, doi:10.1016/0006-291x(66)90225-7.
211. Spinola, M.; Galvan, A.; Pignatiello, C.; Conti, B.; Pastorino, U.; Nicander, B.; Paroni, R.; Dragani, T. Identification and functional characterization of the candidate tumor suppressor gene TRIT1 in human lung cancer. *Oncogene* **2005**, *24*, doi:10.1038/sj.onc.1208687.
212. Lamichhane, T.N.; Mattijssen, S.; Maraia, R.J. Human cells have a limited set of tRNA anticodon loop substrates of the tRNA isopentenyltransferase TRIT1 tumor suppressor. *Molecular and cellular biology* **2013**, *33*, doi:10.1128/MCB.01041-13.
213. Maraia, R.J.; Arimbasseri, A.G. Factors That Shape Eukaryotic tRNAomes: Processing, Modification and Anticodon-Codon Use. *Biomolecules* **2017**, *7*, doi:10.3390/biom7010026.
214. Yamamoto, T.; Fujimura, A.; Wei, F.; Shinojima, N.; Kuroda, J.; Mukasa, A.; Tomizawa, K. 2-Methylthio Conversion of N6-Isopentenyladenosine in

Mitochondrial tRNAs by CDK5RAP1 Promotes the Maintenance of Glioma-Initiating Cells. *iScience* **2019**, *21*, doi:10.1016/j.isci.2019.10.012.
215. Jenner, L.B.; Demeshkina, N.; Yusupova, G.; Yusupov, M. Structural aspects of messenger RNA reading frame maintenance by the ribosome. *Nature structural & molecular biology* **2010**, *17*, doi:10.1038/nsmb.1790.
216. Yarham, J.W.; Lamichhane, T.N.; Pyle, A.; Mattijssen, S.; Baruffini, E.; Bruni, F.; Donnini, C.; Vassilev, A.; He, L.; Blakely, E.L.; et al. Defective i6A37 modification of mitochondrial and cytosolic tRNAs results from pathogenic mutations in TRIT1 and its substrate tRNA. *PLoS genetics* **2014**, *10*, doi:10.1371/journal.pgen.1004424.
217. Grosjean, H.; Westhof, E. An integrated, structure- and energy-based view of the genetic code. *Nucleic acids research* **2016**, *44*, doi:10.1093/nar/gkw608.
218. Kellner, S.; Neumann, J.; Rosenkranz, D.; Lebedeva, S.; Ketting, R.; Zischler, H.; Schneider, D.; Helm, M. Profiling of RNA modifications by multiplexed stable isotope labelling. *Chemical communications (Cambridge, England)* **2014**, *50*, doi:10.1039/c3cc49114e.
219. Dal Magro, C.; Keller, P.; Kotter, A.; Werner, S.; Duarte, V.; Marchand, V.; Ignarski, M.; Freiwald, A.; Müller, R.; Dieterich, C.; et al. A Vastly Increased Chemical Variety of RNA Modifications Containing a Thioacetal Structure. *Angewandte Chemie (International ed. in English)* **2018**, *57*, doi:10.1002/anie.201713188.
220. Pratt-Hyatt, M.; Pai, D.; Haeusler, R.; Wozniak, G.; Good, P.; Miller, E.; McLeod, I.; Yates, J.; Hopper, A.; Engelke, D. Mod5 protein binds to tRNA gene complexes and affects local transcriptional silencing. *Proceedings of the National Academy of Sciences of the United States of America* **2013**, *110*, doi:10.1073/pnas.1219946110.
221. Swoboda, R.; Somasundaram, R.; Caputo-Gross, L.; Marincola, F.; Robbins, P.; Herlyn, M.; Herlyn, D. Antimelanoma CTL recognizes peptides derived from an ORF transcribed from the antisense strand of the 3' untranslated region of TRIT1. *Molecular therapy oncolytics* **2015**, *1*, doi:10.1038/mto.2014.9.
222. Warner, G.J.; Berry, M.J.; Moustafa, M.E.; Carlson, B.A.; Hatfield, D.L.; Faust, J.R. Inhibition of selenoprotein synthesis by selenocysteine tRNA Ser Sec lacking isopentenyladenosine. *The Journal of biological chemistry* **2000**, *275*, doi:10.1074/jbc.M001280200.
223. Vindry, C.; Ohlmann, T.; Chavatte, L. Translation regulation of mammalian selenoproteins. *Biochimica et biophysica acta. General subjects* **2018**, *1862*, doi:10.1016/j.bbagen.2018.05.010.
224. Kim, L.K.; Matsufuji, T.; Matsufuji, S.; Carlson, B.A.; Kim, S.S.; Hatfield, D.L.; Lee, B.J. Methylation of the ribosyl moiety at position 34 of selenocysteine tRNA Ser Sec is governed by both primary and tertiary structure. *RNA (New York, N.Y.)* **2000**, *6*, doi:10.1017/s1355838200000388.
225. Hatfield, D.; Lee, B.; Hampton, L.; Diamond, A. Selenium induces changes in the selenocysteine tRNA Ser Sec population in mammalian cells. *Nucleic acids research* **1991**, *19*, doi:10.1093/nar/19.4.939.
226. Serrão, V.H.B.; Silva, I.R.; Silva, M.T.A.d.; Scortecci, J.F.; Fernandes, A.d.F.; Thiemann, O.H. The unique tRNA Sec and its role in selenocysteine biosynthesis. *Amino acids* **2018**, *50*, doi:10.1007/s00726-018-2595-6.
227. Burk, R.F.; Hill, K.E. Regulation of Selenium Metabolism and Transport. *Annual review of nutrition* **2015**, *35*, doi:10.1146/annurev-nutr-071714-034250.
228. Short, S.P.; Williams, C.S. Selenoproteins in Tumorigenesis and Cancer Progression. *Advances in cancer research* **2017**, *136*, doi:10.1016/bs.acr.2017.08.002.

229. Hariharan, S.; Dharmaraj, S. Selenium and selenoproteins: it's role in regulation of inflammation. *Inflammopharmacology* **2020**, *28*, doi:10.1007/s10787-020-00690-x.
230. Esaki, N.; Nakamura, T.; Tanaka, H.; Soda, K. Selenocysteine lyase, a novel enzyme that specifically acts on selenocysteine. Mammalian distribution and purification and properties of pig liver enzyme. *The Journal of biological chemistry* **1982**, *257*.
231. Zinoni, F.; Birkmann, A.; Stadtman, T.; Böck, A. Nucleotide sequence and expression of the selenocysteine-containing polypeptide of formate dehydrogenase (formate-hydrogen-lyase-linked) from Escherichia coli. *Proceedings of the National Academy of Sciences of the United States of America* **1986**, *83*, doi:10.1073/pnas.83.13.4650.
232. Howard, M.T.; Copeland, P.R. New Directions for Understanding the Codon Redefinition Required for Selenocysteine Incorporation. *Biological trace element research* **2019**, *192*, doi:10.1007/s12011-019-01827-y.
233. Diamond, A.M.; Choi, I.S.; Crain, P.F.; Hashizume, T.; Pomerantz, S.C.; Cruz, R.; Steer, C.J.; Hill, K.E.; Burk, R.F.; McCloskey, J.A.; et al. Dietary selenium affects methylation of the wobble nucleoside in the anticodon of selenocysteine tRNA(Ser Sec). *The Journal of biological chemistry* **1993**, *268*.
234. Leonardi, A.; Evke, S.; Lee, M.; Melendez, J.; Begley, T. Epitranscriptomic systems regulate the translation of reactive oxygen species detoxifying and disease linked selenoproteins. *Free radical biology & medicine* **2019**, *143*, doi:10.1016/j.freeradbiomed.2019.08.030.
235. Moustafa, M.E.; Carlson, B.A.; M.; El-Saadani, A.; Kryukov, G.V.; Sun, Q.A.; Harney, J.W.; Hill, K.E.; Combs, G.F.; Feigenbaum, L.; et al. Selective inhibition of selenocysteine tRNA maturation and selenoprotein synthesis in transgenic mice expressing isopentenyladenosine-deficient selenocysteine tRNA. *Molecular and cellular biology* **2001**, *21*, doi:10.1128/MCB.21.11.3840-3852.2001.
236. Schoenmakers, E.; Carlson, B.; Agostini, M.; Moran, C.; Rajanayagam, O.; Bochukova, E.; Tobe, R.; Peat, R.; Gevers, E.; Muntoni, F.; et al. Mutation in human selenocysteine transfer RNA selectively disrupts selenoprotein synthesis. *The Journal of clinical investigation* **2016**, *126*, doi:10.1172/JCI84747.
237. Arnér, E.S.; Holmgren, A. Physiological functions of thioredoxin and thioredoxin reductase. *European journal of biochemistry* **2000**, *267*, doi:10.1046/j.1432-1327.2000.01701.x.
238. Lu, J.; Holmgren, A. The thioredoxin antioxidant system. *Free radical biology & medicine* **2014**, *66*, doi:10.1016/j.freeradbiomed.2013.07.036.
239. Zhang, Y.; Roh, Y.; Han, S.; Park, I.; Lee, H.; Ok, Y.; Lee, B.; Lee, S. Role of Selenoproteins in Redox Regulation of Signaling and the Antioxidant System: A Review. *Antioxidants (Basel, Switzerland)* **2020**, *9*, doi:10.3390/antiox9050383.
240. Monies, D.; Vågbø, C.; Al-Owain, M.; Alhomaidi, S.; Alkuraya, F. Recessive Truncating Mutations in ALKBH8 Cause Intellectual Disability and Severe Impairment of Wobble Uridine Modification. *American journal of human genetics* **2019**, *104*, doi:10.1016/j.ajhg.2019.03.026.
241. Sarin, L.P.; Leidel, S.A. Modify or die?--RNA modification defects in metazoans. *RNA biology* **2014**, *11*, doi:10.4161/15476286.2014.992279.
242. Popis, M.; Blanco, S.; Frye, M. Posttranscriptional methylation of transfer and ribosomal RNA in stress response pathways, cell differentiation, and cancer. *Current opinion in oncology* **2016**, *28*, doi:10.1097/CCO.0000000000000252.
243. Suzuki, T. The expanding world of tRNA modifications and their disease relevance. *Nature reviews. Molecular cell biology* **2021**, *22*, doi:10.1038/s41580-021-00342-0.

244. Angelova, M.; Dimitrova, D.; Dinges, N.; Lence, T.; Worpenberg, L.; Carré, C.; Roignant, J. The Emerging Field of Epitranscriptomics in Neurodevelopmental and Neuronal Disorders. *Frontiers in bioengineering and biotechnology* **2018**, *6*, doi:10.3389/fbioe.2018.00046.
245. Freude, K.; Hoffmann, K.; Jensen, L.; Delatycki, M.; des Portes, V.; Moser, B.; Hamel, B.; van Bokhoven, H.; Moraine, C.; Fryns, J.; et al. Mutations in the FTSJ1 gene coding for a novel S-adenosylmethionine-binding protein cause nonsyndromic X-linked mental retardation. *American journal of human genetics* **2004**, *75*, doi:10.1086/422507.
246. El-Hattab, A.; Bournat, J.; Eng, P.; Wu, J.; Walker, B.; Stankiewicz, P.; Cheung, S.; Brown, C. Microduplication of Xp11.23p11.3 with effects on cognition, behavior, and craniofacial development. *Clinical genetics* **2011**, *79*, doi:10.1111/j.1399-0004.2010.01496.x.
247. Kirino, Y.; Suzuki, T. Human mitochondrial diseases associated with tRNA wobble modification deficiency. *RNA biology* **2005**, *2*, doi:10.4161/rna.2.2.1610.
248. Kernohan, K.D.; Dyment, D.A.; M.; Pupavac; Cramer, Z.; McBride, A.; Bernard, G.; Straub, I.; Tetreault, M.; Hartley, T.; et al. Matchmaking facilitates the diagnosis of an autosomal-recessive mitochondrial disease caused by biallelic mutation of the tRNA isopentenyltransferase (TRIT1) gene. *Human mutation* **2017**, *38*, doi:10.1002/humu.23196.
249. Balciuniene, J.; DeChene, E.; Akgumus, G.; Romasko, E.; Cao, K.; Dubbs, H.; Mulchandani, S.; Spinner, N.; Conlin, L.; Marsh, E.; et al. Use of a Dynamic Genetic Testing Approach for Childhood-Onset Epilepsy. *JAMA network open* **2019**, *2*, doi:10.1001/jamanetworkopen.2019.2129.
250. Forde, K.M.; Molloy, B.; Conroy, J.; Green, A.J.; King, M.D.; Buckley, P.G.; Ryan, S.; Gorman, K.M. Expansion of the phenotype of biallelic variants in TRIT1. *European journal of medical genetics* **2020**, *63*, doi:10.1016/j.ejmg.2020.103882.
251. Cosentino, C.; Cnop, M.; Igoillo-Esteve, M. The tRNA Epitranscriptome and Diabetes: Emergence of tRNA Hypomodifications as a Cause of Pancreatic β-Cell Failure. *Endocrinology* **2019**, *160*, doi:10.1210/en.2019-00098.
252. Wang, H.; Wei, L.; Li, C.; Zhou, J.; Li, Z. CDK5RAP1 deficiency induces cell cycle arrest and apoptosis in human breast cancer cell line by the ROS/JNK signaling pathway. *Oncology reports* **2015**, *33*, doi:10.3892/or.2015.3736.
253. Xiong, J.; Wang, Y.; Gu, Y.; Xue, Y.; Dang, L.; Li, Y. CDK5RAP1 targeting NF-κB signaling pathway in human malignant melanoma A375 cell apoptosis. *Oncology letters* **2018**, *15*, doi:10.3892/ol.2018.7920.
254. Colombo, F.; Falvella, F.; De Cecco, L.; Tortoreto, M.; Pratesi, G.; Ciuffreda, P.; Ottria, R.; Santaniello, E.; Cicatiello, L.; Weisz, A.; et al. Pharmacogenomics and analogues of the antitumour agent N6-isopentenyladenosine. *International journal of cancer* **2009**, *124*, doi:10.1002/ijc.24168.
255. Simó-Riudalbas, L.; Pérez-Salvia, M.; Setien, F.; Villanueva, A.; Moutinho, C.; Martínez-Cardús, A.; Moran, S.; Berdasco, M.; Gomez, A.; Vidal, E.; et al. KAT6B Is a Tumor Suppressor Histone H3 Lysine 23 Acetyltransferase Undergoing Genomic Loss in Small Cell Lung Cancer. *Cancer research* **2015**, *75*, doi:10.1158/0008-5472.CAN-14-3702.
256. Coffa, J.; Berg, J.v.d. Analysis of MLPA Data Using Novel Software Coffalyser.NET by MRC-Holland. **2011**, doi:10.5772/21898.
257. Wei, F.-Y.; Tomizawa, K. Measurement of 2-methylthio Modifications in Mitochondrial Transfer RNAs by Reverse-transcription Quantitative PCR. *Bio-protocol* **2016**, *6*, doi:10.21769/BioProtoc.1695.
258. Iorio, F.; Knijnenburg, T.; Vis, D.; Bignell, G.; Menden, M.; Schubert, M.; Aben, N.; Gonçalves, E.; Barthorpe, S.; Lightfoot, H.; et al. A Landscape of

Pharmacogenomic Interactions in Cancer. *Cell* **2016**, *166*, doi:10.1016/j.cell.2016.06.017.
259. Ghandi, M.; Huang, F.; Jané-Valbuena, J.; Kryukov, G.; Lo, C.; McDonald, E.; Barretina, J.; Gelfand, E.; Bielski, C.; Li, H.; et al. Next-generation characterization of the Cancer Cell Line Encyclopedia. *Nature* **2019**, *569*, doi:10.1038/s41586-019-1186-3.
260. Rohrbeck, A.; Neukirchen, J.; Rosskopf, M.; Pardillos, G.; Geddert, H.; Schwalen, A.; Gabbert, H.; von Haeseler, A.; Pitschke, G.; Schott, M.; et al. Gene expression profiling for molecular distinction and characterization of laser captured primary lung cancers. *Journal of translational medicine* **2008**, *6*, doi:10.1186/1479-5876-6-69.
261. Karimian, A.; Ahmadi, Y.; Yousefi, B. Multiple functions of p21 in cell cycle, apoptosis and transcriptional regulation after DNA damage. *DNA repair* **2016**, *42*, doi:10.1016/j.dnarep.2016.04.008.
262. Elmore, S. Apoptosis: a review of programmed cell death. *Toxicologic pathology* **2007**, *35*, doi:10.1080/01926230701320337.
263. Dimri, G.; Lee, X.; Basile, G.; Acosta, M.; Scott, G.; Roskelley, C.; Medrano, E.; Linskens, M.; Rubelj, I.; Pereira-Smith, O. A biomarker that identifies senescent human cells in culture and in aging skin in vivo. *Proceedings of the National Academy of Sciences of the United States of America* **1995**, *92*, doi:10.1073/pnas.92.20.9363.
264. Addinsall, A.; Wright, C.; Andrikopoulos, S.; van der Poel, C.; Stupka, N. Emerging roles of endoplasmic reticulum-resident selenoproteins in the regulation of cellular stress responses and the implications for metabolic disease. *The Biochemical journal* **2018**, *475*, doi:10.1042/BCJ20170920.
265. Lee, K.; Tirasophon, W.; Shen, X.; Michalak, M.; Prywes, R.; Okada, T.; Yoshida, H.; Mori, K.; Kaufman, R. IRE1-mediated unconventional mRNA splicing and S2P-mediated ATF6 cleavage merge to regulate XBP1 in signaling the unfolded protein response. *Genes & development* **2002**, *16*, doi:10.1101/gad.964702.
266. Marciniak, S.; Garcia-Bonilla, L.; Hu, J.; Harding, H.; Ron, D. Activation-dependent substrate recruitment by the eukaryotic translation initiation factor 2 kinase PERK. *The Journal of cell biology* **2006**, *172*, doi:10.1083/jcb.200508099.
267. Cabibbo, A.; Pagani, M.; Fabbri, M.; Rocchi, M.; Farmery, M.; Bulleid, N.; Sitia, R. ERO1-L, a human protein that favors disulfide bond formation in the endoplasmic reticulum. *The Journal of biological chemistry* **2000**, *275*, doi:10.1074/jbc.275.7.4827.
268. Papa, S.; Martino, P.; Capitanio, G.; Gaballo, A.; De Rasmo, D.; Signorile, A.; Petruzzella, V. The oxidative phosphorylation system in mammalian mitochondria. *Advances in experimental medicine and biology* **2012**, *942*, doi:10.1007/978-94-007-2869-1_1.
269. Scielzo, C.; Ghia, P. Modeling the Leukemia Microenviroment In Vitro. *Frontiers in oncology* **2020**, *10*, doi:10.3389/fonc.2020.607608.
270. Ellem, S.; De-Juan-Pardo, E.; Risbridger, G. In vitro modeling of the prostate cancer microenvironment. *Advanced drug delivery reviews* **2014**, *79-80*, doi:10.1016/j.addr.2014.04.008.
271. DeNardo, D.; Andreu, P.; Coussens, L. Interactions between lymphocytes and myeloid cells regulate pro- versus anti-tumor immunity. *Cancer metastasis reviews* **2010**, *29*, doi:10.1007/s10555-010-9223-6.
272. Grivennikov, S.; Greten, F.; Karin, M. Immunity, inflammation, and cancer. *Cell* **2010**, *140*, doi:10.1016/j.cell.2010.01.025.
273. Castro-Manrreza, M. Participation of mesenchymal stem cells in the regulation of immune response and cancer development. *Boletin medico del Hospital Infantil de Mexico* **2016**, *73*, doi:10.1016/j.bmhimx.2016.10.003.

274. Castañón, E.; Soltermann, A.; López, I.; Román, M.; Ecay, M.; Collantes, M.; Redrado, M.; Baraibar, I.; López-Picazo, J.; Rolfo, C.; et al. The inhibitor of differentiation-1 (Id1) enables lung cancer liver colonization through activation of an EMT program in tumor cells and establishment of the pre-metastatic niche. *Cancer letters* **2017**, *402*, doi:10.1016/j.canlet.2017.05.012.
275. Kamalian, L.; Forootan, S.; Bao, Z.; Zhang, Y.; Gosney, J.; Foster, C.; Ke, Y. Inhibition of tumourigenicity of small cell lung cancer cells by suppressing Id3 expression. *International journal of oncology* **2010**, *37*, doi:10.3892/ijo_00000708.
276. Zhao, Z.; Bo, Z.; Gong, W.; Guo, Y. Inhibitor of Differentiation 1 (Id1) in Cancer and Cancer Therapy. *International journal of medical sciences* **2020**, *17*, doi:10.7150/ijms.42805.
277. Lejard, V.; Blais, F.; Guerquin, M.; Bonnet, A.; Bonnin, M.; Havis, E.; Malbouyres, M.; Bidaud, C.; Maro, G.; Gilardi-Hebenstreit, P.; et al. EGR1 and EGR2 involvement in vertebrate tendon differentiation. *The Journal of biological chemistry* **2011**, *286*, doi:10.1074/jbc.M110.153106.
278. Zhang, H.; Ding, C.; Li, Y.; Xing, C.; Wang, S.; Yu, Z.; Chen, L.; Li, P.; Dai, M. Data mining-based study of collagen type III alpha 1 (COL3A1) prognostic value and immune exploration in pan-cancer. *Bioengineered* **2021**, *12*, doi:10.1080/21655979.2021.1949838.
279. Wang, Z.; Chen, M.; Qiu, Y.; Yang, Y.; Huang, Y.; Li, X.; Zhang, W. Identification of potential biomarkers associated with immune infiltration in the esophageal carcinoma tumor microenvironment. *Bioscience reports* **2021**, *41*, doi:10.1042/BSR20202439.
280. Si, M.; Lang, J. The roles of metallothioneins in carcinogenesis. *Journal of hematology & oncology* **2018**, *11*, doi:10.1186/s13045-018-0645-x.
281. Zheng, B.; Qu, J.; Ohuchida, K.; Feng, H.; Chong, S.; Yan, Z.; Piao, Y.; Liu, P.; Sheng, N.; Eguchi, D.; et al. LAMA4 upregulation is associated with high liver metastasis potential and poor survival outcome of Pancreatic Cancer. *Theranostics* **2020**, *10*, doi:10.7150/thno.47001.
282. Li, L.; Song, J.; Chuquisana, O.; Hannocks, M.; Loismann, S.; Vogl, T.; Roth, J.; Hallmann, R.; Sorokin, L. Endothelial Basement Membrane Laminins as an Environmental Cue in Monocyte Differentiation to Macrophages. *Frontiers in immunology* **2020**, *11*, doi:10.3389/fimmu.2020.584229.
283. Li, B.; Qian, M.; Cao, H.; Jia, Q.; Wu, Z.; Yang, X.; Ma, T.; Wei, H.; Chen, T.; Xiao, J. TGF-β2-induced ANGPTL4 expression promotes tumor progression and osteoclast differentiation in giant cell tumor of bone. *Oncotarget* **2017**, *8*, doi:10.18632/oncotarget.18629.
284. Zhao, J.; Liu, J.; Wu, N.; Zhang, H.; Zhang, S.; Li, L.; Wang, M. ANGPTL4 overexpression is associated with progression and poor prognosis in breast cancer. *Oncology letters* **2020**, *20*, doi:10.3892/ol.2020.11768.
285. Yagublu, V.; Arthur, J.; Babayeva, S.; Nicol, F.; Post, S.; Keese, M. Expression of selenium-containing proteins in human colon carcinoma tissue. *Anticancer research* **2011**, *31*.
286. Gong, Y.; Wang, N.; Liu, N.; Dong, H. Lipid Peroxidation and GPX4 Inhibition Are Common Causes for Myofibroblast Differentiation and Ferroptosis. *DNA and cell biology* **2019**, *38*, doi:10.1089/dna.2018.4541.
287. Lu, J.; Chew, E.; Holmgren, A. Targeting thioredoxin reductase is a basis for cancer therapy by arsenic trioxide. *Proceedings of the National Academy of Sciences of the United States of America* **2007**, *104*, doi:10.1073/pnas.0701549104.

288. Talbot, S.; Nelson, R.; Self, W. Arsenic trioxide and auranofin inhibit selenoprotein synthesis: implications for chemotherapy for acute promyelocytic leukaemia. *British journal of pharmacology* **2008**, *154*, doi:10.1038/bjp.2008.161.
289. Kutny, M.; Alonzo, T.; Gerbing, R.; Wang, Y.; Raimondi, S.; Hirsch, B.; Fu, C.; Meshinchi, S.; Gamis, A.; Feusner, J.; et al. Arsenic Trioxide Consolidation Allows Anthracycline Dose Reduction for Pediatric Patients With Acute Promyelocytic Leukemia: Report From the Children's Oncology Group Phase III Historically Controlled Trial AAML0631. *Journal of clinical oncology : official journal of the American Society of Clinical Oncology* **2017**, *35*, doi:10.1200/JCO.2016.71.6183.
290. Adès, L.; Thomas, X.; Bresler, A.; Raffoux, E.; Spertini, O.; Vey, N.; Marchand, T.; Récher, C.; Pigneux, A.; Girault, S.; et al. Arsenic trioxide is required in the treatment of newly diagnosed acute promyelocytic leukemia. Analysis of a randomized trial (APL 2006) by the French Belgian Swiss APL group. *Haematologica* **2018**, *103*, doi:10.3324/haematol.2018.198614.
291. Chen, L.; Zhu, H.; Li, Y.; Liu, Q.; Hu, Y.; Zhou, J.; Jin, J.; Hu, J.; Liu, T.; Wu, D.; et al. Arsenic trioxide replacing or reducing chemotherapy in consolidation therapy for acute promyelocytic leukemia (APL2012 trial). *Proceedings of the National Academy of Sciences of the United States of America* **2021**, *118*, doi:10.1073/pnas.2020382118.
292. Hoonjan, M.; Jadhav, V.; Bhatt, P. Arsenic trioxide: insights into its evolution to an anticancer agent. *Journal of biological inorganic chemistry : JBIC : a publication of the Society of Biological Inorganic Chemistry* **2018**, *23*, doi:10.1007/s00775-018-1537-9.
293. Wahiduzzaman, M.; Ota, A.; Hosokawa, Y. Novel Mechanistic Insights into the Anti-cancer Mode of Arsenic Trioxide. *Current cancer drug targets* **2020**, *20*, doi:10.2174/1568009619666191021122006.
294. Huang, W.; Zeng, Y. A candidate for lung cancer treatment: arsenic trioxide. *Clinical & translational oncology : official publication of the Federation of Spanish Oncology Societies and of the National Cancer Institute of Mexico* **2019**, *21*, doi:10.1007/s12094-019-02054-6.
295. de Thé, H. Differentiation therapy revisited. *Nature reviews. Cancer* **2018**, *18*, doi:10.1038/nrc.2017.103.
296. Milkiewicz, M.; Pugh, C.; Egginton, S. Inhibition of endogenous HIF inactivation induces angiogenesis in ischaemic skeletal muscles of mice. *The Journal of physiology* **2004**, *560*, doi:10.1113/jphysiol.2004.069757.
297. Schultz, K.; Murthy, V.; Tatro, J.; Beasley, D. Prolyl hydroxylase 2 deficiency limits proliferation of vascular smooth muscle cells by hypoxia-inducible factor-1{alpha}-dependent mechanisms. *American journal of physiology. Lung cellular and molecular physiology* **2009**, *296*, doi:10.1152/ajplung.90393.2008.
298. Singh, A.; Wilson, J.; Schofield, C.; Chen, R. Hypoxia-inducible factor (HIF) prolyl hydroxylase inhibitors induce autophagy and have a protective effect in an in-vitro ischaemia model. *Scientific reports* **2020**, *10*, doi:10.1038/s41598-020-58482-w.
299. Rossi, A.; Di Maio, M.; Chiodini, P.; Rudd, R.; Okamoto, H.; Skarlos, D.; Früh, M.; Qian, W.; Tamura, T.; Samantas, E.; et al. Carboplatin- or cisplatin-based chemotherapy in first-line treatment of small-cell lung cancer: the COCIS meta-analysis of individual patient data. *Journal of clinical oncology : official journal of the American Society of Clinical Oncology* **2012**, *30*, doi:10.1200/JCO.2011.40.4905.
300. Iwakawa, R.; Takenaka, M.; Kohno, T.; Shimada, Y.; Totoki, Y.; Shibata, T.; Tsuta, K.; Nishikawa, R.; Noguchi, M.; Sato-Otsubo, A.; et al. Genome-wide

identification of genes with amplification and/or fusion in small cell lung cancer. *Genes, chromosomes & cancer* **2013**, *52*, doi:10.1002/gcc.22076.
301. (CLCGP), C.L.C.G.P.; (NGM), N.G.M. A genomics-based classification of human lung tumors. *Science translational medicine* **2013**, *5*, doi:10.1126/scitranslmed.3006802.
302. Coll-SanMartin, L.; Davalos, V.; Piñeyro, D.; Rosselló-Tortella, M.; Bueno-Costa, A.; Setien, F.; Villanueva, A.; Granada, I.; Ruiz-Xiviller, N.; Kotter, A.; et al. Gene Amplification-Associated Overexpression of the Selenoprotein tRNA Enzyme TRIT1 Confers Sensitivity to Arsenic Trioxide in Small-Cell Lung Cancer. *Cancers* **2021**, *13*, 1869, doi:10.3390/cancers13081869.
303. Janin, M.; Ortiz-Barahona, V.; de Moura, M.; Martínez-Cardús, A.; Llinàs-Arias, P.; Soler, M.; Nachmani, D.; Pelletier, J.; Schumann, U.; Calleja-Cervantes, M.; et al. Epigenetic loss of RNA-methyltransferase NSUN5 in glioma targets ribosomes to drive a stress adaptive translational program. *Acta neuropathologica* **2019**, *138*, doi:10.1007/s00401-019-02062-4.
304. Anadón, C.; Guil, S.; Simó-Riudalbas, L.; Moutinho, C.; Setien, F.; Martínez-Cardús, A.; Moran, S.; Villanueva, A.; Calaf, M.; Vidal, A.; et al. Gene amplification-associated overexpression of the RNA editing enzyme ADAR1 enhances human lung tumorigenesis. *Oncogene* **2016**, *35*, doi:10.1038/onc.2015.469.
305. Song, P.; Yang, F.; Jin, H.; Wang, X. The regulation of protein translation and its implications for cancer. *Signal transduction and targeted therapy* **2021**, *6*, doi:10.1038/s41392-020-00444-9.
306. Nebbioso, A.; Tambaro, F.; Dell'Aversana, C.; L, A. Cancer epigenetics: Moving forward. *PLoS genetics* **2018**, *14*, doi:10.1371/journal.pgen.1007362.
307. Yang, S.; Zhang, Z.; Wang, Q. Emerging therapies for small cell lung cancer. *Journal of hematology & oncology* **2019**, *12*, doi:10.1186/s13045-019-0736-3.
308. Linn, P.; Kohno, S.; Sheng, J.; Kulathunga, N.; Yu, H.; Zhang, Z.; Voon, D.; Watanabe, Y.; Takahashi, C. Targeting RB1 Loss in Cancers. *Cancers* **2021**, *13*, doi:10.3390/cancers13153737.
309. Carlson, B.; Yoo, M.; Tsuji, P.; Gladyshev, V.; Hatfield, D. Mouse models targeting selenocysteine tRNA expression for elucidating the role of selenoproteins in health and development. *Molecules (Basel, Switzerland)* **2009**, *14*, doi:10.3390/molecules14093509.
310. Pérez, S.; Taléns-Visconti, R.; Rius-Pérez, S.; Finamor, I.; Sastre, J. Redox signaling in the gastrointestinal tract. *Free radical biology & medicine* **2017**, *104*, doi:10.1016/j.freeradbiomed.2016.12.048.
311. Yoo, S.; Kim, Y.; Yoon, J.; Seo, G.; Keum, C.; Cheon, C. The first Korean cases of combined oxidative phosphorylation deficiency 35 with two novel TRIT1 mutations in two siblings confirmed by clinical and molecular investigation. *Brain & development* **2021**, *43*, doi:10.1016/j.braindev.2020.08.016.
312. Pitts, M.; Hoffmann, P. Endoplasmic reticulum-resident selenoproteins as regulators of calcium signaling and homeostasis. *Cell calcium* **2018**, *70*, doi:10.1016/j.ceca.2017.05.001.
313. Chen, D.; Forootan, S.; Gosney, J.; Forootan, F.; Ke, Y. Increased expression of Id1 and Id3 promotes tumorigenicity by enhancing angiogenesis and suppressing apoptosis in small cell lung cancer. *Genes & cancer* **2014**, *5*, doi:10.18632/genesandcancer.20.
314. Kamalian, L.; Gosney, J.; Forootan, S.; Foster, C.; Bao, Z.; Beesley, C.; Ke, Y. Increased expression of Id family proteins in small cell lung cancer and its prognostic significance. *Clinical cancer research : an official journal of the American Association for Cancer Research* **2008**, *14*, doi:10.1158/1078-0432.CCR-07-4716.

315. Kuivaniemi, H.; Tromp, G. Type III collagen (COL3A1): Gene and protein structure, tissue distribution, and associated diseases. *Gene* **2019**, *707*, doi:10.1016/j.gene.2019.05.003.
316. Kim, J.; Xu, Y.; Xu, X.; Keene, D.; Gurusiddappa, S.; Liang, X.; Wary, K.; Höök, M. A novel binding site in collagen type III for integrins alpha1beta1 and alpha2beta1. *The Journal of biological chemistry* **2005**, *280*, doi:10.1074/jbc.M502431200.
317. Chen, Z.; Soutto, M.; Rahman, B.; Fazili, M.; Peng, D.; Piazuelo, M.; Chen, H.; Washington, M.; Shyr, Y.; El-Rifai, W. Integrated expression analysis identifies transcription networks in mouse and human gastric neoplasia. *Genes, chromosomes & cancer* **2017**, *56*, doi:10.1002/gcc.22456.
318. Deng, T.; Gong, Y.; Wang, X.; Liao, X.; Huang, K.; Zhu, G.; Chen, H.; Guo, F.; Mo, L.; Li, L. Use of Genome-Scale Integrated Analysis to Identify Key Genes and Potential Molecular Mechanisms in Recurrence of Lower-Grade Brain Glioma. *Medical science monitor : international medical journal of experimental and clinical research* **2019**, *25*, doi:10.12659/MSM.913602.
319. Wang, M.; Zhao, J.; Zhang, L.; Wei, F.; Lian, Y.; Wu, Y.; Gong, Z.; Zhang, S.; Zhou, J.; Cao, K.; et al. Role of tumor microenvironment in tumorigenesis. *Journal of Cancer* **2017**, *8*, doi:10.7150/jca.17648.
320. Chen, Y.; Pan, Y.; Ji, Y.; Sheng, L.; Du, X. Network analysis of differentially expressed smoking-associated mRNAs, lncRNAs and miRNAs reveals key regulators in smoking-associated lung cancer. *Experimental and therapeutic medicine* **2018**, *16*, doi:10.3892/etm.2018.6891.
321. Liu, Y.; Liu, L.; Yu, T.; Lin, H.; Chu, D.; Deng, W.; Yan, M.; Li, J.; Yao, M. Systematic analysis of mRNA expression profiles in NSCLC cell lines to screen metastasis-related genes. *Molecular medicine reports* **2016**, *14*, doi:10.3892/mmr.2016.5911.
322. Cheng, Y.; Champliaud, M.; Burgeson, R.; Marinkovich, M.; Yurchenco, P. Self-assembly of laminin isoforms. *The Journal of biological chemistry* **1997**, *272*, doi:10.1074/jbc.272.50.31525.
323. Lugassy, C.; Torres-Muñoz, J.; Kleinman, H.; Ghanem, G.; Vernon, S.; Barnhill, R. Overexpression of malignancy-associated laminins and laminin receptors by angiotropic human melanoma cells in a chick chorioallantoic membrane model. *Journal of cutaneous pathology* **2009**, *36*, doi:10.1111/j.1600-0560.2009.01273.x.
324. Shan, N.; Zhang, X.; Xiao, X.; Zhang, H.; Tong, C.; Luo, X.; Chen, Y.; Liu, X.; Yin, N.; Deng, Q.; et al. Laminin α4 (LAMA4) expression promotes trophoblast cell invasion, migration, and angiogenesis, and is lowered in preeclamptic placentas. *Placenta* **2015**, *36*, doi:10.1016/j.placenta.2015.04.008.
325. Goh, Y.; Pal, M.; Chong, H.; Zhu, P.; Tan, M.; Punugu, L.; Tan, C.; Huang, R.; Sze, S.; Tang, M.; et al. Angiopoietin-like 4 interacts with matrix proteins to modulate wound healing. *The Journal of biological chemistry* **2010**, *285*, doi:10.1074/jbc.M110.108175.
326. Pal, M.; Tan, M.; Huang, R.; Goh, Y.; Wang, X.; Tang, M.; Tan, N. Angiopoietin-like 4 regulates epidermal differentiation. *PloS one* **2011**, *6*, doi:10.1371/journal.pone.0025377.
327. Zhu, P.; Goh, Y.; Chin, H.; Kersten, S.; Tan, N. Angiopoietin-like 4: a decade of research. *Bioscience reports* **2012**, *32*, doi:10.1042/BSR20110102.
328. Nakayama, T.; Hatachi, G.; Wen, C.; Yoshizaki, A.; Yamazumi, K.; Niino, D.; Sekine, I. Expression and significance of Tie-1 and Tie-2 receptors, and angiopoietins-1, 2 and 4 in colorectal adenocarcinoma: Immunohistochemical analysis and correlation with clinicopathological factors. *World journal of gastroenterology* **2005**, *11*, doi:10.3748/wjg.v11.i7.964.

329. Bach, F.; Uddin, F.; Burke, D. Angiopoietins in malignancy. *European journal of surgical oncology : the journal of the European Society of Surgical Oncology and the British Association of Surgical Oncology* **2007**, *33*, doi:10.1016/j.ejso.2006.07.015.
330. Wang, Z.; Han, B.; Zhang, Z.; Pan, J.; Xia, H. Expression of angiopoietin-like 4 and tenascin C but not cathepsin C mRNA predicts prognosis of oral tongue squamous cell carcinoma. *Biomarkers : biochemical indicators of exposure, response, and susceptibility to chemicals* **2010**, *15*, doi:10.3109/13547500903261362.
331. Kim, S.; Park, Y.; Kim, S.; Lee, J.; Wang, D.; DuBois, R. ANGPTL4 induction by prostaglandin E2 under hypoxic conditions promotes colorectal cancer progression. *Cancer research* **2011**, *71*, doi:10.1158/0008-5472.CAN-11-1262.
332. Wang, F.; Li, X.; Pan, M.; Hassan, M.; Sun, W.; Fan, Y. Identification of the prognostic value of elevated ANGPTL4 expression in gallbladder cancer-associated fibroblasts. *Cancer medicine* **2021**, *10*, doi:10.1002/cam4.4150.
333. Speckmann, B.; Bidmon, H.; Pinto, A.; Anlauf, M.; Sies, H.; Steinbrenner, H. Induction of glutathione peroxidase 4 expression during enterocytic cell differentiation. *The Journal of biological chemistry* **2011**, *286*, doi:10.1074/jbc.M110.216028.
334. Yang, W.; SriRamaratnam, R.; Welsch, M.; Shimada, K.; Skouta, R.; Viswanathan, V.; Cheah, J.; Clemons, P.; Shamji, A.; Clish, C.; et al. Regulation of ferroptotic cancer cell death by GPX4. *Cell* **2014**, *156*, doi:10.1016/j.cell.2013.12.010.
335. Zhu, S.; Zhang, Q.; Sun, X.; Zeh, H.; Lotze, M.; Kang, R.; Tang, D. HSPA5 Regulates Ferroptotic Cell Death in Cancer Cells. *Cancer research* **2017**, *77*, doi:10.1158/0008-5472.CAN-16-1979.
336. Ubellacker, J.; Tasdogan, A.; Ramesh, V.; Shen, B.; Mitchell, E.; Martin-Sandoval, M.; Gu, Z.; McCormick, M.; Durham, A.; Spitz, D.; et al. Lymph protects metastasizing melanoma cells from ferroptosis. *Nature* **2020**, *585*, doi:10.1038/s41586-020-2623-z.
337. Liu, J.; Du, J.; Zhang, Y.; Sun, W.; Smith, B.; Oberley, L.; Cullen, J. Suppression of the malignant phenotype in pancreatic cancer by overexpression of phospholipid hydroperoxide glutathione peroxidase. *Human gene therapy* **2006**, *17*, doi:10.1089/hum.2006.17.105.
338. Heirman, I.; Ginneberge, D.; Brigelius-Flohé, R.; Hendrickx, N.; Agostinis, P.; Brouckaert, P.; Rottiers, P.; Grooten, J. Blocking tumor cell eicosanoid synthesis by GP x 4 impedes tumor growth and malignancy. *Free radical biology & medicine* **2006**, *40*, doi:10.1016/j.freeradbiomed.2005.08.033.
339. Marciel, M.; Hoffmann, P. Selenoproteins and Metastasis. *Advances in cancer research* **2017**, *136*, doi:10.1016/bs.acr.2017.07.008.
340. Guillemin, M.; Raffoux, E.; Vitoux, D.; Kogan, S.; Soilihi, H.; Lallemand-Breitenbach, V.; Zhu, J.; Janin, A.; Daniel, M.; Gourmel, B.; et al. In vivo activation of cAMP signaling induces growth arrest and differentiation in acute promyelocytic leukemia. *The Journal of experimental medicine* **2002**, *196*, doi:10.1084/jem.20021129.
341. Muto, A.; Kizaki, M.; Kawamura, C.; Matsushita, H.; Fukuchi, Y.; Umezawa, A.; Yamada, T.; Hata, J.; Hozumi, N.; Yamato, K.; et al. A novel differentiation-inducing therapy for acute promyelocytic leukemia with a combination of arsenic trioxide and GM-CSF. *Leukemia* **2001**, *15*, doi:10.1038/sj.leu.2402162.
342. Selvaraj, V.; Yeager-Armstead, M.; Murray, E. Protective and antioxidant role of selenium on arsenic trioxide-induced oxidative stress and genotoxicity in the fish hepatoma cell line PLHC-1. *Environmental toxicology and chemistry* **2012**, *31*, doi:10.1002/etc.2022.

343. Sobh, A.; Loguinov, A.; Yazici, G.; Zeidan, R.; Tagmount, A.; Hejazi, N.; Hubbard, A.; Zhang, L.; Vulpe, C. Functional Profiling Identifies Determinants of Arsenic Trioxide Cellular Toxicity. *Toxicological sciences : an official journal of the Society of Toxicology* **2019**, *169*, doi:10.1093/toxsci/kfz024.
344. Walker, A.; Stevens, J.; Ndebele, K.; Tchounwou, P. Evaluation of Arsenic Trioxide Potential for Lung Cancer Treatment: Assessment of Apoptotic Mechanisms and Oxidative Damage. *Journal of cancer science & therapy* **2016**, *8*, doi:10.4172/1948-5956.1000379.
345. Kumana, C.; Au, W.; Lee, N.; Kou, M.; Mak, R.; Lam, C.; Kwong, Y. Systemic availability of arsenic from oral arsenic-trioxide used to treat patients with hematological malignancies. *European journal of clinical pharmacology* **2002**, *58*, doi:10.1007/s00228-002-0514-x.
346. Au, W.; Kumana, C.; Kou, M.; Mak, R.; Chan, G.; Lam, C.; Kwong, Y. Oral arsenic trioxide in the treatment of relapsed acute promyelocytic leukemia. *Blood* **2003**, *102*, doi:10.1182/blood-2003-01-0298.
347. Mayorga, J.; Richardson-Hardin, C.; Dicke, K. Arsenic trioxide as effective therapy for relapsed acute promyelocytic leukemia. *Clinical journal of oncology nursing* **2002**, *6*, doi:10.1188/02.CJON.341-346.
348. Ghavamzadeh, A.; Alimoghaddam, K.; Rostami, S.; Ghaffari, S.; Jahani, M.; Iravani, M.; Mousavi, S.; Bahar, B.; Jalili, M. Phase II study of single-agent arsenic trioxide for the front-line therapy of acute promyelocytic leukemia. *Journal of clinical oncology : official journal of the American Society of Clinical Oncology* **2011**, *29*, doi:10.1200/JCO.2010.32.2107.
349. Emadi, A.; Gore, S. Arsenic trioxide - An old drug rediscovered. *Blood reviews* **2010**, *24*, doi:10.1016/j.blre.2010.04.001.
350. Lai, Y.; Chang, H.; Huang, M.; Chang, K.; Su, W.; Chen, H.; Chung, C.; Wang, W.; Lin, L.; Chen, Y. Combined effect of topical arsenic trioxide and radiation therapy on skin-infiltrating lesions of breast cancer-a pilot study. *Anti-cancer drugs* **2003**, *14*, doi:10.1097/00001813-200311000-00008.
351. Zheng, C.; Lam, S.; Li, Y.; Fong, B.; Mak, J.; Ho, J. Combination of arsenic trioxide and chemotherapy in small cell lung cancer. *Lung cancer (Amsterdam, Netherlands)* **2013**, *82*, doi:10.1016/j.lungcan.2013.08.022.
352. Selvaraju, V.; Parinandi, N.; Adluri, R.; Goldman, J.; Hussain, N.; Sanchez, J.; Maulik, N. Molecular mechanisms of action and therapeutic uses of pharmacological inhibitors of HIF-prolyl 4-hydroxylases for treatment of ischemic diseases. *Antioxidants & redox signaling* **2014**, *20*, doi:10.1089/ars.2013.5186.
353. Zhdanov, A.; Okkelman, I.; Collins, F.; Melgar, S.; Papkovsky, D. A novel effect of DMOG on cell metabolism: direct inhibition of mitochondrial function precedes HIF target gene expression. *Biochimica et biophysica acta* **2015**, *1847*, doi:10.1016/j.bbabio.2015.06.016.
354. Gruber, M.; Hu, C.; Johnson, R.; Brown, E.; Keith, B.; Simon, M. Acute postnatal ablation of Hif-2alpha results in anemia. *Proceedings of the National Academy of Sciences of the United States of America* **2007**, *104*, doi:10.1073/pnas.0608382104.
355. Liao, S.; Zhao, X.; Han, Y.; Zhang, J.; Wang, L.; Xia, L.; Zhao, K.; Zheng, Y.; Guo, M.; Chen, G. Proteomics-based identification of two novel direct targets of hypoxia-inducible factor-1 and their potential roles in migration/invasion of cancer cells. *Proteomics* **2009**, *9*, doi:10.1002/pmic.200800922.
356. Song, L.; Zhang, J.; Wu, S.; Huang, Y.; Zhao, Q.; Cao, J.; Wu, Y.; Wang, L.; Chen, G. Hypoxia-inducible factor-1alpha-induced differentiation of myeloid leukemic cells is its transcriptional activity independent. *Oncogene* **2008**, *27*, doi:10.1038/sj.onc.1210670.

357. Toh, C.; Gao, F.; Lim, W.; Leong, S.; Fong, K.; Yap, S.; Hsu, A.; Eng, P.; Koong, H.; Thirugnanam, A.; et al. Differences between small-cell lung cancer and non-small-cell lung cancer among tobacco smokers. *Lung cancer (Amsterdam, Netherlands)* **2007**, *56*, doi:10.1016/j.lungcan.2006.12.016.
358. Li, F.; Peiris, M.; Donoghue, D. Functions of FGFR2 corrupted by translocations in intrahepatic cholangiocarcinoma. *Cytokine & growth factor reviews* **2020**, *52*, doi:10.1016/j.cytogfr.2019.12.005.
359. Graham, R.; Barr Fritcher, E.; Pestova, E.; Schulz, J.; Sitailo, L.; Vasmatzis, G.; Murphy, S.; McWilliams, R.; Hart, S.; Halling, K.; et al. Fibroblast growth factor receptor 2 translocations in intrahepatic cholangiocarcinoma. *Human pathology* **2014**, *45*, doi:10.1016/j.humpath.2014.03.014.
360. Wu, Y.; Su, F.; Kalyana-Sundaram, S.; Khazanov, N.; Ateeq, B.; Cao, X.; Lonigro, R.; Vats, P.; Wang, R.; SF, L.; et al. Identification of targetable FGFR gene fusions in diverse cancers. *Cancer discovery* **2013**, *3*, doi:10.1158/2159-8290.CD-13-0050.
361. Sia, D.; Losic, B.; Moeini, A.; Cabellos, L.; Hao, K.; Revill, K.; Bonal, D.; Miltiadous, O.; Zhang, Z.; Hoshida, Y.; et al. Massive parallel sequencing uncovers actionable FGFR2-PPHLN1 fusion and ARAF mutations in intrahepatic cholangiocarcinoma. *Nature communications* **2015**, *6*, doi:10.1038/ncomms7087.
362. Parker, B.; Engels, M.; Annala, M.; Zhang, W. Emergence of FGFR family gene fusions as therapeutic targets in a wide spectrum of solid tumours. *The Journal of pathology* **2014**, *232*, doi:10.1002/path.4297.
363. Arai, Y.; Totoki, Y.; Hosoda, F.; Shirota, T.; Hama, N.; Nakamura, H.; Ojima, H.; Furuta, K.; Shimada, K.; Okusaka, T.; et al. Fibroblast growth factor receptor 2 tyrosine kinase fusions define a unique molecular subtype of cholangiocarcinoma. *Hepatology (Baltimore, Md.)* **2014**, *59*, doi:10.1002/hep.26890.
364. Nakamura, H.; Arai, Y.; Totoki, Y.; Shirota, T.; Elzawahry, A.; Kato, M.; Hama, N.; Hosoda, F.; Urushidate, T.; Ohashi, S.; et al. Genomic spectra of biliary tract cancer. *Nature genetics* **2015**, *47*, doi:10.1038/ng.3375.
365. Farshidfar, F.; Zheng, S.; Gingras, M.; Newton, Y.; Shih, J.; Robertson, A.; Hinoue, T.; Hoadley, K.; Gibb, E.; Roszik, J.; et al. Integrative Genomic Analysis of Cholangiocarcinoma Identifies Distinct IDH-Mutant Molecular Profiles. *Cell reports* **2017**, *19*, doi:10.1016/j.celrep.2017.06.008.
366. Gupta, A.; Dixon, E. Epidemiology and risk factors: intrahepatic cholangiocarcinoma. *Hepatobiliary surgery and nutrition* **2017**, *6*, doi:10.21037/hbsn.2017.01.02.
367. Everhart, J.; Ruhl, C. Burden of digestive diseases in the United States Part III: Liver, biliary tract, and pancreas. *Gastroenterology* **2009**, *136*, doi:10.1053/j.gastro.2009.02.038.
368. Moeini, A.; Sia, D.; Bardeesy, N.; Mazzaferro, V.; Llovet, J. Molecular Pathogenesis and Targeted Therapies for Intrahepatic Cholangiocarcinoma. *Clinical cancer research : an official journal of the American Association for Cancer Research* **2016**, *22*, doi:10.1158/1078-0432.CCR-14-3296.
369. Chun, Y.; Javle, M. Systemic and Adjuvant Therapies for Intrahepatic Cholangiocarcinoma. *Cancer control : journal of the Moffitt Cancer Center* **2017**, *24*, doi:10.1177/1073274817729241.
370. Administration UF and D. FDA grants accelerated approval to pemigatinib for cholangiocarcinoma with an FGFR2 rearrangement or fusion. Available online: https://www.fda.gov/drugs/resources-information-approved-drugs/fda-grants-accelerated-approval-pemigatinib-cholangiocarcinoma-fgfr2-rearrangement-or-fusion . (accessed on

371. Merz, V.; Zecchetto, C.; Melisi, D. Pemigatinib, a potent inhibitor of FGFRs for the treatment of cholangiocarcinoma. *Future oncology (London, England)* **2021**, *17*, doi:10.2217/fon-2020-0726.
372. Lamarca, A.; Palmer, D.; H, S.W.; Ross, P.; Ma, Y.; Arora, A.; S, F.; Gillmore, R.; Wadsley, J.; Patel, K.; et al. ABC-06 | A randomised phase III, multi-centre, open-label study of active symptom control (ASC) alone or ASC with oxaliplatin / 5-FU chemotherapy (ASC+mFOLFOX) for patients (pts) with locally advanced / metastatic biliary tract cancers (ABC) previously-treated with cisplatin/gemcitabine (CisGem) chemotherapy. *https://doi.org/10.1200/JCO.2019.37.15_suppl.4003* **2019**, doi:4003.
373. Pavlidis, N.; Pentheroudakis, G. Cancer of unknown primary site. *Lancet (London, England)* **2012**, *379*, doi:10.1016/S0140-6736(11)61178-1.
374. Varadhachary, G.; Raber, M. Cancer of unknown primary site. *The New England journal of medicine* **2014**, *371*, doi:10.1056/NEJMra1303917.
375. Fizazi, K.; Greco, F.; Pavlidis, N.; Daugaard, G.; Oien, K.; Pentheroudakis, G.; Committee, E.G. Cancers of unknown primary site: ESMO Clinical Practice Guidelines for diagnosis, treatment and follow-up. *Annals of oncology : official journal of the European Society for Medical Oncology* **2015**, *26 Suppl 5*, doi:10.1093/annonc/mdv305.
376. Vikeså, J.; Møller, A.; Kaczkowski, B.; Borup, R.; Winther, O.; Henao, R.; Krogh, A.; Perell, K.; Jensen, F.; Daugaard, G.; et al. Cancers of unknown primary origin (CUP) are characterized by chromosomal instability (CIN) compared to metastasis of know origin. *BMC cancer* **2015**, *15*, doi:10.1186/s12885-015-1128-x.
377. Pavlidis, N.; Briasoulis, E.; Hainsworth, J.; Greco, F. Diagnostic and therapeutic management of cancer of an unknown primary. *European journal of cancer (Oxford, England : 1990)* **2003**, *39*, doi:10.1016/s0959-8049(03)00547-1.
378. Conway, A.; Mitchell, C.; Kilgour, E.; Brady, G.; C, D.; Cook, N. Molecular characterisation and liquid biomarkers in Carcinoma of Unknown Primary (CUP): taking the 'U' out of 'CUP'. *British journal of cancer* **2019**, *120*, doi:10.1038/s41416-018-0332-2.
379. Shivaji, V.; Wilson, J.; Schmidt, N.; Kolokythas, O.; Lalwani, N. Carcinoma of unknown primary with hepatic metastases: a need of judicious and contemplative diagnostic algorithm. *Abdominal radiology (New York)* **2021**, *46*, doi:10.1007/s00261-020-02630-3.
380. Moran, S.; Martínez-Cardús, A.; Sayols, S.; Musulén, E.; Balañá, C.; Estival-Gonzalez, A.; Moutinho, C.; Heyn, H.; Diaz-Lagares, A.; de Moura, M.; et al. Epigenetic profiling to classify cancer of unknown primary: a multicentre, retrospective analysis. *The Lancet. Oncology* **2016**, *17*, doi:10.1016/S1470-2045(16)30297-2.
381. Chen, T. Karyotypic derivation of H9 cell line expressing human immunodeficiency virus susceptibility. *Journal of the National Cancer Institute* **1992**, *84*, doi:10.1093/jnci/84.24.1922.
382. Wain, E.; Mitchell, T.; Russell-Jones, R.; Whittaker, S. Fine mapping of chromosome 10q deletions in mycosis fungoides and sezary syndrome: identification of two discrete regions of deletion at 10q23.33-24.1 and 10q24.33-25.1. *Genes, chromosomes & cancer* **2005**, *42*, doi:10.1002/gcc.20115.
383. Okuda, T.; Taki, T.; Nishida, K.; Chinen, Y.; Nagoshi, H.; Sakakura, C.; Taniwaki, M. Molecular heterogeneity in the novel fusion gene APIP-FGFR2: Diversity of genomic breakpoints in gastric cancer with high-level amplifications at 11p13 and 10q26. *Oncology letters* **2017**, *13*, doi:10.3892/ol.2016.5386.

384. Mathur, A.; Ware, C.; Davis, L.; Gazdar, A.; Pan, B.; Lutterbach, B. FGFR2 is amplified in the NCI-H716 colorectal cancer cell line and is required for growth and survival. *PloS one* **2014**, *9*, doi:10.1371/journal.pone.0098515.
385. Venetsanakos, E.; Brameld, K.; Phan, V.; Verner, E.; Owens, T.; Xing, Y.; Tam, D.; LaStant, J.; Leung, K.; Karr, D.; et al. The Irreversible Covalent Fibroblast Growth Factor Receptor Inhibitor PRN1371 Exhibits Sustained Inhibition of FGFR after Drug Clearance. *Molecular cancer therapeutics* **2017**, *16*, doi:10.1158/1535-7163.MCT-17-0309.
386. Klijn, C.; Durinck, S.; Stawiski, E.; Haverty, P.; Jiang, Z.; Liu, H.; Degenhardt, J.; Mayba, O.; Gnad, F.; Liu, J.; et al. A comprehensive transcriptional portrait of human cancer cell lines. *Nature biotechnology* **2015**, *33*, doi:10.1038/nbt.3080.
387. Chindaprasirt, P.; Promsorn, J.; Ungareewittaya, P.; Twinprai, N.; Chindaprasirt, J. Bone metastasis from cholangiocarcinoma mimicking osteosarcoma: A case report and review literature. *Molecular and clinical oncology* **2018**, *9*, doi:10.3892/mco.2018.1720.
388. Hahn, F.; Müller, L.; Mähringer-Kunz, A.; Tanyildizi, Y.; Dos Santos, D.; Düber, C.; Galle, P.; Weinmann, A.; Kloeckner, R. Distant Metastases in Patients with Intrahepatic Cholangiocarcinoma: Does Location Matter? A Retrospective Analysis of 370 Patients. *Journal of oncology* **2020**, *2020*, doi:10.1155/2020/7195373.
389. King, G.; Javle, M. FGFR Inhibitors: Clinical Activity and Development in the Treatment of Cholangiocarcinoma. *Current oncology reports* **2021**, *23*, doi:10.1007/s11912-021-01100-3.